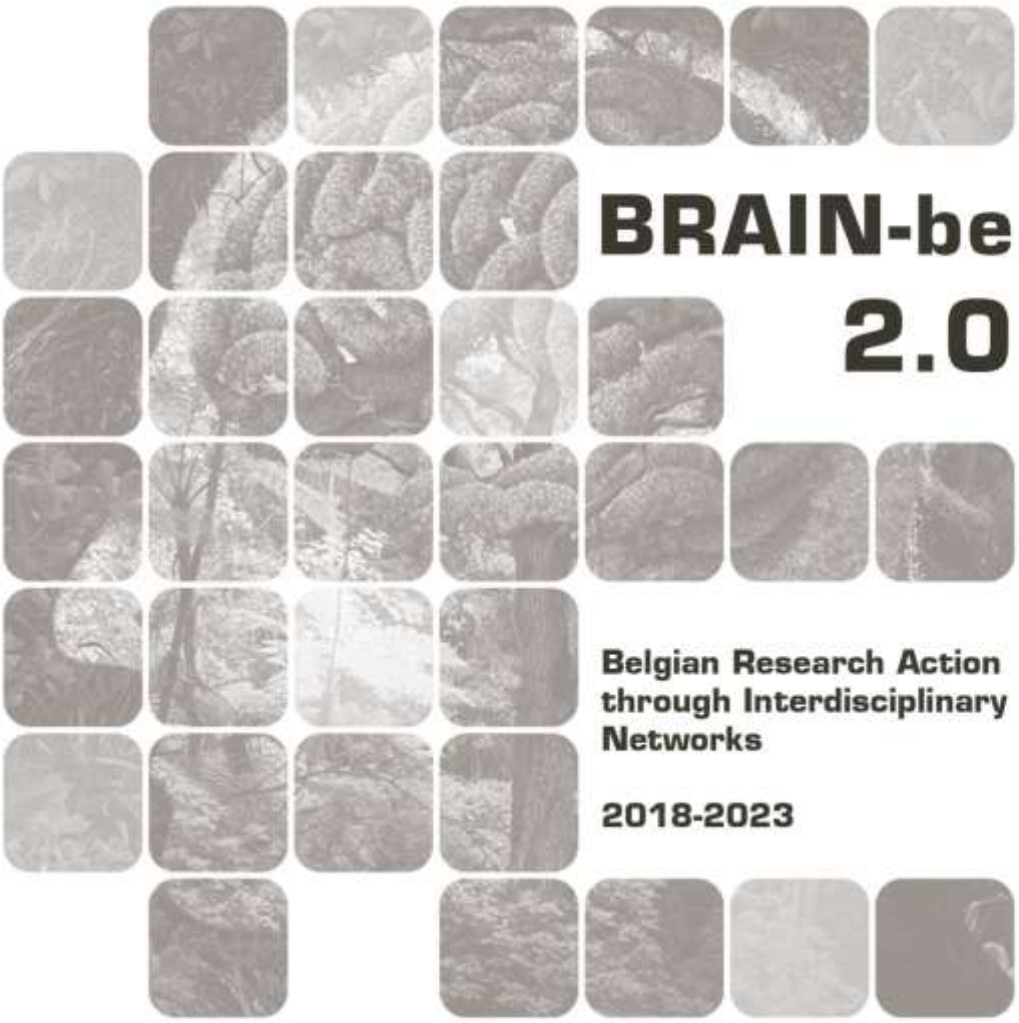

TANGO

Estimating Tipping points in habitability of Antarctic benthic ecosystems under GlObal future climate change scenarios

De Borger Emil (UGent), Ann Vanreusel (UGent), Ulrike Braeckman (UGent, RBINS), Isabelle Schön (RBINS), Gilles Lepoint (ULiège), Bruno Dellile (ULiège), Bruno Danis (ULB), Loïc Michel (ULiège), Lea Katz (ULB), Axelle Brusselmans (ULiège), Anthony Voisin (Univ-Brest), Martin Dogniez (ULiège), Manon Bayat (ULB), Lucas Terrana (ULB), Francesca Pasotti (UGent), Camille Moreau (ULB), Francois Fripiat (ULB), Anton Van de Putte (RBINS)

belspo .be

NETWORK PROJECT

TANGO

Estimating Tipping points in habitability of Antarctic benthic ecosystems under GlObal future climate change scenarios

Contract - B2/212/P1/TANGO

FINAL REPORT

PROMOTORS: Prof. dr. Vanreusel Ann (Universiteit Gent – UGent)
Prof. Dr. Schön Isa (Royal Belgian Institute of Natural Sciences - RBINS)
Prof. Dr. Danis Bruno (Université Libre de Bruxelles - ULB)
Dr. Delille Bruno (Université de Liège - ULiège)

AUTHORS: De Borger Emil (UGent), Ann Vanreusel (UGent), Ulrike Braeckman (UGent, RBINS), Isabelle Schön (RBINS), Gilles Lepoint (ULiège), Bruno Dellile (ULiège), Bruno Danis (ULB), Loïc Michel (ULiège), Lea Katz (ULB), Axelle Brusselmans (ULiège), Anthony Voisin (Univ-Brest), Martin Dogniez (ULiège), Manon Bayat (ULB), Lucas Terrana (ULB), Francesca Pasotti (UGent), Camille Moreau (ULB), Francois Fripiat (ULB), Anton Van de Putte (RBINS)

Published in 2026 by the Belgian Science Policy Office
WTCIII
Simon Bolivarlaan 30 bus 7
Boulevard Simon Bolivar 30 bte 7
B-1000 Brussels
Belgium
Tel: +32 (0)2 238 34 11
http://www.belspo.be
http://www.belspo.be/brain-be

Contact person: David Cox
Tel: +32 (0)2 238 34 03

Authors. ***TANGO: Estimating tipping points in habitability of Antarctic benthic ecosystems under global future climate change scenarios***. Final Report. Brussels: Belgian Science Policy Office 2026 – 86 p. (BRAIN-be 2.0 - (Belgian Research Action through Interdisciplinary Networks))

TABLE OF CONTENTS

ABSTRACT

The TANGO project studied how climate change affects shallow marine ecosystems along the West Antarctic Peninsula (WAP), using a 600 km gradient representing varying sea ice dependence. Two expeditions (2023–2024) sampled five island systems, focusing on biodiversity, food webs, and carbon cycling under changing conditions. Research revealed keystone species' vulnerability: higher temperatures reduced survival and growth in the sea star *Odontaster validus* across generations, suggesting broader ecosystem disruption. Gut microbiota in these species also varied spatially, hinting at their role in resilience. Food web studies showed trophic flexibility in some species, but many are not adaptable. Diatoms and macroalgae are key carbon sources, with rocky habitats supporting more diverse food webs than soft sediments. Glacial retreat is shifting ecosystems toward detrital dependence, altering energy pathways. Primary production and carbon flow analyses found higher chlorophyll in southern, ice-covered stations, with sea ice enhancing organic matter flux to the seafloor. Methane and N_2O emissions were notable, indicating the WAP acts as both a carbon sink and seasonal greenhouse gas source. Ecosystem complexity is driven by macroalgae, ice dynamics, and species interactions at multiple scales. The project therefore recommends monitoring glacial runoff and GHG emissions, using scale-sensitive approaches for marine protected areas, and integrating findings into global climate models.

Keywords: Antarctic, climate change, food web ecology, biogeochemistry, habitat mapping

1. INTRODUCTION

The West Antarctic Peninsula (WAP) is one of Earth's regions where we observe the modest rapid and dramatic environmental changes in marine ecosystems. These changes are driven mostly by warming air and water temperatures, which severely affect ice-dependent polar areas. Observed effects are increasing variation in the duration of the sea ice season, extended glacier retreats, ice shelf collapse, warming of surface waters, and shifts in local primary productivity. Together, these changes are reshaping the WAP marine ecosystem, altering carbon - nutrient cycling, food webs, habitat suitability of key organisms, and more. The response of marine organisms and ecosystem processes to such rapid environmental shifts is not fully understood, especially in shallow, nearshore environments where a myriad of pressures coalesce. Existing studies indicate that many species are highly sensitive to change, suggesting potential vulnerabilities in the ecological processes they support. Understanding resilience, ecological thresholds, and tipping points—critical moments at which small environmental changes can trigger abrupt shifts in ecosystem structure or function—is therefore essential for interpreting and anticipating the impacts of ongoing large-scale changes in the region. **TANGO** approached (future) climate change impacts on coastal ecosystems through a longitudinal gradient along the West Antarctic Peninsula, where a set of research sites spanning ~ 600 km represents a gradient of sea ice dependence. At these sites, an integrated study was performed of the (benthic) ecosystem, combining multiple food web approaches, biogeochemical analyses of nutrient exchange along the sediment-water and water-air interfaces, and detailed habitat mapping. Together, these efforts provide a broad view on the functioning of these nearshore shallow coastal habitats in relation to changing sea-ice conditions.

2. STATE OF THE ART AND OBJECTIVES

The West Antarctic Peninsula (WAP) is among the regions on Earth experiencing rapid environmental change. Over the past decades, atmospheric temperatures in the Antarctic Peninsula have risen up to five times faster than the global average, accompanied by significant warming of surface waters and an increased frequency of extreme temperature anomalies (Ducklow et al., 2013; Intergovernmental Panel On Climate Change (Ipcc), 2022; Massonnet et al., 2023; Pörtner et al., 2019; Turner et al., 2013). These trends contribute to widespread glacier retreat, thinning and collapse of ice shelves, and major reductions in sea-ice extent and seasonality. In the northern WAP, winter sea-ice duration has shortened by more than three months since the 1970s, while historically perennial sea-ice zones in the southern WAP now experience extended ice-free periods (Gutt et al., 2015; Stammerjohn et al., 2008).

Such physical changes have profound implications for the marine environment. Altered sea-ice regimes directly modify light penetration, water-column stability, nutrient cycling, and the phenology of primary production. Observations indicate shifts from large diatom-dominated phytoplankton communities to smaller cryptophyte assemblages in parts of the WAP, linked to changes in stratification and iron availability from meltwater inputs (Constable et al., 2014; Ducklow et al., 2013; Feng et al., 2022; Mendes et al., 2018; Moreau et al., 2015). These changes cascade to higher trophic levels; for example, krill populations, central to Southern Ocean food webs, are affected through reduced sea-ice habitat for juvenile stages and the lower trophic suitability of smaller phytoplankton cells (Atkinson et al., 2019; Kawaguchi et al., 2024; Kohlbach et al., 2017; Moline et al., 2004).

Shallow-water coastal habitats, which are strongly structured by sea-ice cover, glacier influence, and substrate type, are undergoing rapid ecological reorganization. Declining sea-ice cover is expected to favour the expansion of macroalgal beds, while increased iceberg scour and sediment resuspension impose disturbance pressures on benthic communities, altering competitive interactions and functional composition (G. F. Clark et al., 2017; Pasotti et al., 2015; Smale et al., 2007; Torre et al., 2012). Newly exposed rocky habitats following glacial retreat provide substrate for colonisation by macroalgae and sessile invertebrates, whereas soft sediments near glacier fronts may experience higher turbidity and disturbance levels, constraining benthic productivity (Amsler et al., 2023; Braeckman et al., 2019, 2024; Deregibus et al., 2023).

These shallow systems play a key role in carbon and nutrient cycling. Their strong seasonality in primary production leads to pulses of organic material to the seabed, supporting benthic food webs and contributing to carbon storage in long-lived fauna and sediments (Braeckman et al., 2024; Carlini et al., 2009; Constable et al., 2014; Sands et al., 2023; Smith et al., 2012). High rates of organic matter delivery, combined with low temperatures and limited remineralisation, make the WAP one of the more promising regions for "blue" carbon sequestration in Antarctic coastal zones, although empirical evidence remains sparse and spatially fragmented (Isla et al., 2002; Sands et al., 2023; Zwerschke et al., 2022). The magnitude and variability of carbon burial, nutrient regeneration, and benthic-pelagic coupling across the diverse shallow habitats remain insufficiently quantified.

Despite a growing body of field studies and time series, substantial uncertainties persist regarding (i) the biological sensitivity of key species and communities to rapid environmental change, (ii) the mechanistic links between environmental drivers, species interactions, and ecosystem functioning, and (iii) the potential for nonlinear ecological responses. Available studies consistently demonstrate

that Antarctic species are highly sensitive to changes in temperature, food availability, and sea-ice regimes (Chown et al., 2015; Ducklow et al., 2013). However, the resilience capacities of these organisms—particularly in shallow nearshore systems—and the existence of ecological thresholds or alternative stable states remain poorly resolved.

The concept of tipping points is increasingly recognised as critical for understanding Antarctic ecosystem vulnerability. Tipping points represent thresholds at which incremental environmental shifts trigger abrupt, potentially irreversible changes in species performance, community structure, or ecosystem (e.g. biogeochemical) functioning (Convey et al., 2014; Dayton & Jarrell, 2017; Kennicutt et al., 2019; Oliver et al., 2015). Yet, for WAP benthic ecosystems, such thresholds have not been systematically identified, due in part to logistical constraints on long-term observations and the absence of an integrative, multi-level framework capable of linking organismal traits, food-web interactions, and ecosystem processes.

These knowledge gaps have direct relevance for international and Belgian federal science–policy agendas. The Antarctic Treaty System, the Committee for Environmental Protection (CEP), and CCAMLR rely on robust scientific evidence to manage coastal ecosystems, assess climate impacts, and guide conservation measures. Belgium, as a Consultative Party and active contributor to SCAR programmes (e.g., Ant-ICON, AnT-ERA), identifies the understanding of thresholds, habitability, and ecosystem resilience as strategic research priorities under SDG 13 and 14. The limited baseline knowledge on shallow WAP ecosystems limits the capacity of these bodies to anticipate ecosystem change, evaluate management scenarios, and support evidence-based policy decisions.

In summary, the WAP is a highly dynamic natural laboratory where rapid physical changes interact with biological processes across scales. Current knowledge emphasises the urgency of developing mechanistic approaches to (1) detect early-warning signals of ecological thresholds, (2) quantify the impacts of climate-driven alterations in sea-ice and temperature on food webs and carbon cycling, and (3) assess the habitability and long-term stability of Antarctic coastal ecosystems under continued global change.

Objectives

The TANGO project addresses these gaps through an integrative framework capable of detecting and predicting tipping points in Antarctic coastal ecosystems. Building on extensive field experience (RECTO, vERSO, Belgica 121), long-term datasets, and recent methodological advances, TANGO integrates physiological, trophic, biogeochemical, and ecosystem-modelling approaches across a ~600-km environmental gradient along the WAP.

TANGO outlines four main research objectives:

1. **Quantify individual metabolic and physiological responses** of key benthic taxa to temperature and food variability, using Dynamic Energy Budget (DEB) theory to link traits (respiration, growth, reproduction, energy allocation) to changing sea-ice conditions.
2. **Characterize species interactions and trophic niches** along the latitudinal gradient using stable isotopes (C, N, S), and ROV-based habitat mapping to assess competition, trophic flexibility, and habitat use under contrasting sea-ice and disturbance regime.

3. **Determine carbon cycling, storage, export, and burial dynamics** across pelagic, sympagic, and benthic compartments, using sediment-trap deployments, primary-productivity measurements, biogeochemical incubations, and linear inverse modelling to quantify carbon flows and ecosystem functions.
4. **Upscale to ecosystem level and identify ecological thresholds** of species communities across different spatial scales using Bayesian network models, to detect drivers of species occurrence and identify potential tipping points under current and IPCC-projected future scenarios.

Together, these objectives will generate a process-based, predictive understanding of how WAP coastal ecosystems respond to climate-driven alterations in sea-ice cover, temperature, and disturbance regimes. The resulting framework will improve the capacity to identify resilience limits, anticipate irreversible shifts in ecosystem functioning, and support conservation and policy initiatives under the Antarctic Treaty System.

3. METHODOLOGY

3.1. Expeditions

3.1.1. Site selection strategy

Concerted efforts in documenting the Southern Ocean biodiversity have shown that the sampling intensity varies considerably with the considered geographic location (Broyer & Koubbi, 2014; Griffiths et al., 2011). Key elements in the distribution of sampling intensity are the locations of the various national bases and the routes of major research icebreakers. In fact, much of the sampling, tagging, and observation of animals has been done in the coastal areas near the research bases. Based upon the knowledge gained during the B121 expedition (Danis et al., 2021), the TANGO project focused its sampling efforts on areas displaying gradients in (sea)ice conditions.

In the framework of TANGO1, the main challenge was to precisely determine an area suitable for establishing baseline information and displaying sea-ice gradients at various (but workable) spatial scales in uncharted, more Southern locations not visited during the B121 expedition. Within the framework of TANGO2, we leveraged baseline information (bathymetry, ice conditions, geomorphology, etc.) acquired during the B121 expedition. This allowed the consortium to decide on the candidate stations for TANGO2 to best optimize the potential to meet TANGO objectives.

Research sites needed to offer sampling opportunities for food web ecology, biogeochemistry (of sediment, water column, and in southern locations sea-ice), and sheltered from stronger hydrodynamics to allow for ROV work (and diving). The chosen strategy was to leverage RV Australis's agility to explore areas within pre-selected regions. The final decision on the sampling locations was based on a combination of upfront analysis of Sentinel-1 and Sentinel-2 satellite imagery and ground-truthing using RV Australis and the skipper's local knowledge, Ben Wallis (Ocean Expeditions). Ben Wallis, along with the RV Australis and its semi-rigid auxiliary boats, surveyed the bathymetry of the shallow waters of the WAP. He developed a unique bathymetric dataset for Ocean Expeditions, which proved essential for TANGO in selecting the survey and sampling sites, including ROV and diver surveys, sediment core collection, and sediment trap deployment. The combination of this bathymetric data and the RV Australis's shallow draft allows operations close to the coast and within glacier fjords, even enabling surveys of uncharted regions. This was critical, for instance, for sampling the Blaiklock Fjord system, which is uncharted because it has only recently freed from ice-sheet cover. This enabled us to study how the area has been colonized after glacier retreat. To finalize the selection of sampling sites, careful attention was paid to adopting a hierarchical design to account for multiple spatial scales and to feed information into the upscaling work package (WP4) of the TANGO project.

This approach allowed for swift identification of suitable sampling stations, as well as anchorage fit for the deployment of the research gear, ensuring maximal efficiency for finding stations, ice floes, and to carry out gear deployments in a secure fashion. Upon arriving at a new site, additional scouting for the exact sampling locations for different activities was conducted using the RV Australis, two tenders (Bombard C3 and C4), Mavic Pro 2 drones, a BlueROV ROV, and SCUBA divers.

3.1.2. Campaign details

Finally, the TANGO expeditions focused on five island systems (Figure 1): Dodman Island (66°00'S, 65°46'W) and Blaiklock Island (67°33'S, 67°12'W) during TANGO1, and Melchior Island (64°19'S, 62°56'W), Hovgaard Island (65°6'S, 64°4'W), and Føyn Harbor (64°32'S, 61°59'W) during TANGO2. To

increase heterogeneity of the environmental setting of research sites, 2 - 4 subsites were sampled within each island system. During TANGO2, areas were specifically sampled for surface greenhouse gases; they were selected based on features that could serve as sources of atmospheric GHGs. More specifically, glaciers were investigated as a potential source of methane from subglacial meltwater (Lamarche-Gagnon et al., 2019), which has been demonstrated in the Arctic but not yet in the Antarctic. For that, the Leyah (65°8'S, 63°57'W) and Agalina glaciers (64°24'S, 61°28'W) were sampled at the surface. In addition, samples were collected from Deception Island (62°57'S, 60°38'W), a volcanically active island that can be a source of greenhouse gases. This sampling was done in collaboration with the Spanish Gabriel de Castilla research base.

All the stations had features in common, such as depth; every station was shallow (maximum 25m) to allow the diving activities. These were also well-protected stations and coastal. But each station also had specific features: Dodman and Melchior islands had a marine-terminating glacier, while there was no glacier or land-terminating glacier for the others. Hovgaard Island was the only station with the presence of a penguin colony.

The TANGO1 expedition focused on the southern West Antarctic Peninsula and took place from February 9th to March 21st, 2023. Out of the total ship time devoted to the expedition (28 days), 16 days were dedicated to the sampling effort; see details in Table 1.

The TANGO2 expedition focused on the northern West Antarctic Peninsula and took place from February 4th to March 8th, 2024. A total of 16 days were devoted to the sampling effort (excluding birds and marine mammals observations) carried out during transit time (from Ushuaia to the WAP, between the stations, and back to Ushuaia); see details in Table 2.

Full reports of both campaigns can be found in the cruise reports (Danis, 2024; Danis et al., 2023)

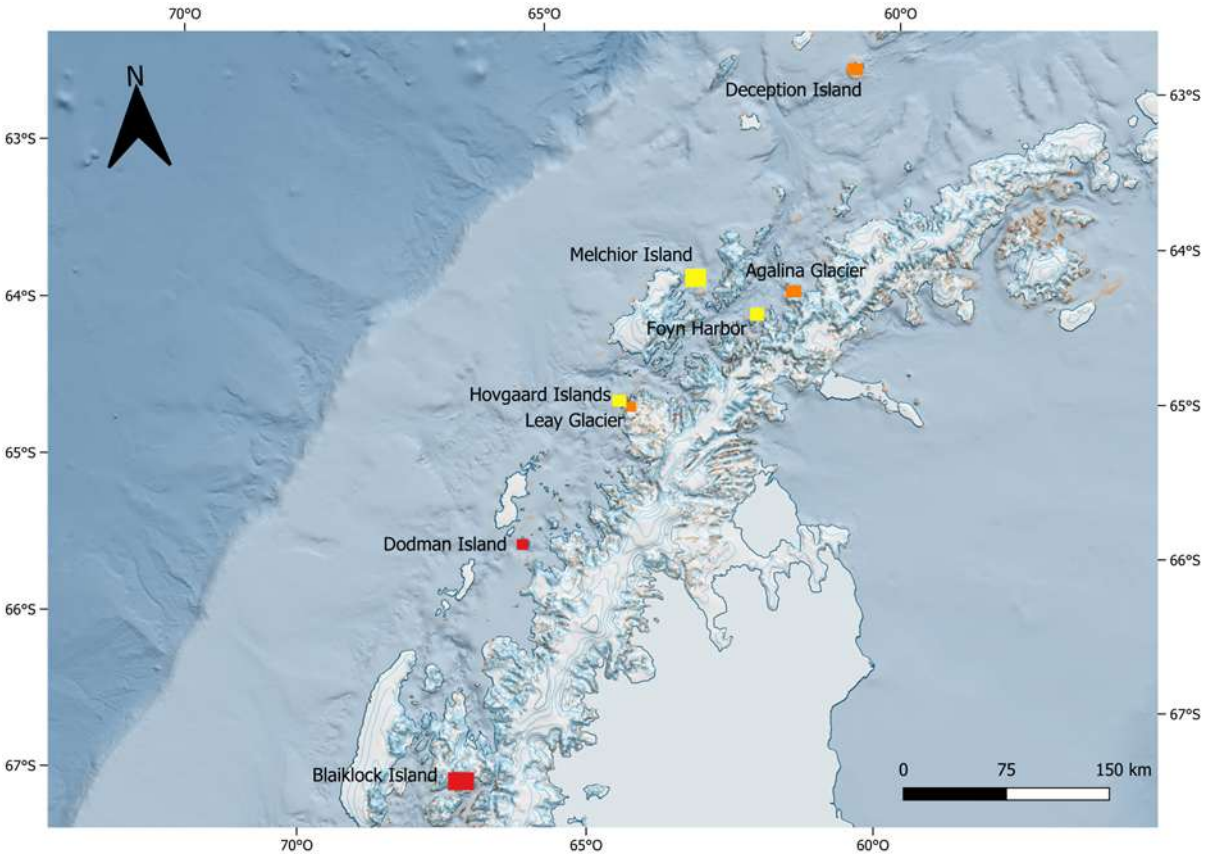

Figure 1: Sampling stations of TANGO1 and TANGO2. Red stations are TANGO1, yellow is for the stations with complete sampling strategy of TANGO2, and orange are the stations with only greenhouse gas sampling of TANGO2

Table 1: Simplified view of the campaign schedule of the TANGO 1 expedition.

	Monday	Tuesday	Wednesday	Thursday	Friday	Saturday	Sunday
February				9	10	11	12
	13	14	15	16	17	18	19
	20	21	22	23	24	25	26
February/March	27	28	1	2	3	4	5
	6	7	8	9	10	11	12
	13	14	15	16	17	18	19
	20	21					

Mobilisation/Demobilisation
CapeHorn/Drake transit
WAP transit
Work at sea

Table 2: Simplified view of the campaign schedule of the TANGO 2 expedition.

	Mon	Tue	Wed	Thu	Fri	Sat	Sun
February							4
	5	6	7	8	9	10	11
	12	13	14	15	16	17	18
	19	20	21	22	23	24	25
February/March	26	27	28	29	1	2	3
March	4	5	6	7	8		

Mobilisation/Demobilisation
CapeHorn/Drake transit
WAP transit
Work at sea

3.2. Data collection and processing

3.2.1. ROV surveys

Fieldwork

A small portable Remotely Operated Vehicle (ROV), the BlueROV2 (Heavy Configuration) from BlueRobotics, was equipped with four 1500-lumen lights, a built-in front-looking camera, a downward looking GoPro HERO 10 camera, a single-beam sonar and a pair of lasers. The ROV was deployed from the Australis itself or from a Bombard C4 tender. With a person managing the tether to assist the pilot. The ROV was deployed using two different methods, serving different purposes for further analysis: squares and line transects. For either method, GPS coordinates were taken on the surface using a handheld GPS (Garmin Oregon 600), then the ROV headed straight downwards until reaching the bottom. It was then flown at a constant altitude above the seafloor (1 meter), either in a "lawn-mower" trajectory (for the squares), covering areas of approx. 10 m^2, or in a straight line (for the line transects) with a known bearing, for approx. 15 minutes at a pace of 0,1m/s, resulting in transects between 90-110 meters, depending on the geomorphological characteristics of the site. Then, it was brought back straight upwards to the surface, and a second GPS point was recorded. If, for weather or logistic reasons, it was not possible to retrieve the second GPS point, it was calculated afterwards using distance and bearing. Square transects were carried out during the first cruise, a total of 32 squares were recorded, including 20 in Dodman Island and 12 in Blaiklock Island. During the second cruise, line transects were carried out in all locations, with 44 transects were performed successfully. Due to some technical complications, such as leaks, breakages or software malfunctions, some transects had to be repeated or performed by divers.

Image analysis

Back in the Laboratory, still images were extracted from the videos and the images resulting from the squares were aligned using Agisoft Metashape to create photomosaics. On the aligned mosaics and the still images from the transects, all organisms and substrate features were annotated using the CATAMI vocabulary along with their size and positioning on the square. This abundance dataset was

used as a base to assess biodiversity, to perform statistical analysis (NMDS and Hierarchical clustering) to differentiate communities between sites and build Bayesian Networks to assess how biotic and abiotic variables are connected in the ecosystem. The aligned mosaics were also used to perform Spatial Point Process Analysis (SPPA).

3.2.2. Benthic trophic ecology

Benthic organism sampling for stable isotopes (SIA), fatty acid (FA) and molecular analysis

WP2 (Species interaction dynamics) involves measurements of stable isotope composition (C, N and S) (hereafter SIA) and determination of fatty acid profiles (hereafter FA). Benthic organisms were collected from the five TANGO locations along the West Antarctic Peninsula (Melchior Islands MI, Føyn Harbour FH, Hovgaard Islands HI, Dodman Island DI and Blaiklock Island BI), with a focus on hard-bottom communities, generally covered by macroalgae (n stations = 5), and soft sedimentary bottom communities (n stations = 5). For these tasks, sampling was standardised to be quantitative and as representative as possible of each sampled site. The collection of organisms was conducted by scientific divers at depths ranging from 15 to 20 m, using a combination of transects (three replicates per station, each 10 m^2) to target mega-invertebrates (> 5 cm), and quadrats (three replicates per station, each 0.16 m^2) to sample smaller invertebrates and benthic primary producers (i.e., macroalgae and their epiphytes, sediment particulate organic matter—hereafter sediment POM—and microphytobenthos). Two exceptions were made to this sampling design. At the hard-bottom station at Dodman Island (station DI1), six transects and six quadrats were used instead of the usual triplicates. At the soft-sediment station at Dodman Island (station DI2), six transects were also deployed, while five Van Veen grab samples replaced the standard quadrats because the station was characterised by very fine sediments. In such environments, quadrats were unsuitable for sampling small macrofauna because most small macroinvertebrates lived buried in the upper sediment layer—a lifestyle that renders sampling by scraping ineffective. Additional specimens of *Cnemidocarpa verrucosa* (Chordate, Ascidiacea) were collected during opportunistic sampling alongside the main sampling units in Melchior Islands, Føyn Harbour and Hovgaard Islands to ensure sufficient replication for fatty acid (FA) analyses. Finally, a special focus was done on the sea urchins *Sterechinus neumayeri* with additional stations and measurement of both stable isotope ratios, metabarcoding of gut content and assessment of microbiomes.

Organisms were sorted and identified morphologically to the lowest possible taxonomic level with the help of well-established field guides on Antarctic Peninsula benthic diversity (Brueggeman, 1998; Schories & Kohlberg, 2016; Watts, 2021). Some individuals were kept for molecular analysis (barcoding and genetic identification (see below)). Organisms were dissected, and the targeted tissues for stable isotope (SI) analysis were placed in 4 mL glass vials and dried in a portable oven at 60 °C for at least 48 h. In parallel, tissues were taken from the same individuals and stored in 4 mL glass vials filled with chloroform/methanol (2:1) solvent and placed in a −20 °C freezer for later analysis of their FA content.

DNA metabarcoding of gut content and microbiomes

More than 700 samples of meiobenthic organisms (e.g. sea stars, ophiuroids, patella, ascidians, sea cucumbers,…) were collected during both cruises for molecular identification of gut content and for the sea urchin *S. neumayeri,* also for the gut-associated microbiome. DNA from the latter samples was extracted with the DNAeasy PoweSoil kit while new DNA extraction protocols for the other meiobenthic organisms were developed using the automated extractor Maxwell® together with the RSC Fecal Microbiome DNA Kit (Promega) or, for *S. neumayeri* samples without subsequent

microbiome analyses, the Promega's Maxwell® RSC PureFood GMO and Authentication Kit on the Maxwell extractor. The selected PCR primers (Geller et al., 2013; Wangensteen et al., 2018) for gut analyses targeted a 313 basepair part of the mitochondrial COI region. Given the wide range of target organisms, extensive PCR optimizations were necessary such as testing different annealing temperatures, Taq polymerases and number of PCR cycles. Amplicons were purified and sent to AllGenetics for pair-end sequencing on an Illumina Novoseq platform. Sequences obtained from a preliminary sequencing run of 20 samples were processed with QIIME2 version 2024.5 (Bolyen et al., 2019) for both the construction of a custom COI reference database with RESCRIPt (Robeson et al., 2021) and the taxonomic assignment of sequences. Certified COI reference sequences for all metazoans present on NCBI GenBank were retrieved, curated and formatted for training a naïve Bayes taxonomic classifier using the *feature-classifier fit-classifier-naive-bayes* function (Bokulich et al., 2018). For characterizing the microbiome and gut content from the same individuals of *S. neumayeri*, two-step PCRs and Illumina sequencing were performed at AllGenetics focusing on the V4-V5 part of the bacterial 16S region for microbiomes and the same COI fragment as in the other gut content study; these sequencing reads were analysed with dada2.

SIA sample preparation and analysis

The carbon, nitrogen and sulphur isotopic ratios, as well as the elemental composition of the samples, were measured (EA-IRMS) at the University of Liège on the ISOTOPY platform, using a continuous-flow system coupling an elemental analyser (Vario PyroCube, ELEMENTAR, Langenselbold, Germany) to an isotope ratio mass spectrometer (precisION, ELEMENTAR, Langenselbold, Germany). In total, 1,579 samples (1,325 consumers and 254 basal sources) were prepared and analysed.

Isotopic values are reported in conventional δ notation in ‰ (Coplen, 2011). Elemental values are reported as percentage of the dry weight (%DW). Samples were analysed alongside certified reference materials from the International Atomic Energy Agency (IAEA): caffeine (IAEA-600; $\delta^{15}N = 1.0 \pm 0.2$ ‰; certified mean ± σ) for nitrogen, sucrose (IAEA-C6; $\delta^{13}C = -10.8 \pm 0.47$ ‰; certified mean ± σ) for carbon, and barium sulphate (IAEA-SO-5; $\delta^{34}S = 0.5 \pm 0.2$ ‰; certified mean ± σ) for sulphur. Two additional reference materials with known isotopic and elemental compositions were analysed to correct values obtained from the elemental analyser: sulphanilic acid (Merck Sigma-Aldrich, Darmstadt, Germany; %C = 41.3–41.8%, %N = 7.7–8.3%, %S = 18.2–18.8%; certified range) and a seabass (*Dicentrarchus labrax*) muscle powder (University of Liège; %C = 46.13 ± 1.05%, %N = 13.98 ± 0.28%, %S = 0.89 ± 0.11%, C:N ratio = 3.30 ± 0.02; measured mean ± σ).

Environmental characterisation for food web approaches

Environmental conditions were obtained by the extraction of satellite data. After analyzing the variance inflation factor to test for possible collinearity, Chlorophyll a (Cha), Suspended Particulate Matter (SPM), and sea ice cover data were used to define the environmental conditions for each site. Chla and SPM data were extracted from the E.U. Copernicus Marine Service Information using the product of Global Ocean Colour (Copernicus-GlobColour), Bio-Geo-Chemical, L4 (monthly and interpolated) from Satellite Observations (pixel resolution 4km). Sea ice cover data were calculated by extracting optical and radar satellite images (i.e., Landsat 9 and Sentinel 1). Sea ice concentrations are the percentage of sea ice cover within an area defined by the sampling effort at each site. A mean was calculated for each month for each variable. Finally, mean values were calculated for the nine months preceding sampling at each site (i.e., May 2022 to January 2023 for TANGO1 and May 2023 to January 2024 for TANGO2) to consider the previous winter and sea ice breakup at each site. This method of

calculating sea ice cover provided values on a smaller scale than those offered by the satellite grids traditionally used (e.g., AMSR2 pixel resolution 6.25km) and the inference of values relative to the nearest pixels.

SIA data analysis and modelling

To investigate differences in food web properties across habitats (i.e. hard-bottom communities [HBs] vs. soft sediment communities [SBs]), organisms sampled at all stations of each habitat were pooled to form two "metacommunities", whose trophic properties were compared.

To investigate differences in trophic properties across sampling locations (i.e. Melchior Islands [MI] vs. Føyn Harbour [FH] vs. Hovgaard Islands [HI] vs. Dodman Island [DI] vs. Blaiklock Island [BL]), organisms sampled in both habitat types at each location were pooled to form five metacommunities in total, The food web properties of these five habitat metacommunities and ten location metacommunities were then computed using R (R version 4.2.2) (R Core Team, 2021) in a RStudio environment (RStudio 2023.06.1) (Posit team, 2022). For each metacommunity, five standard Layman metrics were calculated (Layman et al., 2007):

1. Total Hull Area (TA) – convex hull area encompassed by all species in isotopic bi-plot space. This represents a measure of the total amount of niche space occupied, and thus a proxy for the total extent of trophic diversity within a food web.

2. Carbon Range (CR) – measures the spread in $\delta^{13}C$ values, serving as a proxy for the diversity of basal carbon sources

3. Nitrogen Range (NR) – captures the spread of $\delta^{15}N$ values, providing an estimate of the vertical trophic structure (i.e. range in trophic position and nitrogen sources)

4. Sulphur Range (SR) – captures the spread of $\delta^{34}S$, serving as a proxy for the diversity of basal sulphur resources (i.e. benthic vs. pelagic/sympagic)

5. Centroid Distance (CD) - average Euclidean distance of each species to the convex hull centroid, where the centroid is the mean $\delta^{13}C$ / $\delta^{34}S$ and $\delta^{15}N$ value for all species in the food web (Layman et al., 2007).

Layman metrics were calculated in two isotopic dimensions (C:N and C:S) using a bootstrapping approach. In each comparison unit, *k* individuals were drawn with replacement from each taxon represented by *k* individuals to generate a bootstrapped community. Layman metrics were then computed parametrically using the custom scripts of Bowes et al. (2017). This procedure was repeated 10.000 times to produce, for each comparison unit, a bootstrapped distribution of each metric in both isotopic dimensions.

Trophic positions of invertebrates were computed using the Bayesian model tRophicPosition 0.5.0.1000 in R (Quezada-Romegialli et al., 2018).

For the sea urchins *Sterechinus neumayeri*, the size of the isotopic niche was estimated using the methodology of Skinner et al. (2019), by estimating the volumes of the standard ellipsoids generated with $\delta^{13}C$, $\delta^{15}N$ and $\delta^{34}S$ values in each station.

Fatty acid and highly branched Isoprenoids analysis

Fatty acid analysis was realised at LIPIDOCEAN technical platform (University of Western Brittany (UBO), Brest, France) in collaboration with Prof Gauthier Schaal following Couturier et al. (2020) (n = 650 samples). A TRACE 1300 GC-FID (Thermo-Fisher) was used to separate and quantify the diversity of compounds found in each sample using two Agilent J&W DB-HeavyWAX Polyethylene Glycol columns (30min length, 0.25mm internal diameter, 0.25 µm film thickness). The area underneath the peaks was extracted from Chromeleon 7.2.10 software (Thermo-Fisher) to quantify each peak and then converted in fatty acid proportion (% of Total Fatty Acid). Additional runs were done using a GC-MS TRACE 1300 coupled to an ISQ 7000 single quadrupole mass spectrometer after GC-FID analyses to characterise more precisely unknown compounds or confirm prior identification from lab standards.

Highly branched isoprenoids (HBI) analysis HBI analysis was used to better understand the contribution of sea ice algae to the ecosystem as a food source. Analysis was carried out at the Oceanography and Climate Laboratory (LOCEAN) in Paris, France, according to Amiraux et al. (2021) (n = 180 samples). HBIs are highly branched alkenes, differentiated by the number of double bonds present.

Fatty acid and HBI data treatment and statistical analysis

FA analyses have enabled the identification of numerous compounds (Table 3). To determine which FA have the greatest contribution to the overall variability of the data collected, a Species Contribution of Beta Diversity (SCBD) analysis was performed for all food sources. The purpose of this analysis is to determine the contribution of each response variable in the dataset (i.e., each FA) to the overall variability of the dataset. By selecting FA with values above the mean SCBD value, it was possible to retain only the fatty acids that were the most important in food source differentiation. This analysis was performed using the beta.div() function from the adespatial package (Dray et al., 2026). A Principal Component Analysis (PCA) was performed to evaluate the diversity of the previously selected FA in all food sources sampled, allowing to use fatty acid as a biomarker of potential food sources.

Table 3: List of fatty acids (FA) selected as trophic biomarkers based on obtained data and various documentation, including, but not limited to, Kelly and Scheibling, 2012 (and references within).

Food Source	Biomarker FA
Diatoms	16:1n-7, 16:3n-4, 16:4n-1
Dinoflagellate	22:6n-3
Nanophytoplankton (e.g., Cryptophyte, Haptophyte)	18:3n-3, 18:4n-3
Zooplankton	20:1n-9, 20:1n-11
	22:1n-9, 22:1n-11
Bacteria	18:1n-7
	Odd numbered anteiso
Macroalgae	20:4n-6

The ratio between analysed HBI was calculated using their areas underneath the peak. This ratio is indicative of sea ice algae as they are producing specific forms of Highly Branched Isoprenoids (HBI). In Antarctica, the Diene is used to characterize this source of diatoms (e.g. Amiraux et al., 2021). In this way, the higher the ratio was, the higher the incorporation of sea ice primary production may have occurred in the sample: HBI: Diene (IPSO25) / Triene (HBI III).

Linear inverse modelling

We investigated the effects of glacial meltwater runoff on benthic food webs in a fjord on the northern edge of the WAP. Potter Cove is a shallow bay on King George Island, N-WAP, strongly impacted by glacial melt runoff. The benthic communities of three sites were investigated during three seasons between 2015 and 2017 (Figure 2). Among the three sites, Faro lies upstream of the dominant current in Potter Cove and experiences the weakest glacial disturbance; Isla D is located right in front of the glacier and is frequently disturbed by ice scouring and increased sedimentation from the glacier; Creek lies further from the glacier, downstream of the dominant current and experiences intermediate disturbance in terms of ice scouring and sedimentation. The seasonal and climatic variability in the dataset is evidenced in a warm summer (2015) and warm spring (2016) with strong glacial melt run-off, contrasting with a cold spring (2015) with limited glacial melt run-off, clear waters and strong production by benthic diatoms. For more details, see Braeckman et al., (2021).

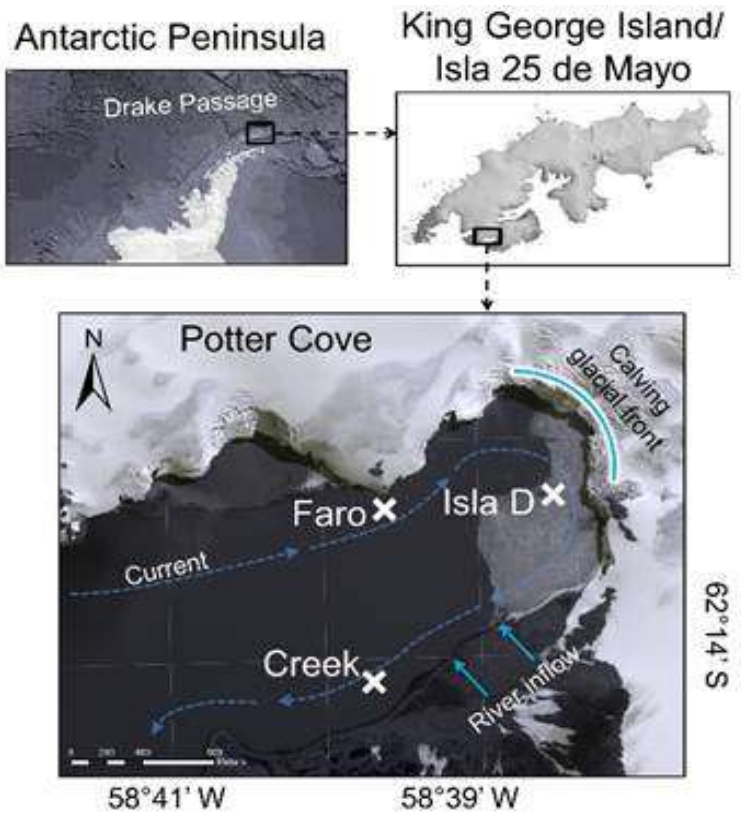

Figure 2: Benthic food web models were constructed for three sites—Faro, Creek, and Isla D (positions are marked with a cross). The curved, bright blue line marks the front of the Fourcade glacier. The bright blue arrows indicate river run-offs from the creeks, supplied mainly by melting glacier, permafrost and snow. The dashed blue arrows indicate the direction of the main current in Potter Cove. Owing to this current direction, Faro is considered an upstream site experiencing little glacial melt disturbance, Isla D is a glacier front site under high glacial melt influence and Creek is located downstream of a melt water river, experiencing glacial melt disturbance in addition to meltwater plume influence.

The food web models were parameterized for the three study sites in Potter Cove, within the three seasons using a Linear Inverse Modelling (LIM) approach. This mass budget model technique resolves fluxes through a food web by creating closed carbon mass balances for each compartment in the ecosystem. It can use various types of field observations, including biomass, stable isotopic composition, rate measurements and isotope tracer experiment data and has proved to be useful to infer carbon flows in benthic food webs in different ecosystems. In this approach, we parameterized

the model, using biomass, rate measurements, stable isotopes composition data and the results from an isotope tracer experiment (Braeckman et al., 2019).

Nine LIMs were constructed, covering each of the three study locations within Potter Cove experiencing different glacial melt disturbances, and three seasons with very different climatic conditions. This entailed complementing the benthic carbon stock data and benthic carbon cycling rate data from Hoffmann et al. (2019) and Braeckman et al. (2021) with extensive literature research on unmeasured stocks and rates. These include for example respiration rates, growth rates, mortality rates of the dominant species and sediment accumulation rates. These rate data are necessary to constrain the LIM.

3.2.3. Molecular analysis

Sampling for molecular analyses

During the sampling of benthic invertebrates and algae for stable isotopes (SI) analyses and fatty acids (FA) analyses, tissues from dominant or unidentified specimens were taken for subsequent DNA barcoding, with the primary goal to complement the existing database of Antarctic invertebrate barcode sequences. In addition to these main samples, environmental DNA samples were also collected at each of the ten stations to characterize general biodiversity using eDNA Dual Filter Capsules from Sylphium Molecular Ecology. At each sampling station, three samples each of 0.96L of seawater were collected two meters above the bottom with a Niskin bottle and filtered into Sylphium capsules, resulting in a total number of 30 samples. In parallel, 462 digestive tracts of selected meta-invertebrates (e.g. sea stars, ophiuroids, patella, ascidians, sea cucumbers,…) and of 252 samples of the sea urchin *Sterechinus neumayeri* were dissected from the same individuals which are processed in SI & FA analyses (see below, WP2).

DNA barcoding

DNA barcoding samples were sub-sampled to preserve original dissections or whole organisms for future morphological analyses. DNA extractions from metazoans were conducted with the Blood & Tissue kit (Qiagen) and from macroalgae with the Plant & GMO kit together with the automated Maxwell R-16 extractor (Promega).

Amplifications with Polymerase Chain Reactions (PCRs) targeted 600 to 800 basepairs of the mitochondrial cytochrome c oxidase 1 gene (CO1, the main sub-unit of the mitochondrial cytochrome c oxidase complex) with the universal primer pair LCO1490-HCO2198 (Folmer et al., 1994). If amplifications were unsuccessful, PCRs were further optimized with different annealing temperatures, TAQ enzymes (DNA polymerases), and PCR primers resulting in novel, optimized PCR protocols for Asteroidea and Ophiuroidea (Echinodermata) and some Mollusca samples. Amplicons were purified and sequenced directly with the PCR primers at Macrogen Europe BV with the Big Dye kit on an ABI 3730xl System.

Raw DNA sequence data were processed with Geneious Prime v.2023.2.1 (Biomatters) including quality control, corrections of sequencing errors and end trimming. The identity of the DNA sequences was confirmed with MEGABLAST searches against the BOLD/GenBank public databases, and the 50 most similar, matching sequences retrieved for further genetic analyses.

3.2.4. Biogeochemistry of water column and sediment trap

We carried out three sampling strategies to answer the question of WP3: What is primary production, pelagic export, benthic storage and carbon flow along climate gradient? These strategies involved seawater collection: I) CTD/Niskin profiles (0m, 6m and bottom) to investigate the dynamic in the whole water column, II) sampling at the bottom to complement organism analysis and III) water collection at the surface to investigate the air-sea exchange for greenhouse gases. The parameters and number of replicates for each strategy are in Table 4.

The three sampling strategies were applied at all the main stations (i.e. Dodman, Blaiklock, Melchior, Hovgaard Islands and Føyn Harbor). At Leyah, Agalina glaciers and Deception Island, only the surface sample strategy was applied.

Table 4: Parameters measured in the water column for each strategy with number of replicates.

Parameter	Profiles/Bottom	Surface	Sediment trap
Salinity	1	1	/
Pigments (including Chl a)	3	/	1
Particulate carbon (PC), particulate nitrogen (PN), particulate sulphur (PS), $\delta^{13}C$ of PC, $\delta^{15}N$ of PN, $\delta^{34}S$ of PS	3	/	1
CH_4 and N_2O concentration	2	2	/
$^{13}CH_4$	2	2	/
Nutrients	1	/	/
Total alkalinity (TA)	1	/	/
Dissolved inorganic carbon (DIC)	1	/	/
Total suspended matter (TSM)	3	/	1
Fatty acid	3	/	/
Environmental DNA (eDNA)	3	/	/

In addition, we measured vertical fluxes of carbon using a sediment trap. One sediment trap was deployed at the main stations for about 7 days for Dodman and Blaiklock Islands and 4 days for Melchior, Hovgaard Islands and Føyn Harbor on a relatively flat bottom ranging between 18 m and 20 m to allow release by divers.

Particular attention was given to the location of the sampling to be as close as possible to the other activities. For that, the agility of the RV Australis but also the two tenders were used. This strategy allowed us to have a better constraint on the environmental parameters of the area which are essential to understand the different interactions and dynamics at each station and in the WAP in general.

CTD casts using ODDI sensors for depth, salinity, temperature, and a HOBO light sensor were performed from the surface to the bottom at all TANGO sites, to produce vertical salinity and temperature sensors. These CTD profiles were completed by water collection with a 2.5L General Oceanic Niskin bottle at three depths: (0m, 6m and 1m from the bottom). Attention has been paid to condition the ODDI sensor in cold seawater for at least 10 min before the CTD profile, then to let the sensor for 3 min at the surface before going down slowly to perform the CTD profile.

CH_4 and N_2O

Gases were the first to be sampled from the Niskin bottle. A Tygon tube was attached to the tip of the bottle and attention was paid to have no bubbles in the tube. 60ml glass bottle were rinced by over filling them during 10 seconds and then poisoned with 60µl of HgCl2. The bottles were then closed with isobutyl stopper and crimped with aluminium cap. The bottles were stored in the dark at room temperature for the rest of the trip and transport to the laboratory.

At home laboratory, samples were analysed using the headspace technique (Weiss et al, 1981). A 20ml headspace made of ultra pure N2 (AirLiquide Belgium®, Alphagaz 2, $N_2 \geq 99.9999\%$) and manually shaken for a few minutes. The bottles were then placed overnight in a water bath at room temperature to let the headspace and water equilibrate. A sub-sample of 10ml was then injected in a gas chromatograph (GC, SRI™ 8610C) with a flame ionization detector (FID) and a Electron Capture Detector (ECD) to analyse CH4 and N2O respectively. The GC was calibrated with precision mixture containing CH_4, N_2O, CO_2, and N_2 with mixing ratios of 0.23, 0.86, and 9.5 ppm for CH4 and 0.53, 0.19 and 0.94 ppm for N2O, manufactured and certified at ± 2% by AirLiquide Belgium®.

Salinity

Salinity was collected from the Niskin bottle and stored in 80 mL brown glass bottles with a headspace. The bottles were stored in the dark at room temperature for the rest of the cruise and taken back to the home laboratory in Belgium. It was analysed using a Guildline 8400B Autosal.

Total alkalinity

Total alkalinity was collected from the Niskin bottle and stored in 80 mL brown glass bottles with a headspace. The bottles were stored in the dark at room temperature for the rest of the cruise and taken back to the home laboratory in Belgium. It was analysed using a Gran titration.

DIC and Nutrients

DIC was collected from the Niskin bottle and stored in 80 mL brown glass bottles with a headspace, and 80 µL of $HgCl_2$ was added to stop biological activity. The bottles were then stored in the dark at room temperature for the rest of the cruise. Nutrients were collected from the Niskin bottle in 60 ml HDPE bottle with a headspace and directly put at -20°C. The samples were returned to Belgium frozen. DIC and nutrients were sent to NIOZ (Royal Netherlands Institute of Sea Research) for analysis.

Phytoplankton pigments

Pigments were collected by filtering 1L of seawater on 25mm GF/F filters. Filters were stored in cryovials in a liquid nitrogen container for the rest of the cruise, then transferred to a -80°C freezer on the RV Hesperides and finally to the home laboratory.

Pigments were extracted at home laboratory. 4 mL of HPLC-grade acetone was added to the filters, and the samples were sonicated for 15 minutes in an ice bath. Extraction lasted overnight at 4°C, followed by a second 15-minute sonication in an ice bath. 2ml of the sample was then transferred to HPLC brown glass vials. Attention was paid during the entire process to keep the samples as cold and in the dark as possible. Samples were then run on a Waters Alliance 2695 with a Waters 2996 PDA detector, equipped with a Waters NovaPak C18 column, using a protocol adapted from Wright & Mantoura (1997). Quantification of chlorophyll a and marker pigments for different phytoplankton

groups was achieved using calibration curves established with pure pigments standards (DHI, Denmark).

Particulate carbon, nitrogen, and sulfur

Particulate carbon (PC), particulate nitrogen (PN), particulate sulfur (PS), $\delta^{13}C$ of PC, $\delta^{15}N$ of PN, $\delta^{34}S$ of PS for vertical profiles were collected by filtering 1L of seawater on 25mm pre-combusted (12 hours at 450°C) GF/F filters. Filters were stored in petri dishes and dried at 60°C for at least 12 hours. The samples were then analysed by ICP-MS at the Laboratoire d'Ecologie trophique et isotopique (LETIS) in Belgium.

Sediment trap

The sediment trap was attached to three floaters to keep it vertical and to collect organic matter (Figure 3). The first floater was 9m below the surface to avoid wave influence and tilting the sediment trap.

Only one collecting cup was used for each deployment. The cup was filled with brine prepared with filtered seawater (FSW), and NaCl was added to increase the salinity by 5 psu. No preservatives were added. Filtered seawater was prepared by filtering surface seawater collected close to the vessel and filtered on a Sartorius Sartroban 0.45/0.2 µ cartridge using a peristaltic pump set at 1l/min. Filtered seawater was kept in the dark at room temperature.

To prevent sample mixing during sediment trap recovery, the divers recovered the sample bottle before releasing the trap. We carefully divided the sample bottle into two subsamples of equal sediment content to allow two filtrations. Subsamples were filtered for pigments and particulate carbon, nitrogen, and sulfur following the same protocol as for seawater.

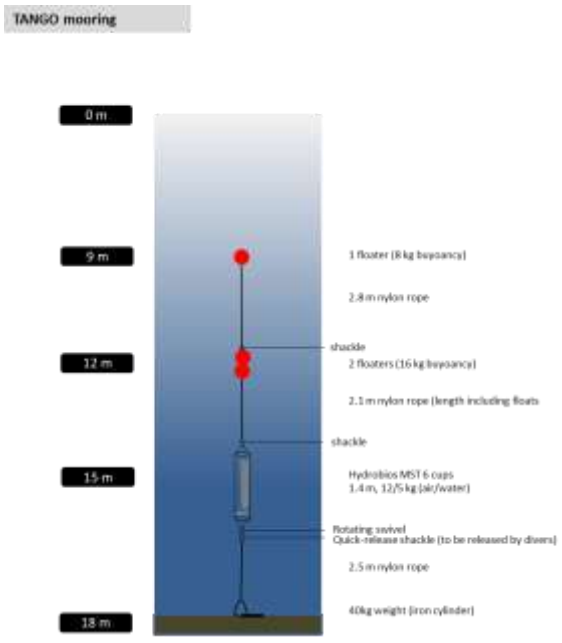

Figure 3: Diagram of the sediment trap.

3.2.5. Biogeochemistry of ice cores

Sea ice sampling was only conducted during TANGO1 at the two stations (i.e. Dodman and Blaiklock Island). Sea ice work was designed to complement the sampling strategy of the water column, providing the same information for sea ice as for the water column to cover carbon fluxes over the benthic-pelagic-sympagic continuum. Hence consistent physical, biological, and biogeochemistry parameters were captured for sea ice, as for the benthic and pelagic compartments, but involving different techniques. For instance, primary production in sea ice will be assessed using O_2:Ar ratio rather than O_2 incubation. In addition, we collected additional cores to investigate the spatial variability of gas concentration at small scale (1 to 10 m).

Two ice floes have been sampled as close as possible to the two main sites. Suitable floes have been chosen according to safety concerns (large and thick enough to deploy several people on the floe), accessibility, and ice thickness of less than 2m (limitation of the gear). At each ice station 12 to 14 ice cores were collected covering the full ice thickness. Details of the core collected, purpose and cutting resolution and treatment are presented in Table 5. Ice cores were collected with an 8 cm-diameter ice corer (Lichtert Industry®, Belgium) coupled to a battery-powered drill. Core was sampled along two lines in a preserved, untouched area at a similar snow thickness. The distance between the two cores was about 50 cm.

All cutting was done on-site just after ice collection with stainless steel ice saw. All personnel were wearing laboratory gloves for ice manipulation. Archives ice cores dedicated to treatment at home laboratories were wrapped in polyethylene plastic bags and stored immediately in a cool box with cool packs at -20°C and transferred within less than one hour in a -20°C freezer. After the ice melted, water was transferred to ad hoc containers and then analysed following the same protocol as seawater for salinity, pigments, CH_4, N_2O, particulate carbon, nitrogen, and sulfur, and their isotopes.

Table 5: Details of cores collected, purpose, cutting resolution and treatment.

Core	Parameter	Resolution	Melting procedure
Physical core	Temperature Bulk salinity Water stable isotopes	10 cm from top; 10 cm in the middle; one piece with adjustable resolution in the middle	Room temperature in the dark
Pigments core	Pigments	Ice 1: 20 cm from top. Bottom 10 cm then 20 cm towards the top Ice 2: 10 cm from top, 10 cm from bottom; one adjustable resolution in the middle	Room temperature in the dark, with addition of FSW
Biogeochemical core	Nutrients	Ice 1: 20 cm from the top. Bottom 10 cm, then 20 cm towards the top Ice 2: 20 cm from the top, 10 cm from bottom.	Room temperature in the dark
	PC, PN, PS, $\delta^{13}C$ of PC, $\delta^{15}N$ of PN, $\delta^{34}S$ of PS	Ice 1: 20 cm from top; 10 cm in the middle; one piece with adjustable resolution in the middle	Room temperature in the dark
Greenhouse gas cores (bags method)	CH_4, N_2O	Ice 2: 10 cm from top; 10 cm in the middle; one piece with adjustable resolution in the middle	Melted in sealed vacuum bags in the dark at room temperature

Fatty acid core (Ice 2 only)	Fatty acid	60-70 cm from bottom	Room temperature in the dark
eDNA core (Ice 2 only)	eDNA	40-60 cm & 86-106 cm	Room temperature in the dark
Archive cores stored at -20°C	/	/	/
Gas cores (full core)	N_2, O_2, Ar, CH_4, N_20, CO2 and Thin sections	5 cm	/

Gases (N_2, O_2, Ar, CH_4, N_2O, CO2)

We used the wet-extraction method to extract gases from sea ice for continental ice (Raynaud et al., 1982). Briefly, 100 g of ice sample was put in a small container, using a 5 cm vertical resolution. The container was placed under vacuum (10-3 mbar) and then heated in a bain-marie at 100°C to melt the ice. It was then slowly refrozen from the bottom, using an ethanol (96 %) bath that was cooled to −30 ◦C and after 1h at -80°C by the addition of liquid N_2. After refreezing, the whole gas content (both dissolved and in the bubbles) was expelled into the headspace of the container. The expelled gas was then injected into a gas chromatograph (Trace GC) equipped with a flame ionization detector (FID), an electron capture detector (ECD), and a thermal conductivity detector (TCD) for CH_4-CO_2, N_2O, and Ar-O_2-N_2 measurements, respectively.

3.2.6. Biogeochemistry of sediments

Approach to sampling

Sediment sampling for biogeochemical analyses was performed in 2 - 4 subsites within each island location, with the goal to generate within-site contrasts in driving factors of sediment biogeochemistry, as well as between-site contrasts related to the longitudinal gradient. Prior to sediment sampling, potential sites with soft sediment were highlighted with the help of bathymetry maps, and were often first scouted during diving work for other work packages.

At each site, scientific divers collected a series of samples from the seafloor. To determine the quantity and distribution of carbon present in the seafloor sediment from different sources (organic matter, inorganic carbon, algal origin,..), divers pushed 3 cores (perspex, Ø 3.6 cm) into the seafloor sediment at each site, aiming for a sediment column of at least 10 cm. To determine the consumption and/or production of oxygen (O_2), nutrients (NHx, NOx, PO_4, Si), greenhouse gases (CH_4, N_2O), and carbon (C) by the benthic community, 3 larger incubation cores (Ø 10 cm Perspex) were pushed into soft sediments, aiming for a sediment height of 15 – 20 cm in the cores. Once in the sediment, the top of the cores was carefully sealed with rubber stoppers, extracted from the seafloor, and then the bottom was sealed as well.

Environmental variables

After retrieval, the cores were sliced as follows into sections: 0.5 cm intervals for the first two centimeters, in 1 cm intervals down to 6 cm, and 2 cm intervals for the remaining sediment, all into aluminium cryo-vials. All samples were immediately stored into a -20 °C freezer.

Grain size distribution was determined on oven dried samples through laser diffraction method in a Malvern Mastersizer 2000 with Hydro 2000S module. Total carbon (TC), total nitrogen (TN) and total organic carbon (TOC; after acidification) were measured on a Flash 2000 NC Sediment Analyzer.

Pigments (Chl a and its degradation products) were extracted with acetone, and analyzed through fluorometry following Wright & Mantoura (1997).

Core incubations

The 10 cm Ø incubation cores were immediately placed in a thermostatic bath controlled by an external chiller (LAUDA thermocirculator), set to the water temperature at the seafloor as determined by the divers (± 0.5 °C). We provided oxygen to the cores through bubbling stones, and the cores were left to acclimatize overnight until further treatment.

Incubation experiments lasted from 8 to 12 hours, depending on the sediment oxygen consumption rates, and consisted of the following steps. First a T0 sample was collected for nutrient analysis, for DIC, for alkalinity (TA), and for greenhouse gases (CH_4, N_2O). Subsequently, the cores were closed with airtight transparent lids, which contained sampling ports and a Teflon stirrer to keep the water column in the cores homogenized. Through an airtight septum, we placed a rigid oxygen probe (Pyroscience Firesting optodes), to measure the oxygen concentration in the water at 30 second intervals. At time intervals of 2 – 3 hours (depending on the oxygen consumption rates), repeat measurements for nutrients and DIC were collected through sampling ports. Incubations lasted until most cores reached an oxygen concentration of around 70 % of the starting concentration, after which all measurements of the T0 sample were repeated. The DIC, TA, and greenhouse gas samples were stabilized with mercury chloride ($HgCl_2$), and the nutrient sample was immediately frozen at –20 °C.

Two types of incubations were performed: dark incubations where the cores were kept in the dark throughout the experiment, and light incubations where the sediment surface was subjected to a light intensity of 400 lumens, representing the light intensity on the seafloor on a partially overcast day (as measured with HOBO loggers (Scaled instruments) on CTD profiles). The first incubation was the dark incubation, after which the overlying water was replaced with filtered seawater, bubbled with oxygen, and left to acclimatize again overnight until the light incubation was performed the following day.

To calculate oxygen consumption rates within the cores, a linear regression line was fitted through the Firesting water column oxygen concentration data. The height of the overlying water column was used to express the oxygen consumption rates in mmol O_2 m^{-2} d^{-1}.

Porewater profiling

After finishing the incubations, we extracted porewater from the sediment column in 1 cm intervals through pre-drilled holes in the cores using rhizon samplers (Rhizosphere research products), attached to 5 mL plastic syringes. The extracted porewater was split into 2 mL for DIC, and 2 – 3 mL for nutrients. The nutrient samples, and DIC vials were stored at -20 °C and room temperature respectively. Finally, the contents of the cores were sieved over a 1 mm mesh to collect the macrofaunal community present in the cores, which was preserved on ethanol.

Upon thawing, nutrient samples of porewater and incubation experiments were analysed in the lab.

Van Veen sampling

At each site, an effort was made to collect three Van Veen samples. The Van Veen grab (0.1 m2) was lowered to the seafloor, and retrieved slowly. The content of the grab were subsequently sieved on a 1 mm sieve to retain the macrofauna. Macrofauna were then stored on ethanol.

3.3. Long-term exposure experiment of keystone species to elevated temperature conditions

While short-term to medium-term experiments have identified the maximum temperature range of various Antarctic invertebrates (Morley et al., 2022, 2024; L. Peck et al., 2008; L. S. Peck et al., 2007), the long-term consequences of exposure to higher temperature conditions are rarely assessed yet given its logistic challenges. The cushion sea star *Odontaster validus* is one of the most abundant benthic species in the Southern Ocean, a generalist with trophic plasticity (e.g. Michel et al. (2019; Voisin et al. (2025)), and thus an ecologically high relevant key stone species. Its reproductive and developmental cycle is well known (McClintock et al., 1988) and temperature appeared to have a positive effect on larval development (Hoegh-Guldberg & Pearse, 1995). The upper lethal temperature limit of adult *Odontaster validus* of 7.5° C in short term experiments (L. Peck et al., 2008; L. S. Peck et al., 2007) suggests that it might be more resistant to global warming than other species, and this has been attributed to its slow metabolism and resistance to extended starvation (Agüera et al., 2015).

In a long-term experiment that started in 2016, adults of this species were collected from the Southern Ocean and exposed to two different temperatures: warming conditions of 3°C and ambient conditions of 0°C. Subsequently, the reproductive and nutrition status of adults was followed. After two years, gametes of these sea stars were obtained; larvae fertilized and reared under temperatures ranging from 0°C to 4°C. Until the end of larval development after 145 days, survival, growth, morphology and development were compared among the different treatments also taking the pre-exposure of adults to ambient or elevated temperatures into account.

3.4. Modelling

Studying the structure and drivers of biological communities in patchy environments is inherently complex, as multiple biotic and abiotic factors interact in nonlinear and indirect ways. Network-based approaches, such as Bayesian Network Inference (BNI), can handle this complexity by quantifying, visualizing, and comparing these interactions, offering insights into community structure that traditional statistical methods often struggle to capture (Hui et al., 2022; Milns et al., 2010; Yu et al., 2004). Bayesian Network Inference (BNI) represents ecosystems as a network, with variables being treated as nodes and dependencies between them as edges. Here, the nodes are taxa (morphotypes or groups) and physical parameters (substrate granulometry, distance to the glacier, slope and maximum depth). These dependencies are found based on frequent colocalizations (or lack thereof).

Bayesian Network Inference (BNI) analysis will be performed on different spatial scales: the regional scale (Northern or Southern WAP), the station scale (Dodman Island, Blaiklock Islands, Melchior Islands, Hovgaard Islands and Føyn Harbor) and the site scale (contrasting sites within each station).

Performing BNI on this data allows for a naïve approach on how the different variables in our benthic habitats are connected to each other, regardless of their nature (taxonomic and/or functional groups, substrate, depth, water characteristics, etc.). Causal relationships between each node will be statistically inferred using Banjo v2.2.0. Then, we can simulate the removal of a taxa or changes in an environmental variable and see how this affects the other nodes in the network.

3.5. Data-management

At the onset of the Project a Data Management Plan was created and shared in dmponline (see below). The data management plan was reviewed annually and if pertinent updated.

During the first year a dedicated Data Management workshop was organised. This included a General Introduction to Open data, Data Management Plans and sample and data collection with each partner giving an overview of the samples and data to be collected. A data flow template was discussed and developed.

The data management plan is available here : https://dmponline.dcc.ac.uk/public_plans, as TANGO - Estimating Tipping points in habitability of ANtarctic benthic ecosystems under GlObal future climate change scenarios, and as a download: https://dmponline.dcc.ac.uk/plans/84809/export.pdf?export%5Bquestion_headings%5D=true

As some of the scientific work is still ongoing not all data are ready to be published, data custodians will work with the team at RBINS to ensure proper publication of all data inline with the DMP

Published datasets include:

Robert H, Danis B (2025). Expedition TANGO 1 & 2 At Sea Top Predator survey. Version 1.4. SCAR - AntOBIS. Samplingevent dataset. https://ipt.biodiversity.aq/resource?r=tango-topp&v=1.4 https://doi.org/10.15468/x53vmd accessed via GBIF.org on 2025-12-05.

Voisin A, Lepoint G, Danis B, Guillaumot C, Kristiansen A, Pasotti F, Saucède T, Gan Y, Michel L N (2025). Stable isotope ratios and elemental contents of C, N and S in benthic organisms sampled during the Belgica 121 campaign in the Gerlache Strait, West Antarctic Peninsula (2019).. Version 2.1. SCAR - AntOBIS. Samplingevent dataset. https://doi.org/10.48361/ptbggs

4. SCIENTIFIC RESULTS AND RECOMMENDATIONS

4.1. WP1 Individual responses of selected key species

RO: What is the respective importance of environmental descriptors such as temperature and food resources on the physiological performance of keystone species?

Contributors: Martin Doignez, Deborah Dupont, Manon Bayat, Loic Michel, Bruno Danis

4.1.1. Introduction

Polar amplification has led to the most rapid warming of the globe at the poles (Alexeev et al., 2005; Barnes & Tarling, 2017; Byrne & Lamare, 2024; Rantanen et al., 2022) and the Western Antarctic Peninsula is among the fastest warming regions on Earth with record temperatures being recorded in February 2022 (Gorodetskaya et al., 2023). Likewise, the Antarctic sea ice regime has been reduced due to a recent regime shift (Abram et al., 2025). In view of this fast global warming, it is absolutely essential to better understand the physiological response of keystone species to higher temperatures including life history traits and microbiome diversity (Buschi et al., 2025; Song et al., 2016), and to document biodiversity of the Southern Ocean under different sea ice conditions.

4.1.2. Molecular identification of key organisms

Morphological identifications in the field are challenging. Furthermore, cryptic diversity has been reported for a wide range of Antarctic invertebrates both from pelagic (e.g. Jossart et al., 2019) and benthic habitats (e.g. Brasier et al., 2016; Havermans et al., 2018) requiring integrative taxonomic approaches using morphological and molecular data for realistic assessments of biodiversity. We successfully verified morphological identifications with DNA barcoding approaches. Our initial aim was to complement reference databases for gut metabarcoding approaches to identify food items of key stone species for WP2. Despite the 10,000s of DNA barcodes that were already generated during initiatives like the Polar Census year and the Census of Antarctic Marine Life (CAML; Dettai et al., 2011; Grant et al., 2011), DNA barcode databases of Antarctic organisms are still far from complete. We generated 110 novel DNA barcodes identifying multiple key species at our sampling locations, mainly for the phyla Echinodermata, Mollusca, Polychaeta, and Crustacea. Our DNA barcoding approach identified at least 10 novel species, and detected several instances of potential cryptic diversity, which can be further explored. DNA barcodes improved taxonomic resolution of 50% of the initial morphological classifications, a similar number as in a DNA barcoding study on Antarctic Demosponges (Vargas et al., 2015). We also corrected and refined another 25% of the initial morphological identifications.

In summary, these novel molecular data increased estimates of species richness by at least one order of magnitude. They also provide important baseline data for future investigations of biogeography, gene flow, and evolution of this wide range of taxa. The most significant contribution for the TANGO project was the complementation of reference databases, which are essential for molecular identifications, for example of food items in gut content analyses but also for environmental and microbial DNA studies of the Antarctic biodiversity. Processing of the eDNA samples of TANGO is still ongoing, but eDNA techniques are already successfully implemented in Antarctic waters (e.g. Nester et al., 2024) and expected to become an important tool for future biodiversity assessments.

4.1.3. Temperature effects on physiological performance of an Antarctic sea star

Adult sea stars were sampled in the Southern Ocean and exposed to natural (0° C) or higher temperatures (3° C) for 2 years. After this period, their larvae were reared under different temperature conditions, and larval life history and morphology followed for another 5 months. This long-term experiment of the cushion sea star *Odontaster validus* (Lamare et al., 2024) revealed that the effects of elevated temperatures differed greatly between developmental stages. Adult sea stars could survive at the elevated temperature and kept similar energy reserves as adults under ambient temperatures. However, they produced smaller eggs and thus had lower reproductive output. Surprisingly, in this study, the largest effect of increased temperatures appeared to be acting across generations on the offspring. Instead of being preadapted to elevated temperatures, larvae originating from adults that were reared under 3°C developed poorly, with significantly reduced sizes, decreased survival and arresting larval development after 50 days (of the 145 days of the larval stage). These results are highly relevant for assessing the effects of global warming on endemic, cold-adapted Antarctic organisms. If *O. validus* and other species suffer lower reproductive success and recruitment, this will have huge effects on the functioning of Antarctic marine ecosystems and food webs.

Up to now, temperature exposure experiments have been successfully conducted on more than dozen Antarctic animal species from various taxonomic groups, and these studies have shown that some species can tolerate high temperatures and survive for up to 300 days (Morley et al., 2024); some species furthermore show escape behavioural responses, (Morley et al., 2022). Given that metazoan and bacterial responses to elevated temperatures are drastically different (M. S. Clark et al., 2019) and that multiple ecological and physiological factors influence thermal response (Morley et al., 2024), the diversity in thermal sensitivity needs urgently to be further studied, also including the temperature effects across generations to improve our ability to predict future responses of Antarctic ecosystems to global change.

4.1.4. Environmental drivers of microbiome diversity

The gut microbiota (in the food pellets) of the key stone sea urchin species *S. neumayeri* showed a high diversity across sampling sites but also core bacterial genera, matching the results of Buschi et al. (2025) in an Antarctic mollusc and Ferchiou et al. (2025) on seabirds. In contrast, Song et al. (2016) and González-Aravena et al. (2024) did not observe core microbiomes in an Antarctic clam and various Antarctic fish species, respectively. In the TANGO experiment, both, the alpha and beta diversity of the gut microbiome of *S. neumayeri* differed significantly among sampling sites ($p < 0.001$). Similar spatial patterns in microbiome diversity were also observed for epibionts on krill (Clarke et al., 2021), Antarctic seabirds and in sponges of the Southern hemisphere (summarized by Ochoa-Sánchez et al. (2023)). Geography was also one of the drivers of variation in the gut microbiome of the plunderfish in the Southern Ocean (Schwob et al., 2024) while Heindler et al. (2018) reported temporal not spatial shifts in microbiome composition between historical and recent fish samples.

4.1.5. Recommendations for society and policy

The poles and polar seas are among the fastest warming regions on our planet. The effects of elevated temperatures on polar marine ecosystems remain unstudied and can be surprising. A long-term study on an Antarctic key stone sea star species (Lamare et al., 2024) resulting from the Belspo projects RECTO and TANGO illustrates that higher temperatures can have dramatic effects across generations. In this experiment, exposure of adults to higher temperatures did not preadapt the population to

global warming; on the contrary, the offspring of these adults showed reduced survival, and growth, and larval development stopped altogether. Such cross-generational effects of raised temperatures could disturb the functioning of Antarctic marine ecosystems to a much larger extent than expected. Furthermore, we observed spatial structuring of gut microbiata in the key stone species *S. neumayeri*; such **local diversity patterns inside Antarctic invertebrates add an additional layer of biodiversity that needs to be considered for conservation of the Southern Ocean, even more so, because microbiota are known to shape the physiological response of their host organisms and might be crucial for coping with the extreme environmental conditions in the Southern Ocean (Buschi et al., 2025) and their predicted changes**.

Given the potentially severe negative cross-generational temperature effects discovered for a sea star species during TANGO, such **research needs to be extended to other Antarctic key stone species and must also unravel the underlying genetic and physiological mechanisms for a better understanding of the response of polar taxa to higher temperatures**. Likewise, the observed spatial variation in gut microbiota in a sea urchin species is different to most other microbiome studies targeting organisms in the Southern Ocean (Buschi et al., 2025; Clarke et al., 2019; Thibodeau et al., 2022), and illustrates the need to also characterize the microbiome for a wide range of endemic Antarctic species. Despite large international efforts such as CAML, DNA barcoding databases still have major gaps for Antarctic taxa. **Integrated molecular and morphological taxonomic identifications are a requirement for all subsequent scientific studies and essential to characterize polar marine biodiversity, especially in view of threats from global warming and invasive species.** The new DNA barcoding data that TANGO generated provide important references for metabarcoding and eDNA studies and can serve as the foundation for future studies on phylogeography and evolution of these taxa.

4.2. WP2 Species interaction dynamics

4.2.1. Introduction

In this work package, we aimed to identify and quantify interactions among key taxa along a latitudinal gradient to understand how habitats and local constraints influence species interactions for food resources across the studied natural gradient at five locations sampled during the two TANGO cruises along the WAP. Species diversity results have led us to compare two habitats—hard substrates colonised by macroalgae and soft sediments. Firstly (RO1), we have assessed general food web properties and tried to delineate potential food sources at the basis of the food web. General food web properties, as well as species interactions such as competition for resources, can be intensified by factors such as rising temperatures, shifts in food regimes, changes in community composition, and the arrival of invasive species. Our second goal (RO2) is to determine whether key taxa in the WAP exhibit trophic flexibility that enables them to cope with environmental changes. Coastal ecosystems of WAP are characterised by the complexity of potential food sources at the basis of the food web, including the contribution of sea ice algae (Figure 4).

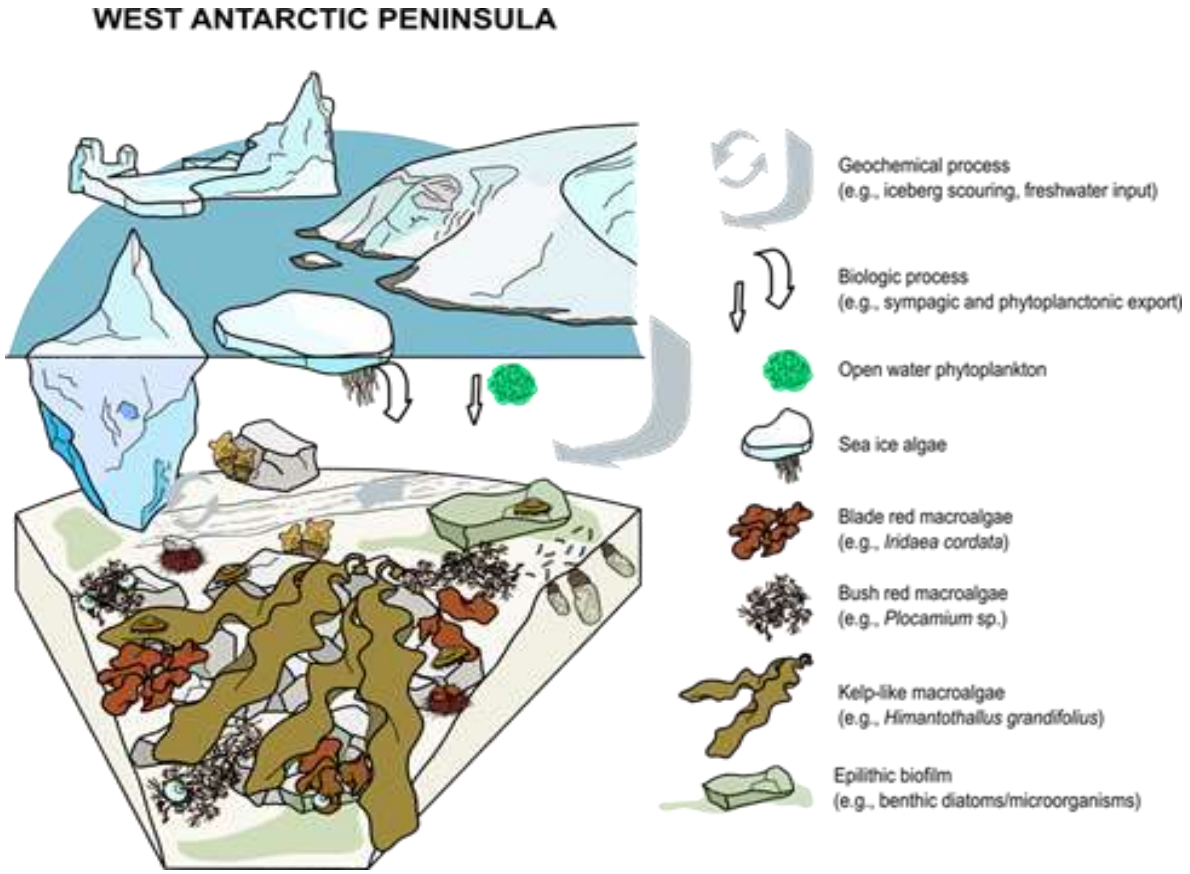

Figure 4: Schematic representation of the environmental characteristics of coastal benthic habitats along the West Antarctic Peninsula. © Anthony Voisin

Here, we present observations based on stable isotope and fatty acid analyses. Stable isotopes were used to characterise the trophic web at both habitat level (hard substrate vs soft sediment) and location level, applying established isotopic niche metrics (see Materials and Methods) to describe food web properties at multiple scales—from species to communities. Fatty acid profiles and HBI contents were primarily used to assess the relative importance of different basal food sources for dominant grazers and suspension feeders across the two habitats and five locations. These results form part of the PhD theses of Martin Dogniez (SI, metabarcoding of gut content), Anthony Voisin (FA, HBI) and Manon Bayat (SI, Metabarcoding of *S. neumayeri* gut content). Both approaches were applied to the same individuals, enabling subsequent integration of the two datasets to model contributions of food sources to individual diets. For this purpose, metabarcoding data will also be incorporated as priors in a Bayesian mixing model.

4.2.2. Latitudinal changes in environmental conditions

A hierarchical clustering analysis using Ward's method grouped the sites into two environmental clusters: Blaiklock Island and Føyn Harbor, with higher sea ice cover and SPM concentrations, in contrast to Dodman, Hovgaard, and Melchior Island (Figure 5) showing that sites differ not only according to latitude but also at smaller scale, notably by their sea ice cover before and during the cruise.

Variables	Blaiklock Island	Foyn Harbour	Dodman Island	Hovgaard Island	Melchior Islands
Chla (mg/m^3)	0.22 ±0.16	0.20 ±0.05	0.25 ±0.14	0.31 ±0.16	0.34 ±0.24
SPM (g/m^3)	3.28 ±2.40	3.53 ±1.57	0.62 ±0.16	1.41 ±0.58	1.53 ±1.04
Sea ice (%)	78.00 ±37.90	38.20 ±44.80	0	42.40 ±31.80	16.00 ±17.20
Cluster	1	1	2	2	2

Figure 5: Environmental variables (mean ± standard deviation) used to cluster research sites along the WAP with the corresponding dendrogram. Chlorophyll a (Chl a) concentration in mg m^{-3}, Suspended particulate matter (SPM) in g m^{-3} and Sea ice cover in percentage of site area (%).

4.2.3. Benthic morphospecies diversity (morphological approach)

Our sampling design of the two TANGO expeditions aimed at characterizing benthic communities with contrasting effects of sea ice and SPM. Based on morphological identifications, for which most taxa could be classified to the species level, we found that substrate type (hard or soft bottom) was an important driver of the specific composition of benthic communities and therefore have decided to study separately these two habitats in addition to inter-site comparison. While about 50% of entire invertebrate communities were shared between the two types of benthic habitats, we observed 28% of unique taxa in hard substrates and 21% in soft bottoms, respectively (Figure 6, left). Hard substrates were dominated by macroalgae forests. Our results are supported by other studies, which found relatively high diversity on hard bottoms in the South Shetland Islands (Ferrero et al., 2026)(Ferrero et al. 2026) and higher diversity on hard than soft bottoms close to Rothera (Vause et al., 2019).

We also found that 19.6% of all taxa were shared among our 5 sampling locations (Figure 6, right), but also that each location displays unique biodiversity. Blaiklock Island had a high number of unique benthic taxa. These patterns suggest differences in benthic biodiversity at small scales as also reported by Angulo-Preckler et al. (2023) for the West Antarctic Peninsula. Such variability in specific diversity can have important effects on food web structure.

Our results on diversity based on morphological analyses advance our knowledge on how substrate type drives benthic Antarctic biodiversity and were conducted by direct sampling as recommended by Angulo-Preckler et al. (2023). Our novel data furthermore confirm differences in biodiversity at small spatial scales including hard substrates with high heterogeneity by Angulo-Preckler et al. (2023), which are important to consider in overall biodiversity assessments.

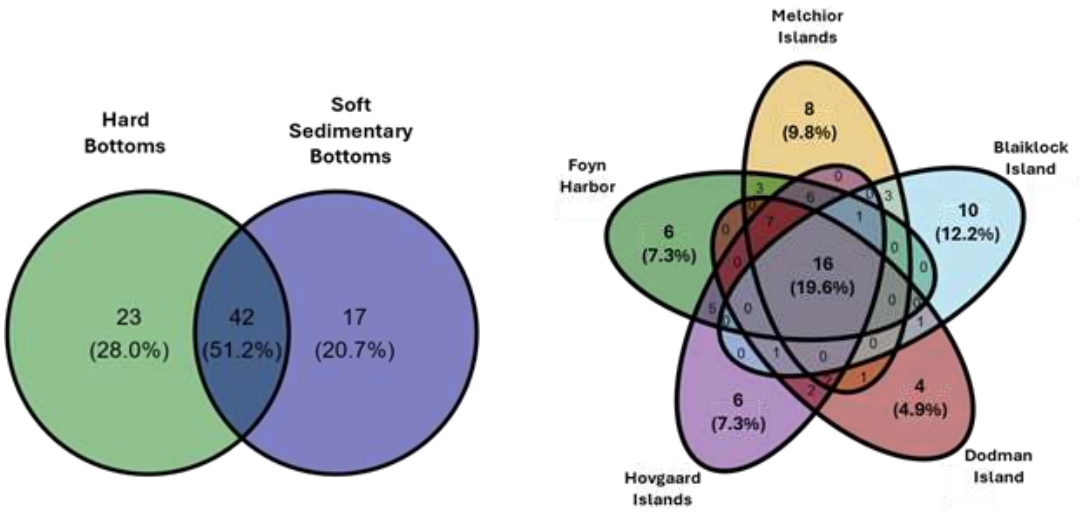

Figure 6: Venn diagrams comparing morphospecies diversity between hard and soft substrate habitats (left) and between sampled locations along the West Antarctic Peninsula during TANGO 1 and TANGO 2 cruises.

4.2.4. Individual diets trough gut content DNA metabarcoding

A preliminary gut content DNA metabarcoding analysis was performed on six Antarctic mega-invertebrate species collected during the TANGO1 campaign. After processing with DADA2 and VSEARCH, each individual yielded 40,006–71,047 sequencing reads (mean 50,552 ± 10,916), with most sequences (69.4–99.4%) assigned to the host. Non-host amplicon sequence variants (ASVs) abundances were highly variable, ranging from six in *Diplasterias* sp. to 54 in *Cnemidocarpa verrucosa*, and occasionally included a large proportion of unassigned sequences. The number of reads assigned to potential food sources varied widely, from 150 in *Sterechinus neumayeri* to 17,385 in *Odontaster validus*, corresponding to 2–30 ASVs after filtering. Additional data (for more than 150 individuals) have been obtained but bioinformatic analysis is still in process.

Gut content diversity revealed recurrent detection of Hexanauplia ASVs, likely indicating contamination, followed by the frequent presence of Bacillariophyceae (diatoms) in several host species, including *Navicula glacie*i and *Nitzschia cf. promare,* and being consistent with diatoms' ecological role in Antarctic food webs (Ha et al., 2019). In contrast, the sea cucumber *Heterocucumis steineni* did not contain any diatom DNA but was dominated by macroalgal sequences (Phaeophyceae and Florideophyceae), suggesting ingestion of resuspended detrital macroalgae, in accordance with the result from the fatty acid approach. Similar macroalgal taxa appeared in the sea star *C. verrucosa,* even in soft bottom substrates highlighting potential trophic links to macroalgal forests through the detrital food web (i.e. brown food web).

Future analyses could explore habitat-related patterns and latitudinal trends in macroalgal occurrence

4.2.5. Characterisation of food web properties at habitat scale using stable isotopes approach

The metacommunities created to compare the fundamental characteristics of trophic networks in hard bottom vs. soft sedimentary bottom do not occupy the C:N or C:S isotopic spaces in the same way (Figure 7).

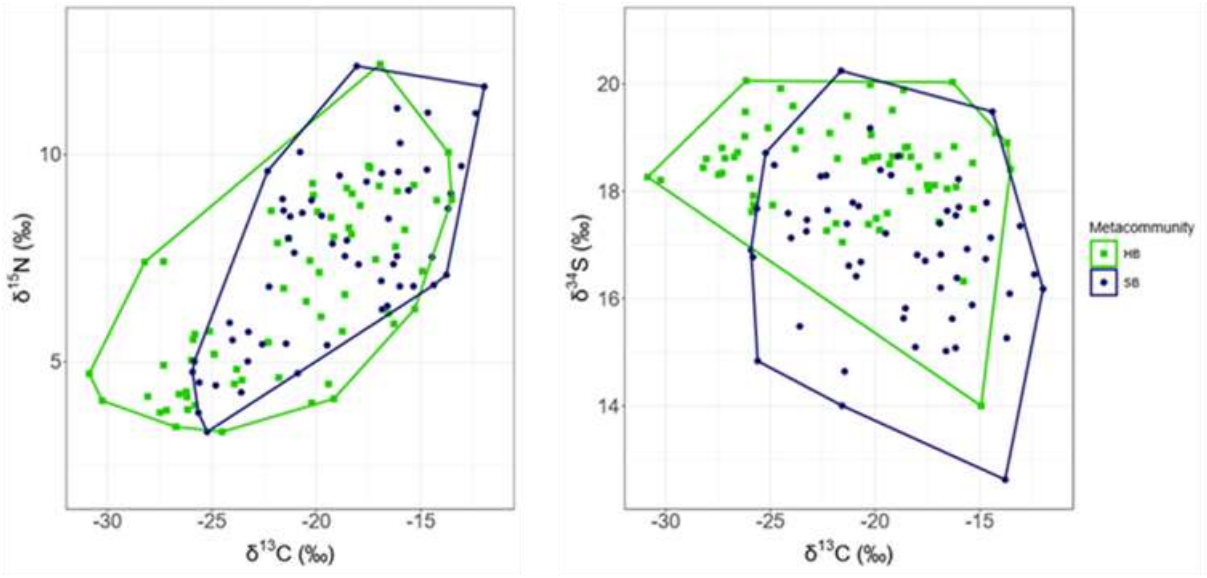

Figure 7: Stable isotopes Convex Hull of Hard Bottom (HB) and Soft Bottom habitats (SB) sampled along the West Antarctic Peninsula (2023 & 2024) either in the C:N (left) or C:S (right) isotopic space. Full communities are presented here and each point representing the mean stable isotopes ratios of one morphotaxon.

They also differ with respect to several Layman metrics (Figure 8): the convex-hull area and the carbon range are significantly larger in rocky substrate habitats than in soft sediment habitats. These two metrics indicate that the diversity of carbon sources used in rocky habitats is greater than in soft sediment habitats, with the probable use of carbon derived from macroalgae in rocky habitats.

Conversely, the ranges of sulphur values are higher in soft sediment substrate habitats than in hard substrate habitats (Figure 9). This indicates that in sedimentary habitats, there is a coupling with processes occurring in the sediment linked to the decomposition of organic matter and the assimilation by benthic producers (i.e. microphytobenthos) of sulphur species showing lower isotopic values than those generally found in the water column or sea ice. This would suggest a less pronounced coupling with the sediment in rocky habitats.

There is no significant difference in the nitrogen range nor in the positioning of the two habitats in the C:N isospace along the nitrogen axis. This could indicate trophic chain lengths with a similar number of trophic positions in both habitat types and/or similar nitrogen sources. Indeed, nitrogen isotopic ratios are often used to characterise the vertical dimension of a trophic network (i.e. the trophic position of organisms).

Finally, the distances to the centroids of the different morphotypes are significantly higher in hard substrate habitats than in soft sediment substrates. This would indicate greater trophic, and therefore functional, diversity in rocky substrate habitats than in soft sediment habitats. This coincides quite well with the morpho-specific diversity recorded during this project. This diversification is made possible by a greater diversity of primary sources at the base of trophic networks in rocky substrate.

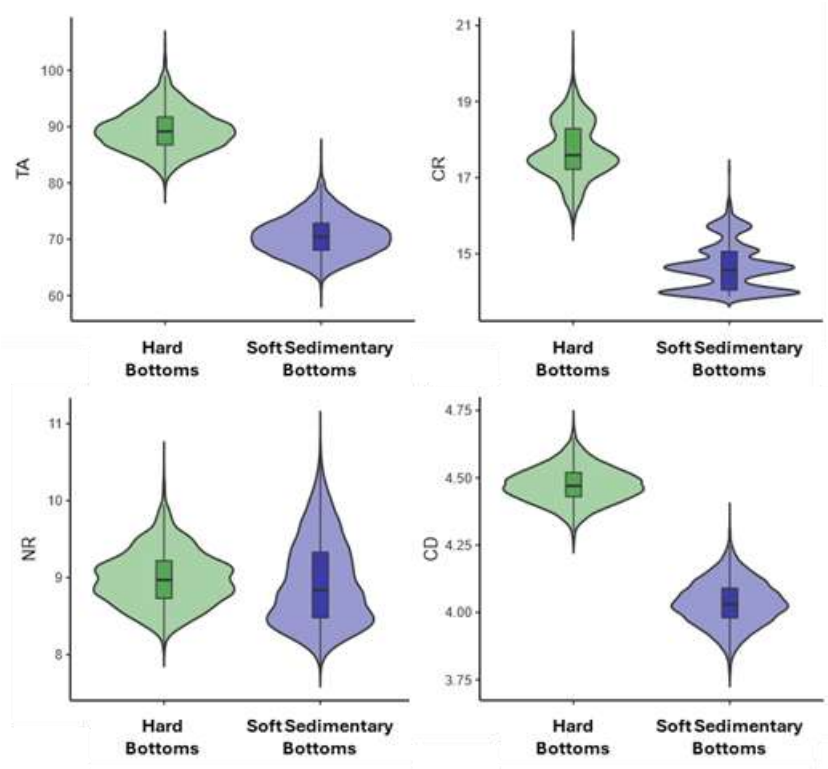

Figure 8: Bootstrapped distribution of Layman Metrics (C:N dimension) for full Metacommunities of invertebrates in Hard Bottom and Soft Bottom habitats sampled along the West Antarctic Peninsula (2023 & 2024). TA: Total Area of convex hull; CR: Carbon isotopic ratio Range; NR: Nitrogen isotopic ratio Range; CD: Distance to convex-hull Centroid.

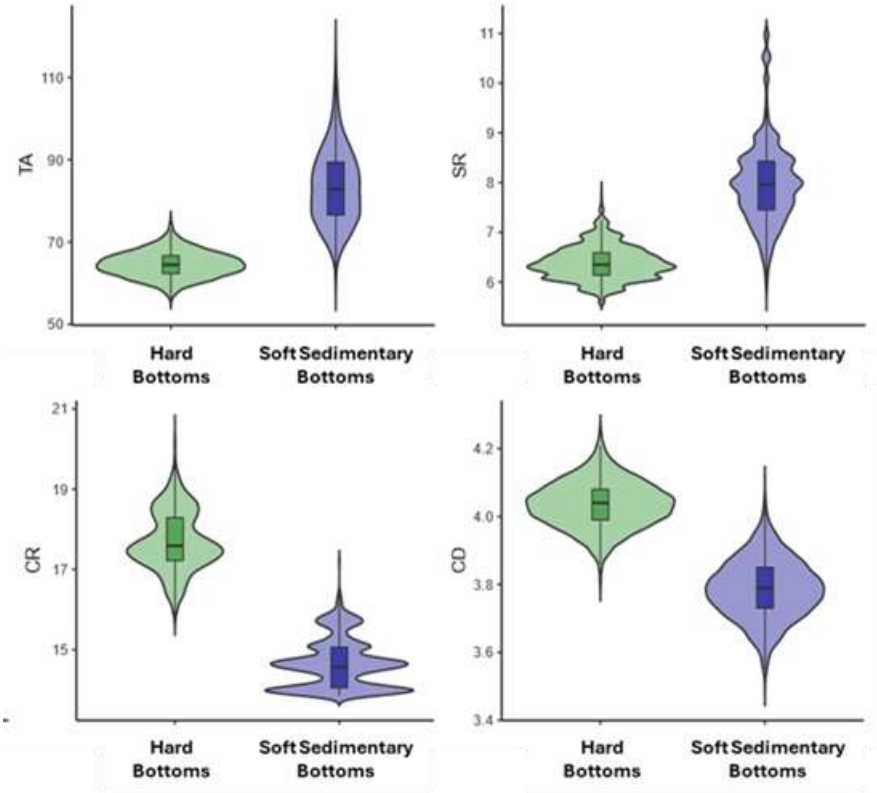

Figure 9: Bootstrapped distribution of Layman Metrics (C:S dimension) for Full Metacommunities of invertebrates in Hard Bottom and Soft Bottom habitats sampled along the West Antarctic Peninsula (2023 & 2024). TA: Total Area of convex hull; CR: Carbon isotopic ratio Range; SR: Sulphur isotopic ratio Range; CD: Distance to convex-hull Centroid.

4.2.6. Food web properties and variability according to latitudinal gradient

The metacommunities created to compare the fundamental characteristics of trophic networks in the five investigated locations along the latitudinal gradient do not occupy the C:N or C:S isotopic spaces in the same way (Figure 10). Nevertheless, except for Blaiklock Island, differences in isotopic space, but also for calculated metrics (Figure 11), between locations were lower or in the same range than differences between habitats of a same location, indicating the importance of habitat diversity at small scale compared to large scale variability.

Blaiklock Island shows the lowest Total convex hull area, but also the lowest isotopic range for carbon (CR), indicating a lower trophic diversity and a lower number of carbon sources used by organisms. This could be related to the lower diversity in sampled habitat, notably the absence of "true" macroalgae forest sites.

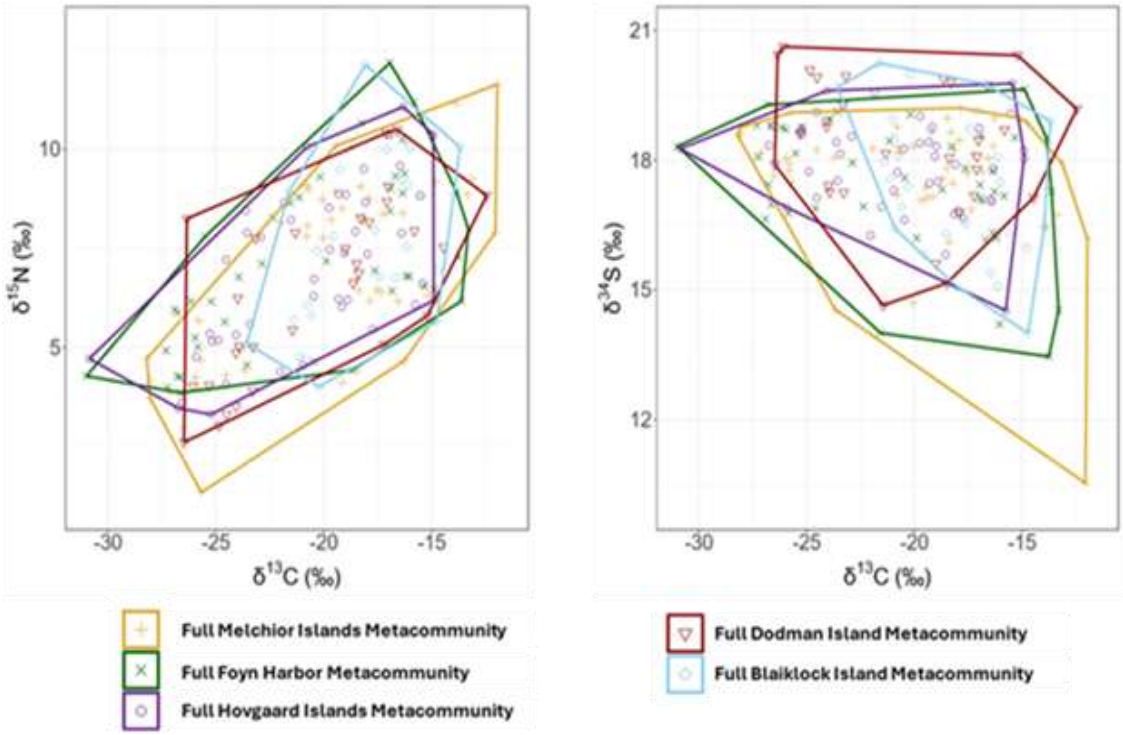

Figure 10: Stable isotopes Convex Hulls of Melchior Island, Føyn Harbor, Dodman Island & Blaiklock Island Full Metacommunities along the West Antarctic Peninsula, either in the C:N (left) and C:S (right) isotopic space, each point representing the mean stable isotopes ratios of one morphotaxon in one location of interest.

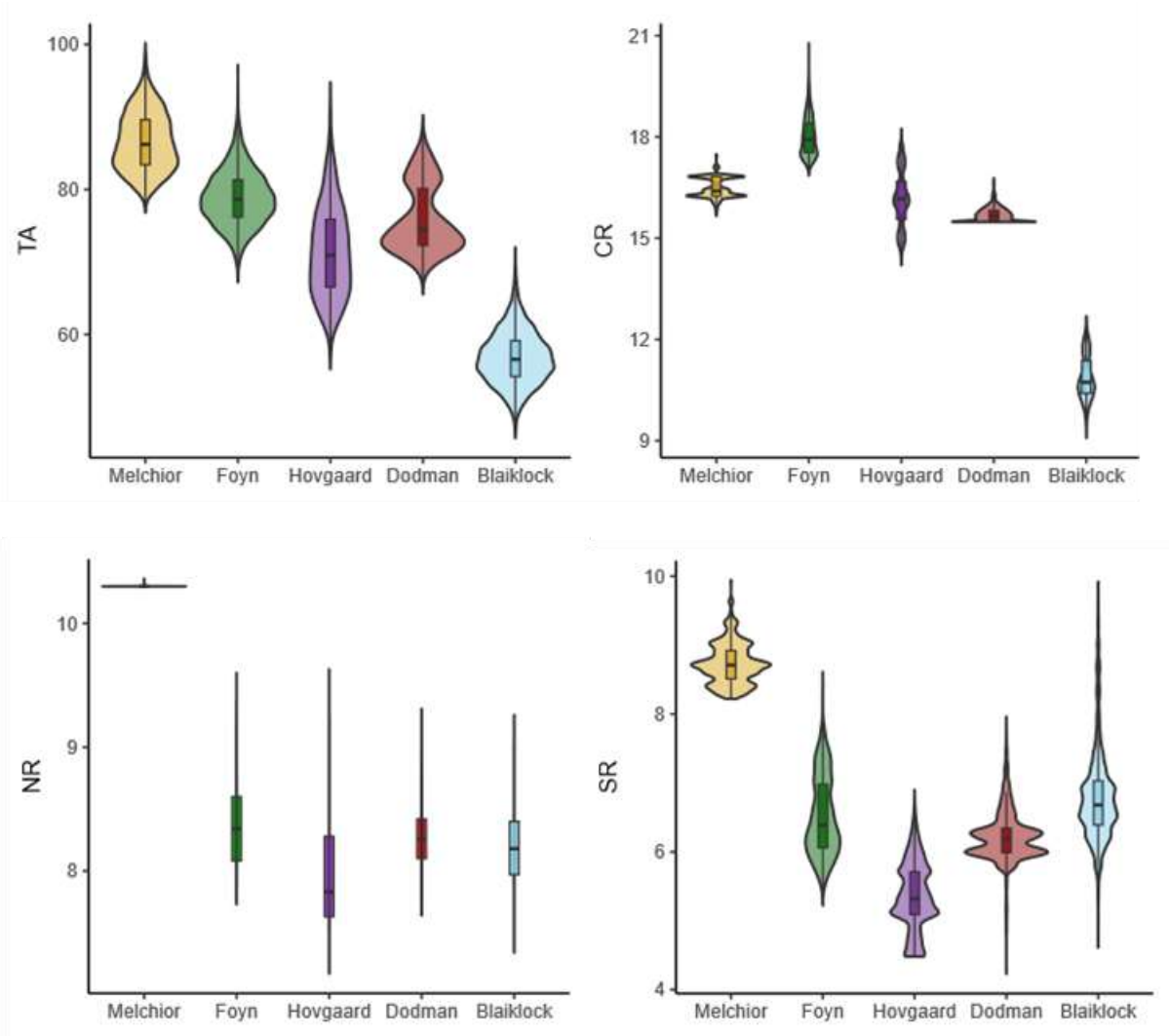

Figure 11: Bootstrapped distribution of Layman Metrics (C:N and C:S dimension) for full Metacommunities of invertebrates in five locations sampled along the West Antarctic Peninsula (2023 & 2024). TA: Total Area of convex hull; CR: Carbon isotopic ratio Range; NR: Nitrogen isotopic ratio Range; SR: Sulphur isotopic ratio range.

On the contrary, the Melchior Island site showed a convex hull area significantly larger than the other sites. This corresponds to a greater diversity of habitat and morphospecies. The range of isotopic values for sulphur would also indicate, for this site, a more intense coupling with the sedimentary compartment, while that of nitrogen would suggest either a greater number of trophic levels or, more likely, a greater diversity of nitrogen sources than in the other sites. This diversity of nitrogen sources could possibly be linked to different levels of organic matter degradation. Conversely, the greater trophic diversity observed does not seem to be related to a diversification of carbon sources, as shown by a range of carbon isotopic values equivalent to the other stations, with the exception of Blaiklock Island. All this highlights the importance of local habitat diversity in understanding the trophic functioning of the benthic compartment at the scale of a site.

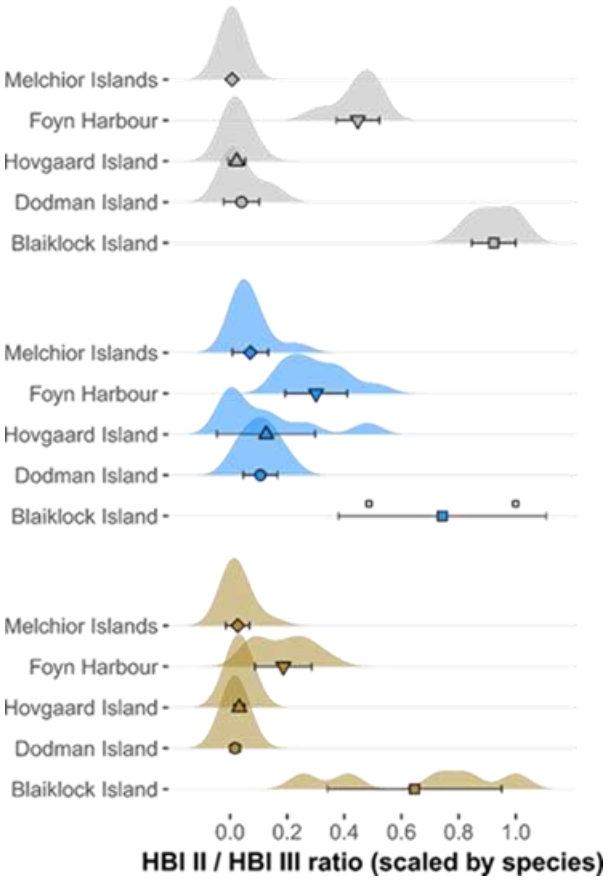

Figure 12: Density plot of the ratio between two forms of HBI II (Diene) and HBI III (Triene), scaled by type of sample between 0 and 1, in (a.) sediments, (b.) M. antarcica and (c.) N. concinna, collected along the WAP. The mean and standard deviation were computed for each sample in each site. Lack of density plot is related to an insufficient number of replicates, represented by the scattering of empty points.

One aspect of the local diversity of sources is determined by the presence or absence of sea ice at the location before and during the cruise, and therefore, the presence or absence for the benthic compartment of microalgae sedimented during the sea ice break-up. The two locations characterised by a greater ice cover show higher HBI II/HBI III ratios in the organic matter of the sediment, probably indicating the presence of sympagic algae sedimented on the surface of the substrate (Figure 12). The use of HBI also highlighted variability in the diet of animals. For example, in locations with greater ice cover and higher HBI ratios in the sediment, two grazing molluscs also showed higher HBI ratios, indicating consumption of algae sedimented from sea ice to the benthic compartment. This trend was also observed in Terebellidae (Annelid, Polychaetes), a deposit feeder family (data not shown). Here the contrast between locations is much more marked, and the southernmost station, namely Blaiklock Island, shows the highest HBI ratios in relation to greater ice cover and longer ice duration. The disappearance of ice cover in the northernmost stations has clear implications for these two mollusc species. Indeed, in the absence of sea ice, the two species modify their diets and consume other sources of carbon (macroalgae and/or microphytobenthos depending on the species).

4.2.7. Do key taxa in the WAP exhibit trophic flexibility that enables them to cope with environmental changes?

Evidences from fatty acid approach

The ability of organisms to adapt to environmental changes lies partly in their capacity to modify their diet according to environmental conditions, particularly food availability. This project allowed us to compare the variability of fatty acid profiles and, therefore, the diet of dominant benthic species along the WAP (Figure 13). The data showed that the studied species occupy distinct trophic niches, but these change subtly between different locations, demonstrating a certain dietary flexibility according to environmental conditions. Indeed, although fatty acid profiles do not change drastically, some proportions shift slightly. This supports the information provided by HBIs, showing that in stations where sea ice and sympagic algae are present, some organisms incorporate algal material released during ice melt. The fatty acid profiles demonstrate the assimilation of planktonic and benthic microalgae as well as macroalgae, either through direct ingestion (grazing) or in detrital form, even in soft sediment habitats, once again demonstrating the connection between different habitats and the importance of understanding habitat diversity to comprehend ecosystem functioning at the site scale.

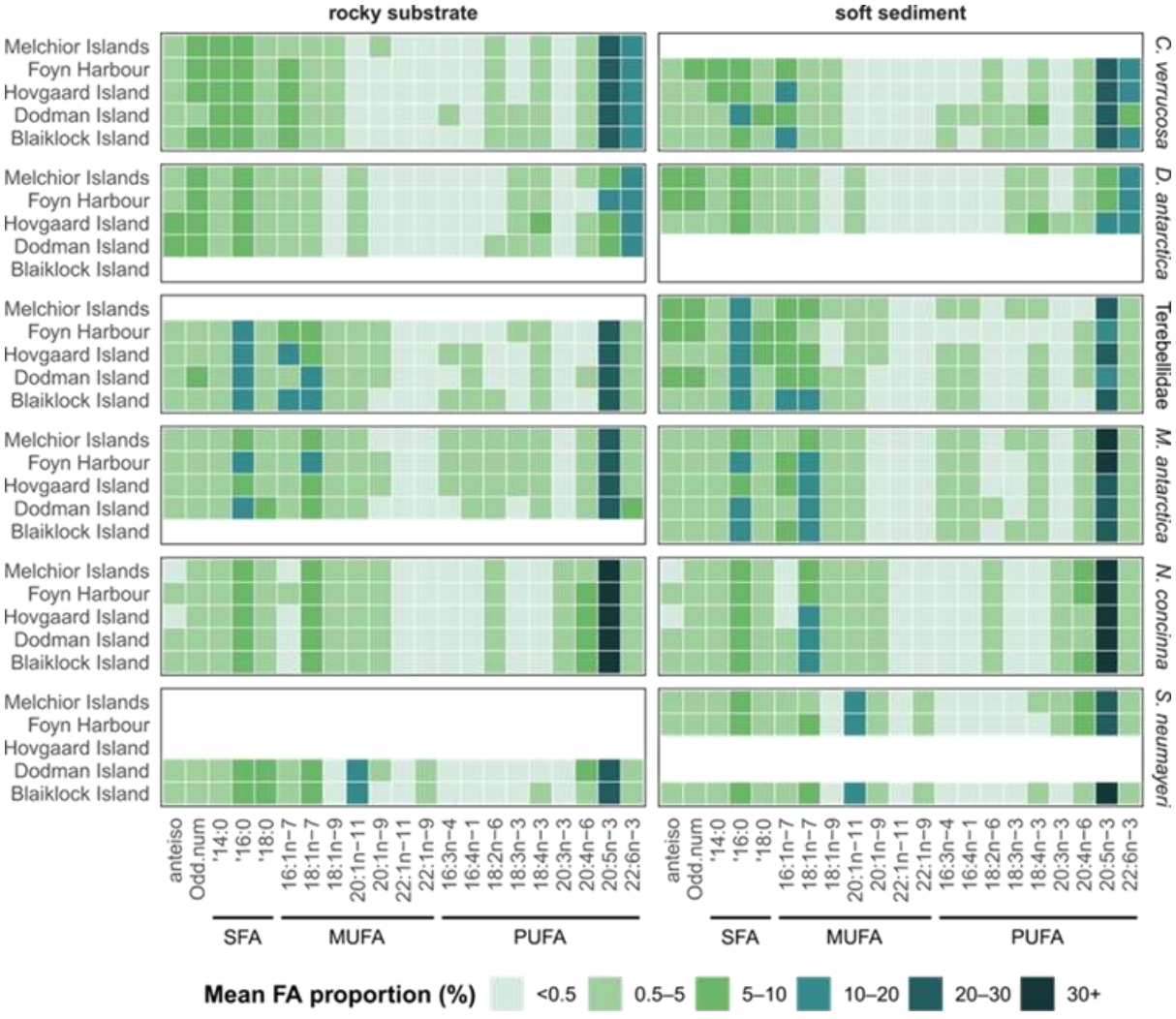

Figure 13: Heatmap of selected FA mean proportion (%) in sampled benthic consumers of the site and habitat studied along the WAP (see supplementary material for mean and standard deviation values).

Evidences from stable isotope approach

The isotopic approach also made it possible to study the variability of the trophic position of dominant organisms within each location (Figure 14). Here too, the results show that subtle changes in trophic position can occur between different locations for organisms occupying distinct trophic niches in the ecosystem. This is particularly true for organisms at the lowest trophic positions (herbivores, suspension feeders, deposit feeders) but also for opportunistic predators such as nemerteans and the sea star *Odontaster validus*.

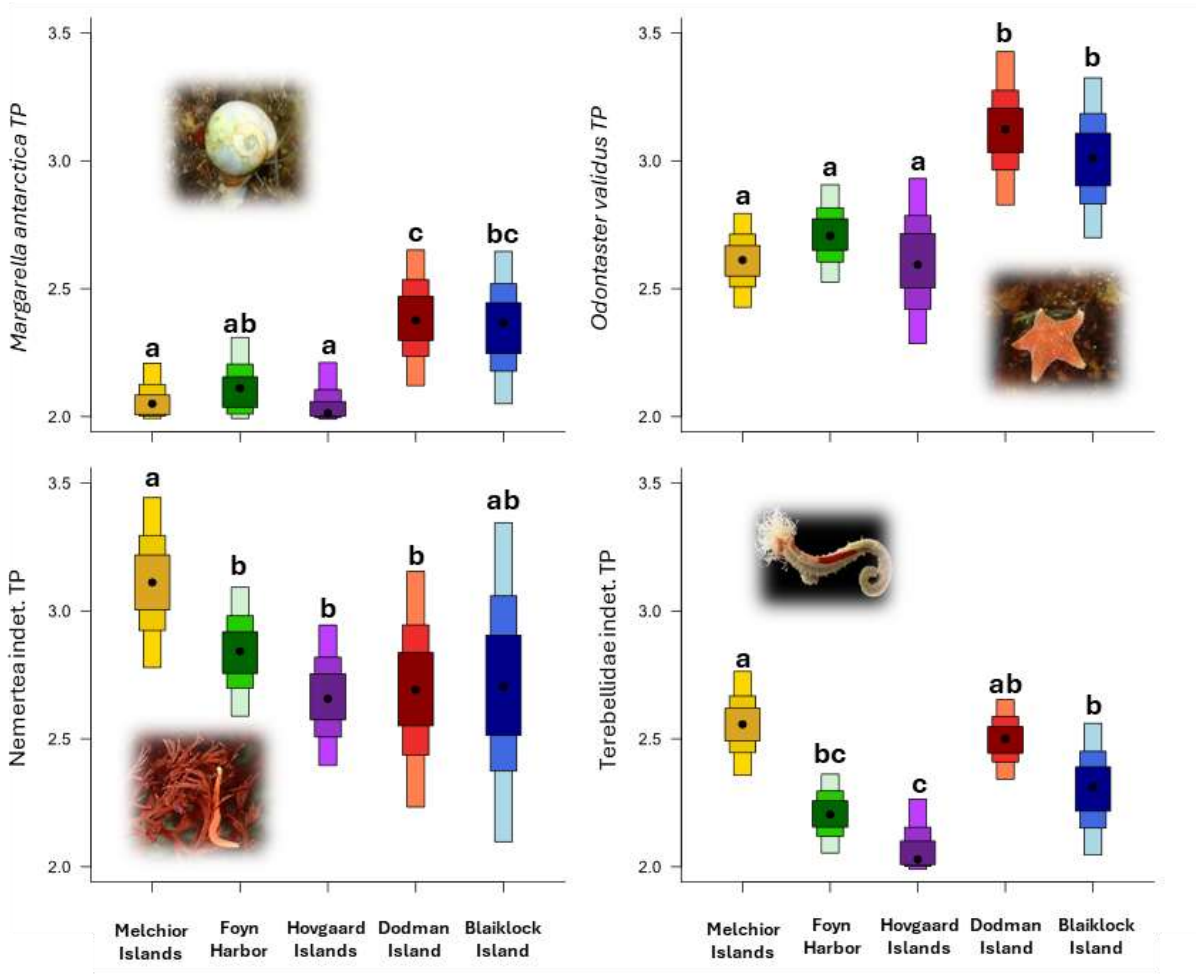

Figure 14: Estimated Trophic Position (Bayesian model, Mollusc Nacella concinna as baseline) of invertebrate with at least five individuals sampled in all TANGO locations, lowercase letters indicate post-hoc groups after pairwise comparison of the Bayesian TP distributions (significance threshold fixed at 90%).

The case of Sterechinus neumayeri: stable isotopes and gut meta barcoding

These results are confirmed by the focused study on the urchins *Sterechinus neumayeri.* Metabarcoding of gut content revealed that *S. neumayeri* consumes a broad prey spectrum dominated by diatoms, with site-specific variations in the proportions of macroalgae and invertebrates. Shannon diversity varied significantly among sites (1.6 – 3.7), with some sites displaying high within-site variability while others were more homogeneous. Although PcoA (Figure 15) showed considerable overlap in diet composition across sites, shifts in dominant prey groups produced a significant site effect.

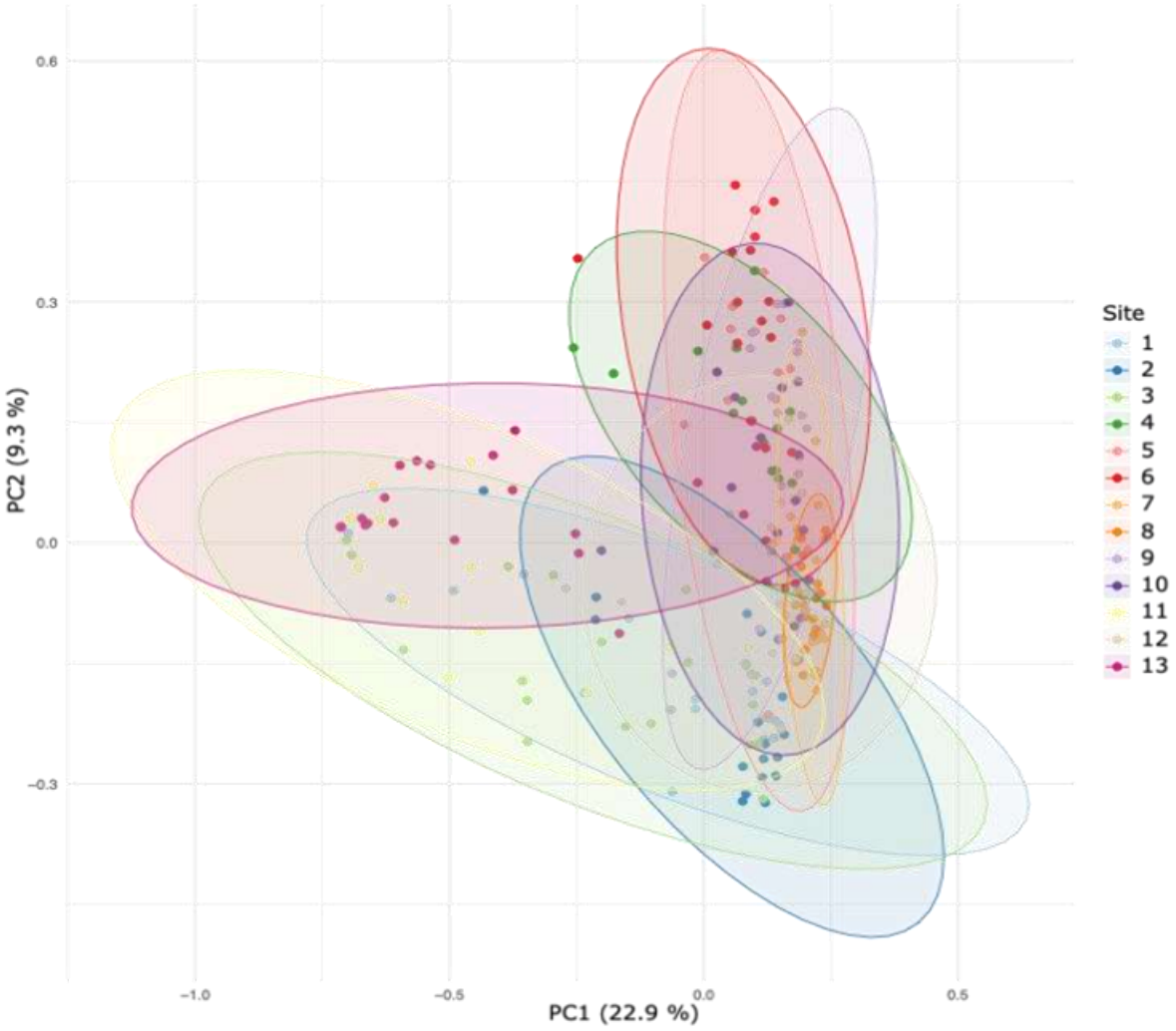

Figure 15: Principal Coordinate Analysis (PCoA) based on Bray-Curtis dissimilarity matrix of dietary composition in Sterechinus neumayeri individuals across sites. Each point represents an individual, and ellipses denote the 95% confidence interval for site-level grouping

Using the stable isotope approach, the three-dimensional $\delta^{13}C$–$\delta^{15}N$–$\delta^{34}S$ ellipsoids (Figure 16) revealed also substantial spatial variation confirming strong spatial structuring of isotopic composition.

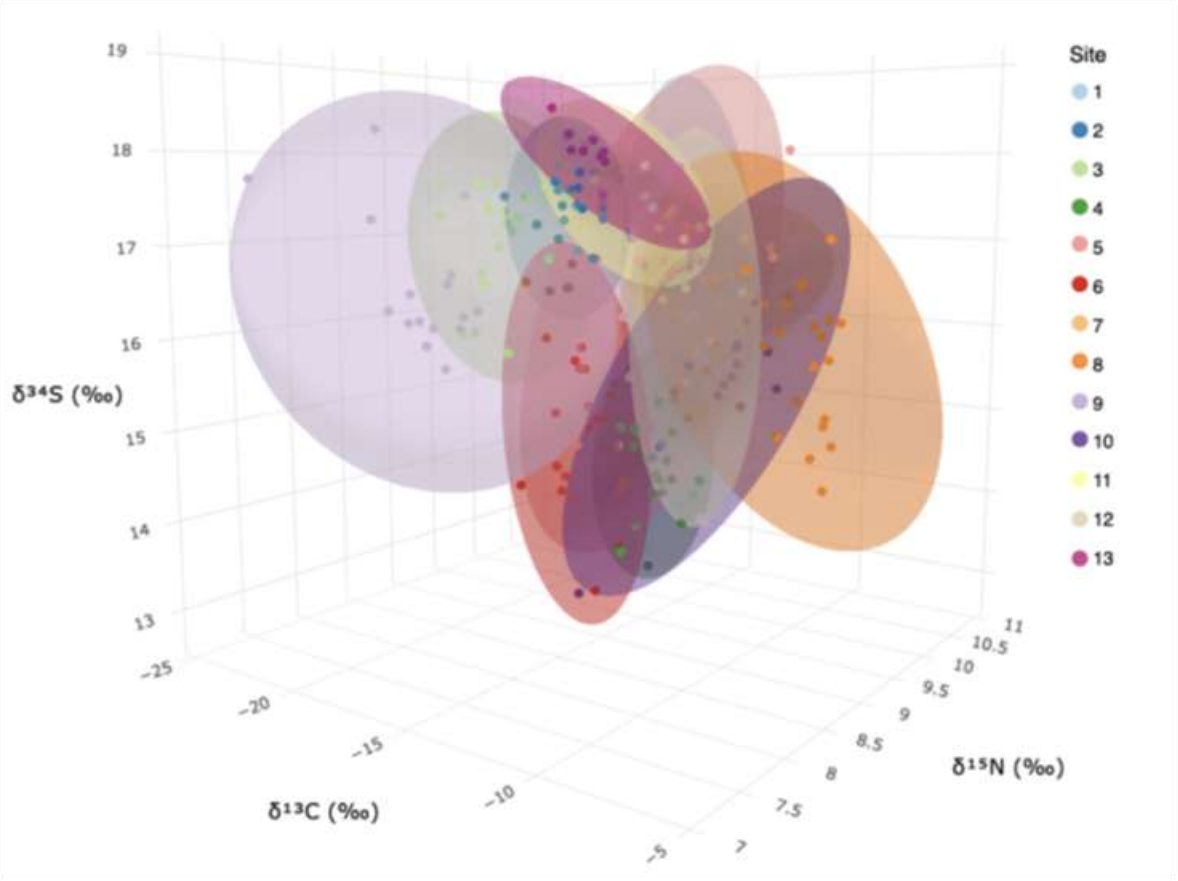

Figure 16: Three-dimensional isotopic niche space of Sterechinus neumayeri individuals across thirteen sampling sites, based on $\delta^{13}C$, $\delta^{15}N$, and $\delta^{34}S$ values. Each point represents an individual, and ellipsoids depict the 95% Bayesian isotopic niche for each site.

All these results evidence that these organisms, to some extent, can adapt to environmental conditions in terms of trophic resources. However, to what extent they can do so remains questionable in the context of the drastic changes currently occurring along the WAP.

4.2.8. Linear inverse modelling of food webs

Figure 17 and Figure 18 show how carbon pathways in the Potter Cove food web reorganize under varying degrees of glacial melt. The microphytobenthos (MPB) pathway (Figure 17 A) is consistently suppressed at the glacier-proximal site Isla D, particularly during periods of high meltwater discharge such as summer 2015 and spring 2016. During these seasons, gross MPB production contributed only 14–35% of total carbon input, compared to 41–59% in the clearer waters of spring 2015. The reduced MPB pathway aligns with the strong physical disturbance regime at Isla D: high turbidity limits light availability, and rapid sedimentation buries diatoms, inhibiting their ability to maintain position in the photic layer. Even under favourable conditions in spring 2015, Isla D retained the lowest MPB pathway intensity, confirming that chronic disturbance constrains benthic primary production regardless of seasonal variation.

The microbial loop (Figure 17 C) shows a similarly clear sensitivity to meltwater inputs. During high disturbance seasons, bacterial recycling of DOC is significantly reduced, resulting in a weaker microbial

loop at Isla D. Only in spring 2015, when melt was anomalously low, was microbial recycling in glacier-proximal sediments nearly as strong as at Faro. This was supported by higher detritus dissolution and elevated DOC uptake by bacteria during that season. These modelled patterns reinforce experimental findings indicating that frequent resuspension events depress bacterial biomass and carbon cycling efficiency.

In contrast, the macroalgal pathway (Figure 17 B) shows little response to meltwater gradients. Macroalgal fragments typically contribute 19–40% of carbon input, and grazing remains the dominant fate of these fragments at all stations. However, despite substantial inputs, macroalgal carbon contributes only 2–5% to consumer ingestion flows. This indicates that macroalgal detritus does not compensate for reduced benthic primary production in soft sediments, even though macroalgal abundance is increasing across newly ice-free habitats.

These pathway alterations propagate to consumers (Figure 18). Secondary production patterns reflect the uneven reorganization of carbon flows: *Aequiyoldia eightsii* and other macrofauna show significantly lower production near the glacier, consistent with reduced food quality and frequent disturbance. In summer 2015, for instance, *A. eightsii* production at Isla D was markedly lower than at Faro and Creek. Conversely, *Laternula elliptica* and meiofauna exhibit significantly higher production at Isla D, especially during spring 2016 when total secondary production near the glacier surpassed that at Faro. This suggests that taxa with flexible feeding strategies, small body size, or adaptations to burial and resuspension can capitalize on altered resource landscapes, whereas more disturbance-sensitive infauna decline.

Together, Figure 17 and Figure 18 illustrate that glacial melt does not merely reduce overall carbon availability; it shifts which pathways dominate and which consumers benefit. The system becomes less reliant on autotrophic benthic production and internal recycling, and more dependent on detrital inputs and opportunistic taxa, signalling a functional reorganization of the benthic food web under intensified melt. As glacial retreat along the Antarctic Peninsula accelerates, such shifts are likely to intensify, reshaping benthic community structure, reducing carbon transfer efficiency, and altering energy pathways in shallow Antarctic fjords.

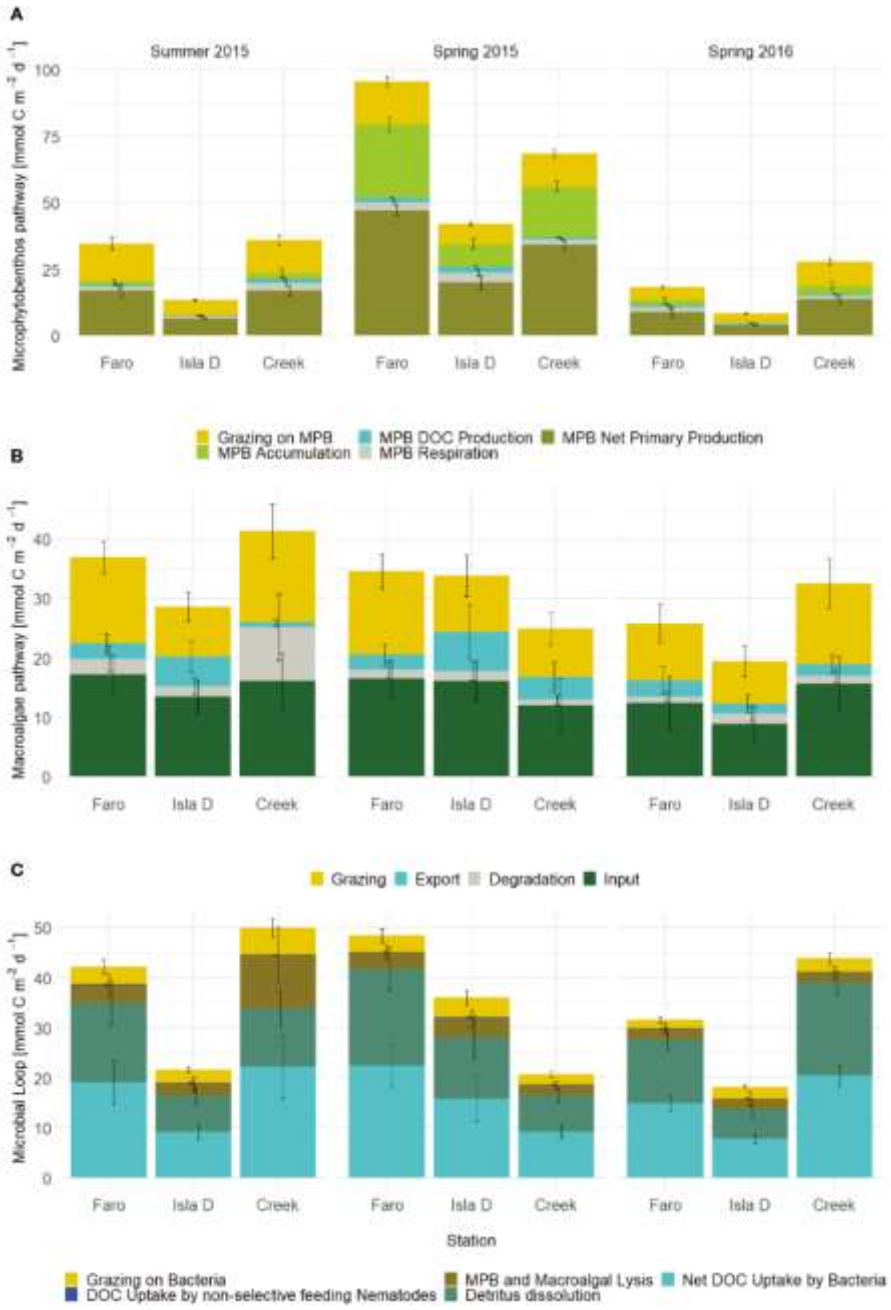

Figure 17: Adopted from Braeckman et al., 2025. Contributions to three pathways at the three locations and three seasons with different glacial melt impacts: (A) Microphytobenthos (MPB) pathway, (B) Macroalgae pathway and (C) Microbial loop. Means and standard deviations of 1000 simulations

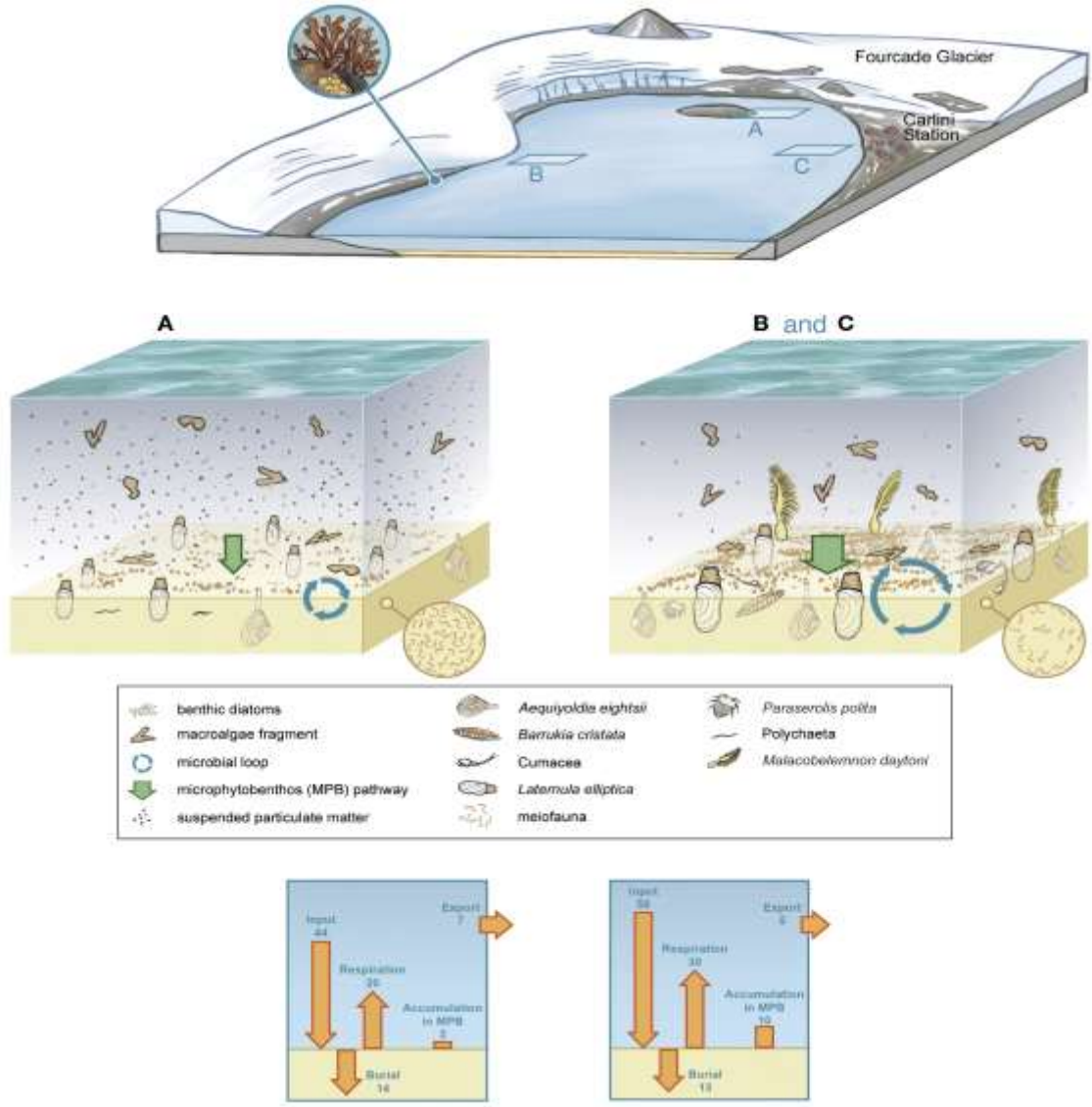

Figure 18: Adopted from Braeckman et al., 2025. Summary of alterations to carbon flows in the benthic food web as a result of glacial melt disturbance. Location A: Isla D; Location B and C: Faro and Creek, respectively. Carbon flows in mmol C m^{-2} d^{-1}.

4.2.8. Synthesis and Recommendations

In WP2, we investigated the main characteristics of benthic trophic webs at different spatial scales, from very local (i.e. a fjord) to very large (i.e. locations separated by about 500 km), using stable isotopes, fatty acids, highly branched isoprenoids (HBIs) and linear inverse modelling (LIM). We compared different habitats (mainly hard substrates and soft-bottom habitats). Many analyses are still in progress, and this is a preliminary synthesis.

Our results varied according to the spatial scale investigated. At fine scales (hundreds of metres to kilometres, i.e. station and fjord levels), food-web characteristics were determined by both habitat type and local environmental conditions, particularly glacier melt, summer sea-ice persistence, and microphytobenthic primary production. At larger scales (i.e. locations along the Peninsula), we observed major variability in the diversity of carbon sources used by benthic organisms, linked to

habitat type and summer sea-ice persistence. No clear latitudinal gradient emerged, but carbon-source diversity was influenced by the presence of benthic macroalgae on hard substrates and by the presence or absence of summer sea ice. This may indicate that the predicted future expansion of macroalgal habitats will strongly affect carbon fluxes and dynamics within the benthic compartment, including in soft-bottom habitats where macroalgae enter the food web as detritus. We also observed that some species were able to cope with this variability in carbon sources, benefiting from the presence of macroalgae. However, this is likely not the case for all species investigated. This could suggest that future changes may lead to greater food-web complexity and drastic shifts in community composition along the Peninsula.

Nevertheless, comparisons at broader scales were partly hampered by effects at the local-scale. We therefore recommend that future studies take such fine-scale variability into account when designing sampling strategies, particularly when the aim is to compare habitats at broader scales. In particular, it is important to consider the level of local habitat variability in sampling design in order to better capture processes at the Peninsula scale.

At the scale of the Peninsula, we showed that the presence of macroalgae increases the diversity of carbon sources in the ecosystem, shifting it from a water-column/sea-ice-dominated system to one that is more benthic-dependent, with more diverse carbon sources and potentially higher species diversity. However, this is not necessarily positive for the conservation of characteristic Antarctic ecosystems. Many species endemic to the Peninsula and adapted to current carbon sources may not be able to adapt to future food-web changes. We therefore recommend caution when interpreting the trophic parameters used here, and emphasise that an increase in the diversity (or even the quantity) of carbon sources is not necessarily beneficial for the highly specific ecosystems found in the region.

4.3. WP3 Ecosystem carbon cycling

4.3.1. Introduction

Sea-ice retreat, glacier retreat, and ocean warming in habitats along the West Antarctic Peninsula are potentially altering organic matter – organic carbon cycling, from production to mineralization. These environments integrate processes spanning the full continuum from primary production in the water column to pelagic export, benthic storage, and long-term deposition, while also mediating exchanges among the ocean, atmosphere, and cryosphere. A shift from sympagic production to water column production (e.g. Moline et al., 2004), increased water column primary production and subsequent deposition on the seafloor (e.g. Henley et al., 2020; Sands et al., 2023), and increased habitat for benthic primary producers (e.g. Amsler et al., 2023; Deregibus et al., 2016), are several pathways that will affect C-cycling in the Antarctic ecosystem. In this work package, we aim to quantify baseline carbon cycling typologies along a longitudinal gradient of sea-ice cover, by executing detailed measurements on the transfer of carbon throughout the cycle from production to mineralization. There is additional emphasis on the production of greenhouse gases (GHG, CO2, CH4), as these are products of (partial) mineralization of organic matter, and have been linked to subglacial meltwater (Lamarche-Gagnon et al., 2019). This starts with the quantification of primary production in the water column, and in sea-ice (sympagic production), quantifying deposition of organic carbon - matter, and how this organic carbon is subsequently remineralized in the seafloor and released back to the water column and atmosphere.

RO: What is primary production, pelagic export, benthic storage and carbon flow along climate gradient?

4.3.2. Production of carbon in the water column and sea ice

Sea ice was sampled during the TANGO1 expedition at two stations (Dodman and Blaiklock Islands). The gas content of these cores was analysed, including argon and oxygen. The ratio of these two gases makes it possible to distinguish physical processes from biological ones. It is possible to deduce the biological oxygen, which is therefore that produced by biological processes. In our case, we observe variations in $[O_2]_{bio}$ concentration in the cores.

For the sea ice of Doman Island (Figure 19, left), the highest peaks (at 10 cm and 80 cm) correspond to the location where the gas content was lowest. The injection pressures were extremely low and therefore close to the GC detection limit. These data should therefore be treated with caution.

At Dodman Island, we observed higher $[O_2]_{bio}$, between 30 and 70 cm and at the bottom of the core. At Blaiklock Island (Figure 19, right), however, the highest concentrations are found between 40 and 70 cm. This corresponds to locations that we have identified as gap layers. A gap layer is a mixture of ice and seawater that has infiltrated the ice. This zone is particularly rich in chlorophyll a, which certainly indicates higher primary production in this type of ice.

These preliminary results show possible primary production within the ice, particularly in gap layers, which are more commonly found at the end of summer.

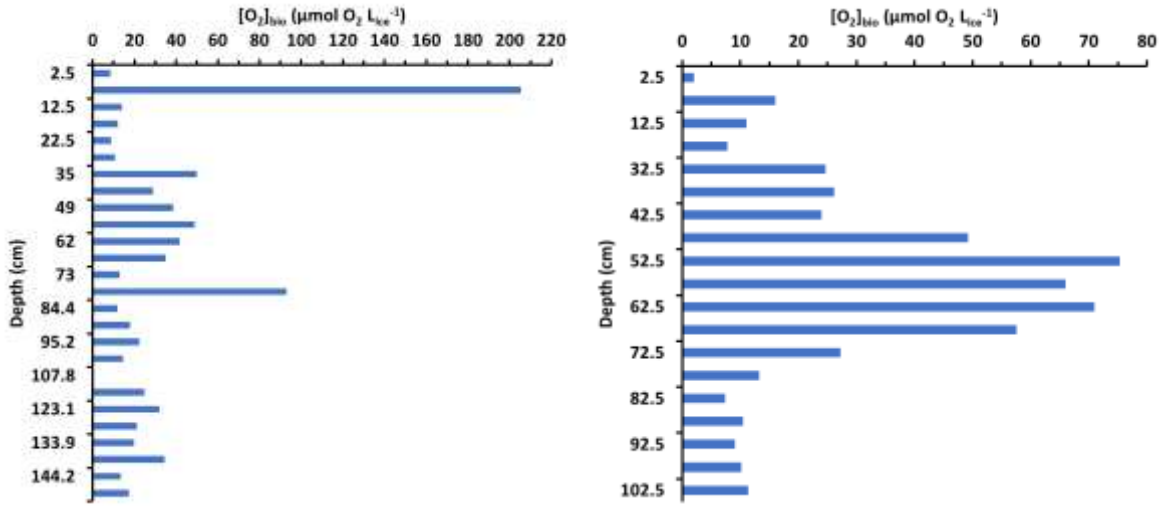

Figure 19: $[O_2]_{bio}$ in sea ice core from Dodman Island (left) and Blaiklock Island (right).

Analyses to quantify primary production in the water column are not yet complete. However, chlorophyll analyses have been carried out and can serve as an initial indicator. We note that chlorophyll concentrations are two to three times higher in the south (i.e., Dodman and Blaiklock Island) than in the north (i.e., Melchior and Hovgaard Island and Føyn Harbor).

4.3.3. Depositional setting of the TANGO sites

The sediment trap was deployed at all main stations (i.e., Dodman, Blaiklock, Melchior and Hovgaard Island, and Føyn Harbor). The results highlight a vertical flow of material that is five times greater at the southern stations than at the northern stations (Figure 20).

The composition of these flows is relatively similar from one site to another, consisting on average of 98.35%+-0.03% diatoms (Figure 21). The only other algal group present is haptophytes, representing up to 6.7% at Hovgaard Island.

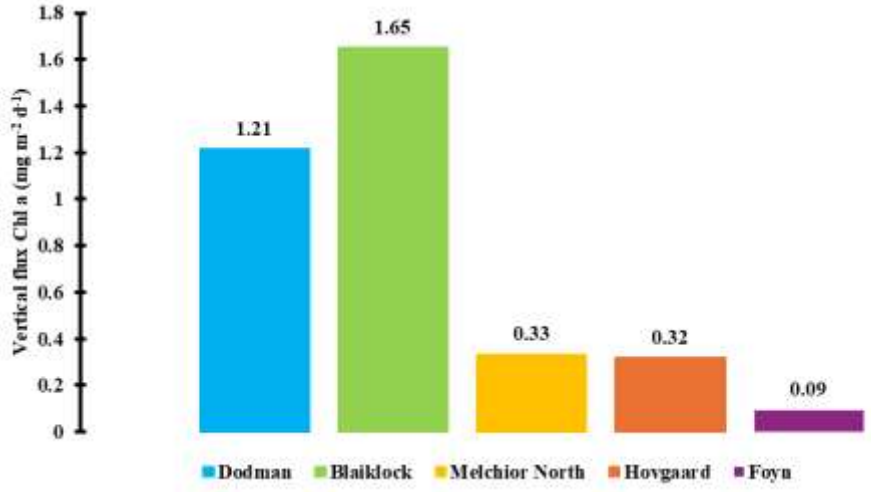

Figure 20: Chl a flux from the sediment trap at the main stations of TANGO 1 and 2.

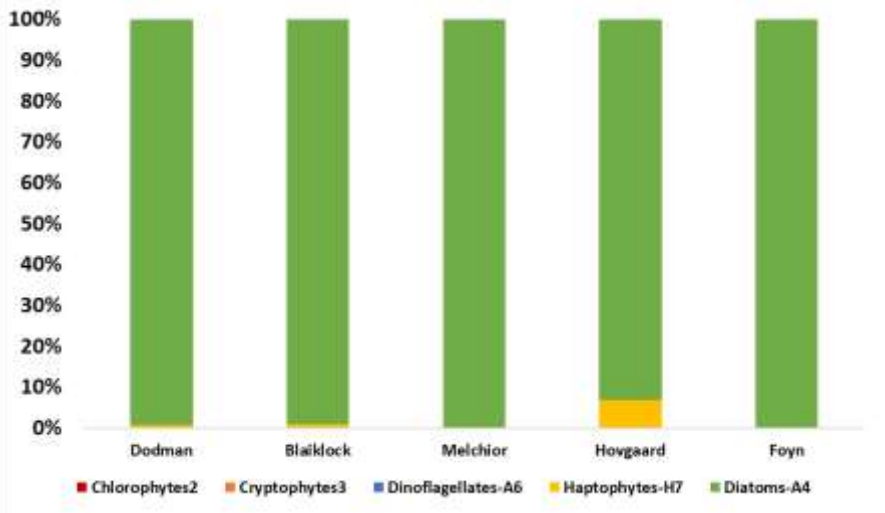

Figure 21: Composition of different algal group in the sediment trap at every location.

By performing a Spearman correlation between chlorophyll a and the environmental parameters of the stations, we find that the concentration of chl a is positively correlated (correlation = 0.39) with the concentration of sea ice. This highlights that the stations most covered by sea ice have higher concentrations of chl a. It also appears that this leads to greater vertical flux, distinguishing between northern and southern stations.

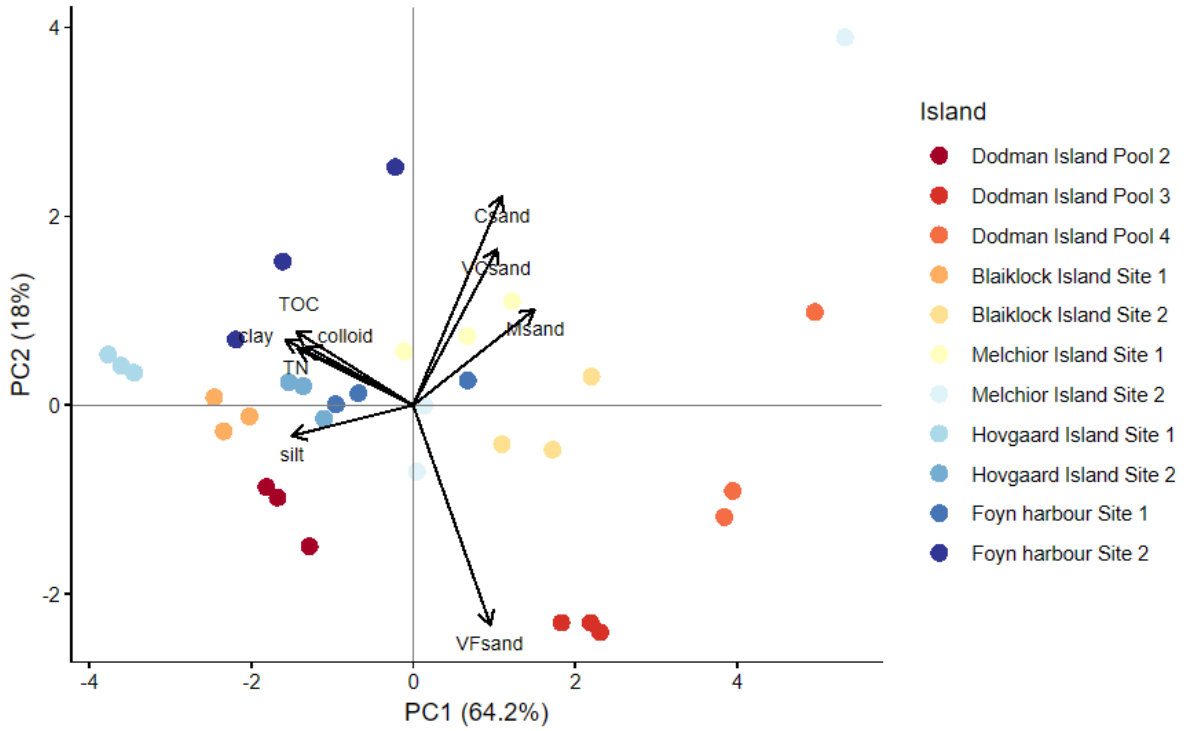

Figure 22: Centred principal component analysis (PCA) of TANGO sites based on surface sediment characteristics. Points represent individual replicates, with colours indicating stations. Percentages on the axes show the proportion of total variance explained by each principal component. Arrows depict the loadings of environmental variables, indicating their direction and relative contribution to the ordination.

Sites differed strongly in their granulometry and organic matter (organic carbon and nitrogen) contents (Table S. 1, Figure 22). The latter did not only reflect deposition from the water column, but also the presence of microphytobenthos, which were observed in several sites. In general, sites could be classified between silty- fine sandy, as values for median grain size (MGS) were generally below 63 µm. MGS seldomly exceeded 125 µm with the exception of one core in Melchior 2 where surface median grain size was 251 µm, and Dodman Island pool 4 cores, where surface values ranged from 136 - 172 µm. Grain size, driven by clay and silt content mostly, was strongly correlated to total organic carbon (TOC) and total nitrogen (TN) content in the sediment, which was highest in sites with the finest, clay rich sediments.

These fine, organic matter rich sediments were found either closest to glacier outputs (see the gradient of Dodman island, where pool 2 is closest to the glacier, and pool 4 furthest away, and Blaiklock Site 1 - Site 2), or in strongly sheltered sites such as Hovgaard Island (site 1 especially), and Føyn harbour.

4.3.4. Exchange of fluxes across the sediment water interface and underlying biogeochemistry

Mineralization of organic matter dynamics

O_2 consumption was generally comparable between most of the studied sites (Table S. 2); rates were relatively similar throughout the different study locations, with average values per site ranging from 8.4 ± 8.2 mmol O_2 $m^{-2}d^{-1}$ at Blaiklock site 2, to 32.9 ± 15.7 mmol O_2 $m^{-2}d^{-1}$ at Føyn harbor site 2. As a result, oxygen consumption does not strongly differentiate the biogeochemical pattern of the different research sites (Figure 23). In terms of absolute values of oxygen fluxes, a contrast is visible

between the most organic matter rich, finest sediments of Dodman Island pool 2 compared to the other sites, and in the contrasting Blaiklock sites. Ammonia release shows similar narrow differentiation, indicating relatively similar mineralization rates across the studied sites differences). Strongest differentiation (first axis, Figure 23) is caused by dynamics of nitrate, phosphate, and silica fluxes, indicating differing contributions of denitrification and phosphate trapping (see below).

Going from dark to light incubation tends to move pairs downwards on PC2 (Figure 23), consistent with lower SCOC often seen at these stations (and even oxygen production on occasion). This also reduces ammonia release, likely as a result of uptake by microphytobenthos. For several stations this is paired to a shift right on PC1 (Blaiklock 1, Melchior, Hovgaard), indicating increased oxygenation (by microphytobenthos) leads to increased release of oxygenated nutrients (NO^{3-}, PO_4^{3-}), a secondary explanation for the decreasing efflux of ammonia from the sediment. This consistent trend between dark and light incubations was confirmed with a between-class-analysis (randomization test, p = 0.002, 10 % of exchange structure explained by incubation mode).

The rather unexpected shift towards decreased nutrient release in light incubations of Dodman pool 2 is driven by strong nitrate and silica uptake. Dodman pool 3, is the only site where oxygen consumption and ammonia release increased in light over dark incubations.

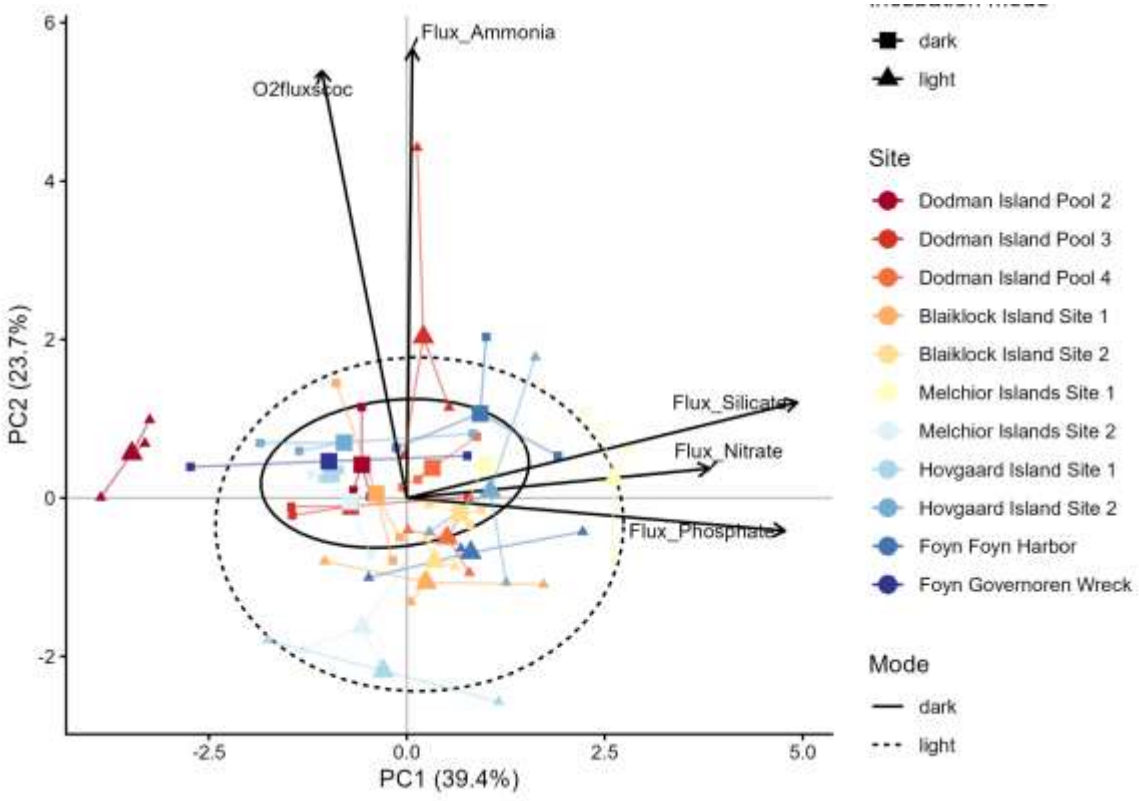

Figure 23: Scaled principle component analysis (PCA) plot of measured fluxes. Arrows depict variable loadings on PC1 and PC2; higher flux values (along the direction of the axis) indicate release of a given nutrient to the water column, except for the sediment community oxygen consumption (SCOC - O_2Flux), where a higher value represents higher uptake of oxygen by the seafloor. Axis labels report the % variance explained by the axes. Larger symbols represent centroids per station x subsite combination, connected by spokes to the individual replicates (smaller symbols). Ellipses show the 95 % normal confidence region of the scores for each incubation type (dark - full line, light - dotted line) group.

Dissolved inorganic carbon (DIC) fluxes vary more strongly between sites when compared to oxygen fluxes Figure 24. For this report, we will not discuss the DIC exchange measured in TANGO 1, as the validity of these values is in question due to possible contamination of the samples due to long storage. There is a consistent pattern of DIC release (negative values) in light incubations, as opposed to uptake in dark incubations, consistent with the photosynthetic activities of MPB, and oxygen dynamics reported above.

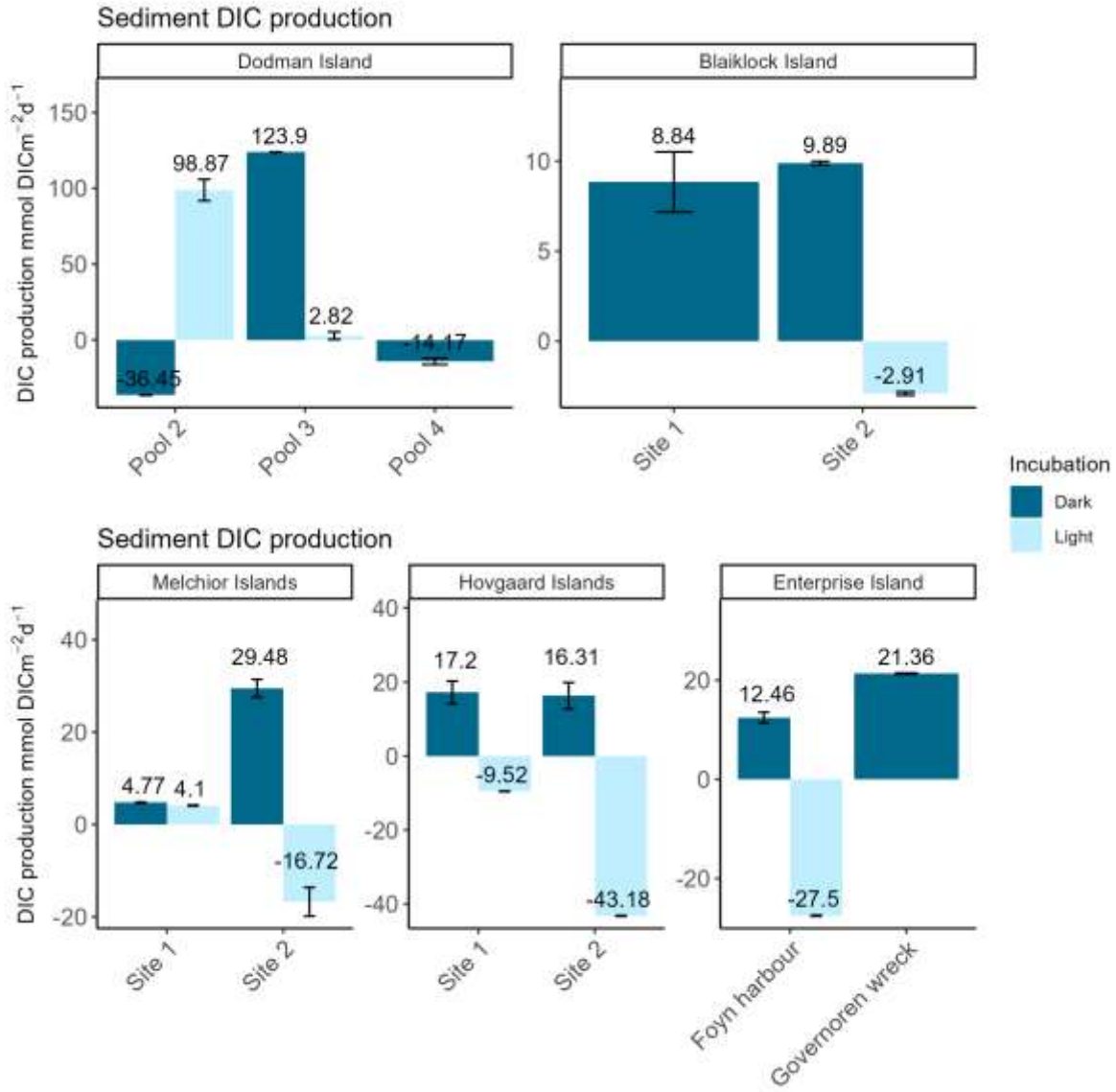

Figure 24: Dissolved inorganic carbon fluxes (mmol DIC m^{-2} d^{-1}) into (positive) or out of (negative) the sediment measured during dark and light incubations (see legend). Bars represent averaged values for core replicates and error flags the standard deviation (SD).

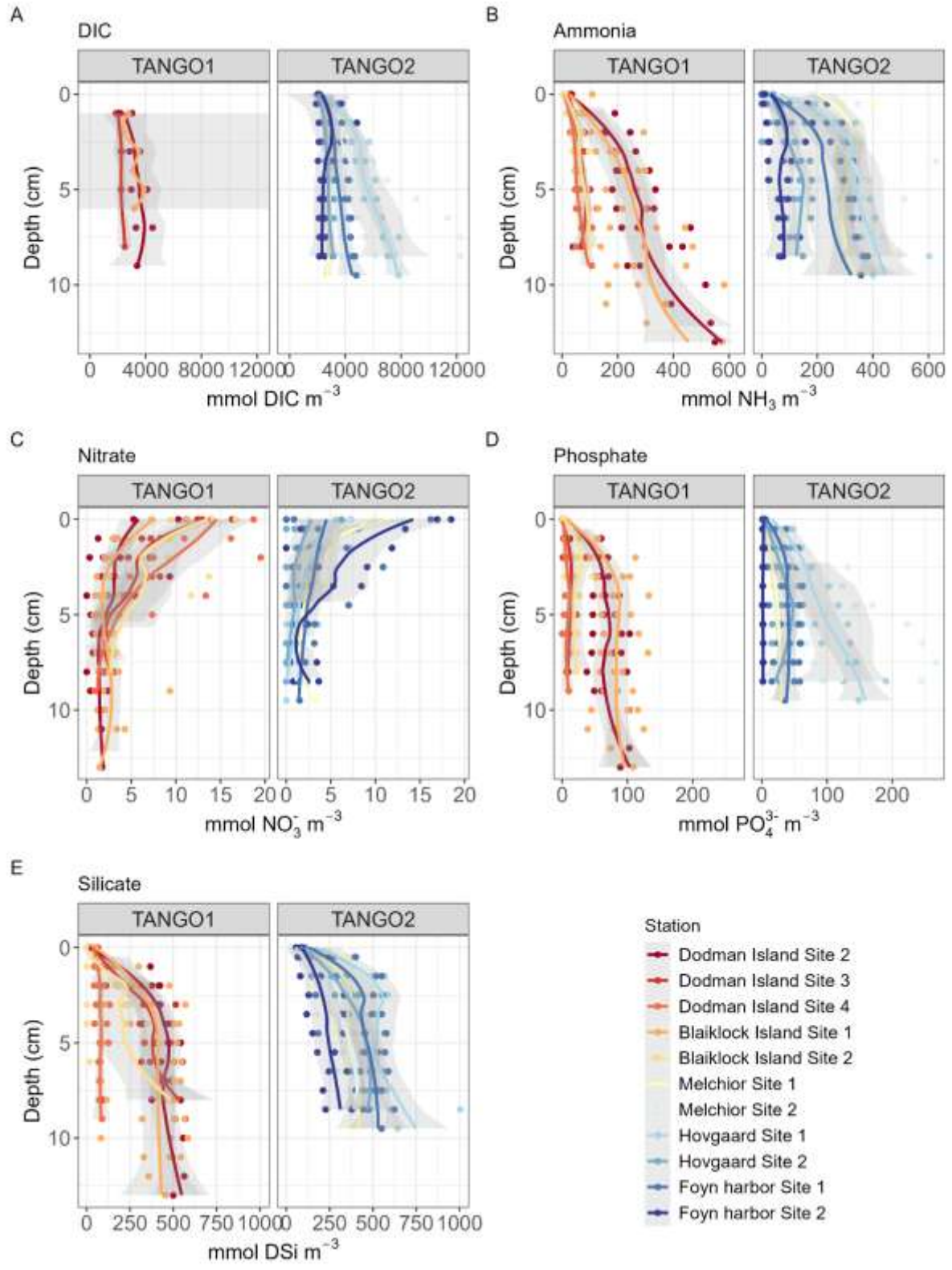

Figure 25: Porewater concentrations of (A) dissolved inorganic carbon, (B) ammonia, (C) nitrate, (D) phosphate, and (E) silicate in mmol m^{-3} (x-axis) and depth in the sediment in cm (y-axis).

Porewater DIC concentrations (and other nutrients) reflected the depositional environment reported above (Figure 25). DIC concentrations were consistently highest in Hovgaard site 1 (up to 8000 mmol DIC m^{-3} at depth), with similar values in Melchior 2, where concentrations were much more variable

between replicates (Figure 25 A). Strongest surface mineralization evidence is seen in Hovgaard site 1, and individual cores of Melchior 2, and Føyn harbour site 2, but most of the profiles exhibit rather straight lines, indicating lower mineralization rates (or stronger exchange flattening gradients). In TANGO 1, DIC concentrations were deemed as unreliable for the same reasons as for the exchange fluxes.

Subsurface gradients in ammonia profiles are stronger (Figure 25 B). The near-glacier sites of TANGO 1 show strongest ammonia buildup, as well as subsurface activity, with concentrations exceeding 500 mmol NH_3 m^{-3} at depth in Dodman Island site 2, and Blaiklock island site 1. Similarly, profiles of Melchior and Hovgaard islands show strong subsurface ammonia buildup, and build up in depth to values around 400 mmol NH_3 m^{-3}. Nitrate profiles exhibit a similar glacier dependent pattern in TANGO 1, where there is virtually no nitrate build up in the sediment except near the surface, indicating a shallow oxic layer (Figure 25 C). Higher values occur further away, implying that stronger nitrification occurs in less fine-grained sites at greater distance from the glacial outflow. Also in TANGO 2 nitrate profiles values are highest in less fine sites (Melchior site 1, individual replicates of Føyn harbour site 2), whereas muddier sediments in other sites prevent high nitrate buildup deeper into the sediment column.

In the porewater phosphate concentrations we see again the depositional effect in TANGO 1, with high buildup of PO_4^{3-} in sites closest to the glaciers, with concentrations increasing to ~ 100 mmol PO_4^{3-} m^{-3} at depth (Figure 25 D). In TANGO 2 phosphate profiles covary with ammonia profiles (Melchior site 2, Hovgaard site 1), with exceptions in Melchior site 1, which does not see higher PO_4^{3-} buildup following NH_3. Interestingly there is no phosphate buildup in the iron-rich sediments surrounding the Governoren wreck of Føyn harbor site 2.

Dissolved silica concentrations are remarkably low in Dodman pool 4; whereas all concentrations at depth range from 250 – 700 mmol DSi m^{-3}, values at Dodman pool 4 do not exceed 125 mmol DSi m^{-3} (Figure 25 E). Surface values at all sites show a considerable mineralization signature, in line with ammonia profiles.

When comparing the ratios of nutrients expressed in porewaters to idealized Redfield ratios of 106:16:15:1 (C:N:DSi:P), several strong deviations are seen. For C:N ratios, especially Melchior 1 expresses far higher DIN concentrations than expected, indicating desorption of NH_3 to explain such high values. Hovgaard 1 and Melchior 2, in contrast, express much lower DIN:DIC ratios, especially at depth, indicating substantial N removal, e.g. through denitrification and potentially increasing DIC through carbonate dissolution. A general trend in TANGO was also an oversaturation of dissolved inorganic phosphate (DIP) compared to DIN. In more fine, TOC rich sites (Dodman site 2, Blaiklock 1, Hovgaard), DIP:DIN ratios correspond to reducing conditions where it is likely that Fe-oxide cycling releases PO_4^{3-} to porewaters. In contrast, DIN rich Melchior site 1 and Føyn 2, where excessive DIP-trapping takes place has decreased DIP:DIN ratios. Lastly, high DSi values (compared to DIN) in most sites (barring Melchior site 1 – 2) indicate strong contributions of silica rich deposition to organic matter depositions (diatoms), which remain trapped in the sediment.

Summarized, the benthic biogeochemical patterns across TANGO sites display a contrast between close and far glacier influence sites, which is especially clear in the TANGO 1 sites where the range of sediment types is wider as opposed to TANGO 2. This is visible in both the nutrient exchange fluxes

(short-term signal), as well as the porewater profiles (long-term signal). Finest sediments containing highest porewater solute buildup rates and a signature of a strong reducing environment closest to glacier outputs. It is interesting that Blaiklock 1 displays similar dynamics as Dodman 1, as the former has only been ice-free since 2001. TANGO 2 sites span a more narrow range in terms of environmental characteristics, which results in more similar biogeochemical signatures overall, though several sites do vary as a result of site specifics (e.g. iron rich sediments near Governoren wreck, strongly enclosed basin of Hovgaard 1). Microphytobenthos appear to play a profound role in nutrient cycling in shallow habitats of the West Antarctic peninsula, generally increasing retention of nutrients in the seafloor during periods of photosynthetic activity.

Greenhouse gas fluxes

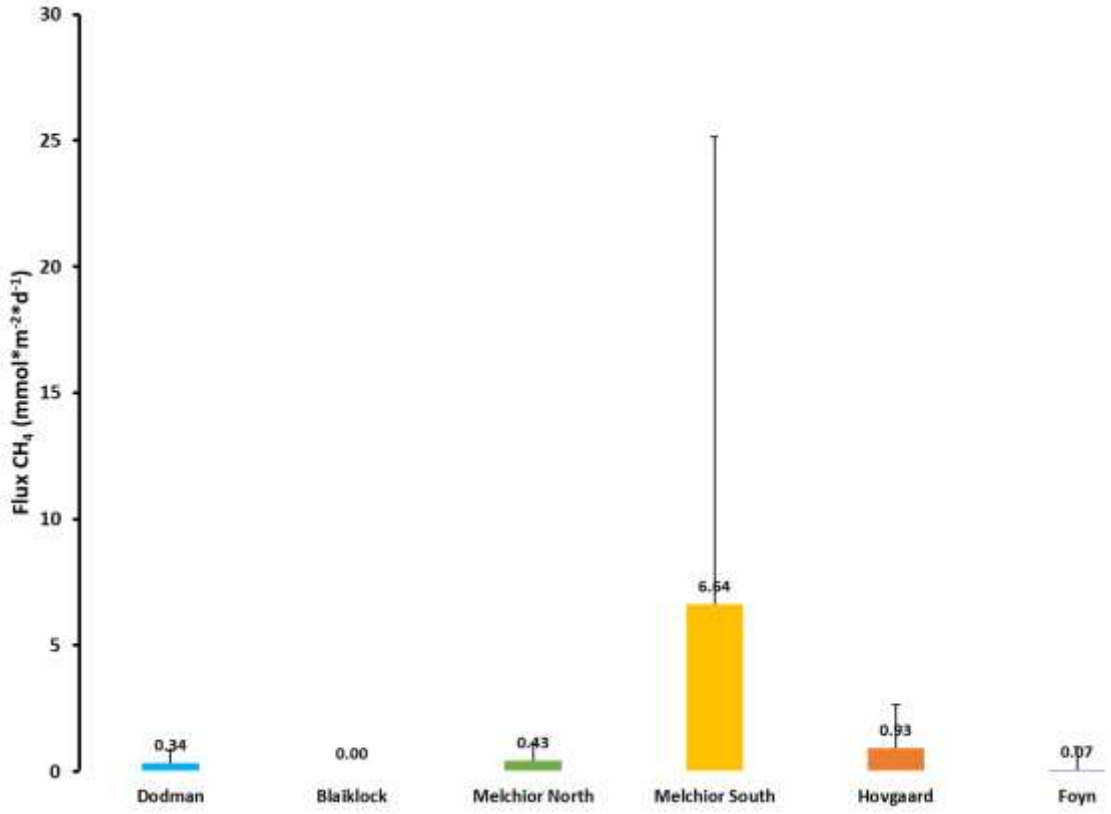

Figure 26: Flux of methane at the interface sediment water column. Positive flux means methane is going from the sediment to the water column. The fluxes are a mean value from dark and light incubation.

Methane fluxes at the sediment-water column interface were measured at each main station. As shown in Figure 26, fluxes range from 0 to 6.64 mmol m^{-2} d^{-1} at Blaiklock Island and Melchior South, respectively. During dives to recover sediment cores, no visual evidence of bubble degassing from the sediment was observed. Furthermore, no evidence of seep in these areas has been described in the literature. It is therefore likely that methane from sediments is mainly due to methanogenesis occurring in the anoxic zone. Nevertheless, the flux from Melchior South is of the same order of magnitude as the fluxes measured near the seeps at Ross Island (3.1 ± 9 mmol m^{-2} d^{-1}) (Thurber et al., 2020). This could either indicate their presence or indicate the presence of a source allowing for a similar flux.

The error bars highlight the heterogeneity of the samples. This is particularly true at Melchior South, where the flux could vary by an order of magnitude between replicates. These flows were nevertheless always positive, indicating a source of methane from sediments to the water column.

The flux at Blaiklock is zero, which is not surprising given that the sediment there is relatively young. The area was covered by a glacier but has been completely free of ice since 2001 (Fox & Vaughan, 2005). The retreat of the glacier has exposed the rock, and the sediment present is therefore relatively young and shallower, making it less active in terms of methane production.

The remaining stations show flows above the average flows measured in Antarctica. However, very few measurements exist and they are relatively heterogeneous. Ni et al. (2025) show an estimated flux in Antarctica at shallow depths between 0.15 and 0.2 mmol m^{-2} d^{-1}. Most of our stations show a higher flux and therefore a source of methane from sediments.

4.3.5. Exchange of fluxes across the water - air interface

Part of the air-sea fluxes have been calculated. The DIC shows rather low concentrations at the surface (between 1993.24 and 2228.32 µmol kg^{-1}, Figure 27). However, these concentrations are similar to those found in the literature for February in Antarctica (concentrations of 2124 µmol kg^{-1}) (Roden et al, 2013). These low concentrations can be explained by air-sea CO_2 exchanges that occur in summer when the ice is no longer present, but also by the increase in primary production during this period. Indeed, as the ice retreats, light becomes available and enhance the primary production.

Alkalinity was calculated for the first expedition in order to determine pCO_2. For Dodman and Blaiklock Island, pCO_2 varies between 137.2 and 316.6 µatm. These partial pressures induce a flow of CO_2 from the atmosphere into the water column, highlighting that these stations are CO_2 sinks during the summer.

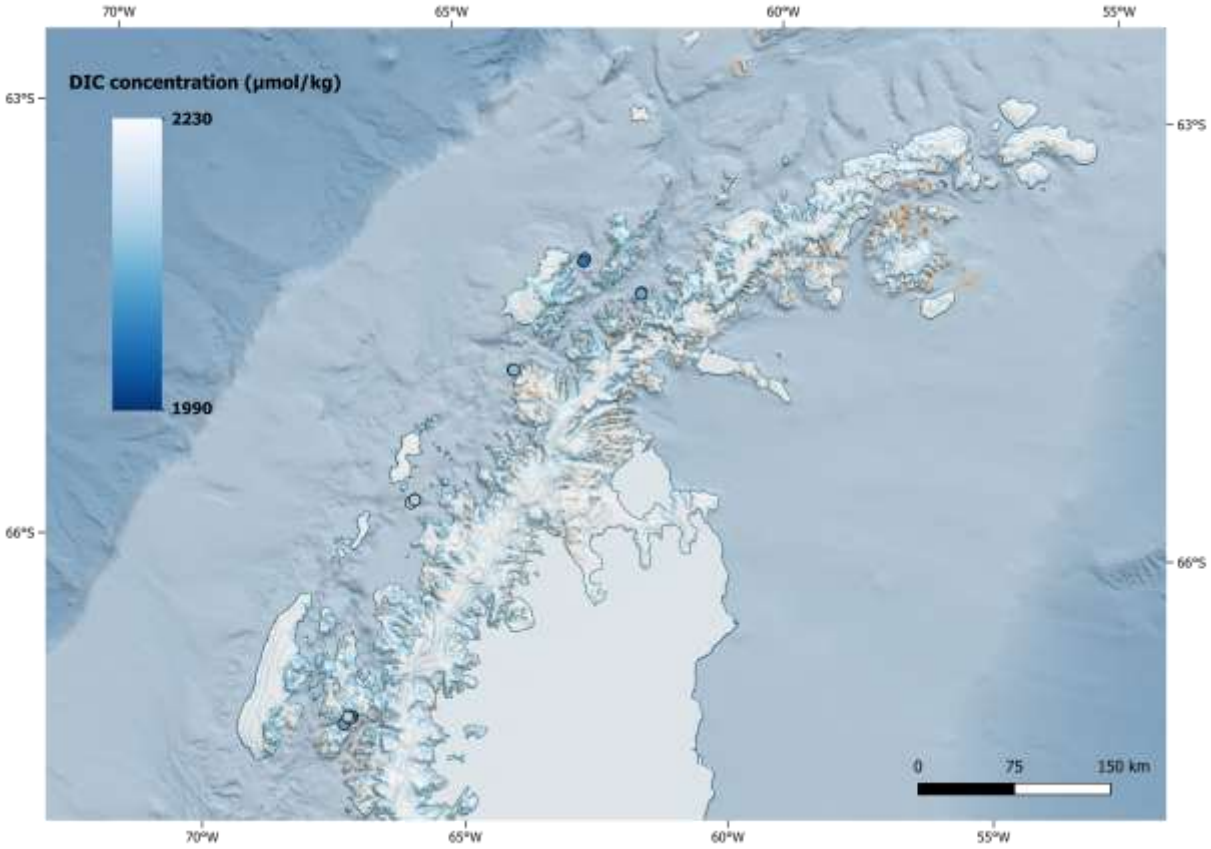

Figure 27: DIC surface concentration in the West Antarctic Peninsula.

As for the other greenhouse gases (CH_4 and N_2O), both are oversaturated at all the stations visited. This highlights the coastal role of the WAP as a source of these gases.

4.3.6. Overall view on C-cycling over longitudinal gradient and recommendations

Not all results are accessible and interpretable yet and no carbon budget can be presented, so below is a summary of observed patterns.

On the production side, sea ice was only found in the southern stations (TANGO 1), in accordance with out longitudinal gradient. This sea ice was found to contain significant concentrations of chlorophyll a, indicating sympagic production. Primary productivity in the water column itself, currently estimated through chlorophyll a concentrations, was estimated to be 2 – 3 times higher in TANGO 1 sites as opposed to the more northern TANGO 2 sites. As a result, the deposition of chlorophyll a on the seafloor (almost exclusively of diatomaceous origin) correlated to the annual percentage of sea-ice cover, with deposition values higher in the more southern sites as opposed to the northern TANGO 2 sites.

These differences in deposition rates did not relate to differences in mineralization rates or sediment properties (grainsize, % TOC). Total mineralization rates were mostly a function of proximity to glacial deposition sources as seen in the gradients of Dodman and Blaiklock. The carbon dynamics on the seafloor were strongly altered by the activities of microphytobenthos, which were present throughout the study area as evidenced by the results of the dark-light incubations. In dark conditions MPB respire organic carbon and consume oxygen, in light conditions photosynthesis causes oxygen production and

uptake of DIC from the water column. This also affects dynamics of other nutrients (N – P) as the sediment surface becomes oxygenated. Observations of surface waters, expected to represent an integrated picture of biogeochemical processes below, indicate that demand of DIC by water column and benthic primary producers makes the WAP act as a sink during Antarctic summer.

The fine-grained nature of the visited sites where anoxic mineralization is expected to dominate OM mineralization, and the presence of GHG in glacial outflow, translated to an oversaturation of GHG in the water column throughout the region, making the WAP a source of GHG.

Based on our current findings, we recommend **increased sampling intensity of the carbon cycle in the WAP, focussing on the mechanistic basis behind the transfer of carbon from primary production, to mineralization locations, to eventual release of CO_2 (and other GHG) to the atmosphere. In addition, we recommend mapping or predictive modelling of sites containing soft sediments where benthic mineralization can occur.**

4.4. WP4 Upscaling to ecosystem level (lead Bruno Danis, ULB)

4.4.1 Quantifying spatial heterogeneity

Our results highlight that shallow benthic communities of the WAP are characterized by very high spatial heterogeneity, which manifests across multiple scales and in different ways. In Dodman Island, we observed remarkable heterogeneity between different sites (Figure 28, Figure 29) and we documented a wide range of typical WAP habitats (Figure 30), including large rocks dominated by grazing limpets, soft sediment plains with piles of *Parborlasia corrugatus* and *Laternula elliptica*, with the occasional dropstone colonized by suspension feeders, as well as dense macroalgal forests hosting a high diversity of fauna. Nearly all studied areas were dominated by different assemblages, resulting in a very high variability both within and among sites, encompassing taxonomic and functional differences.

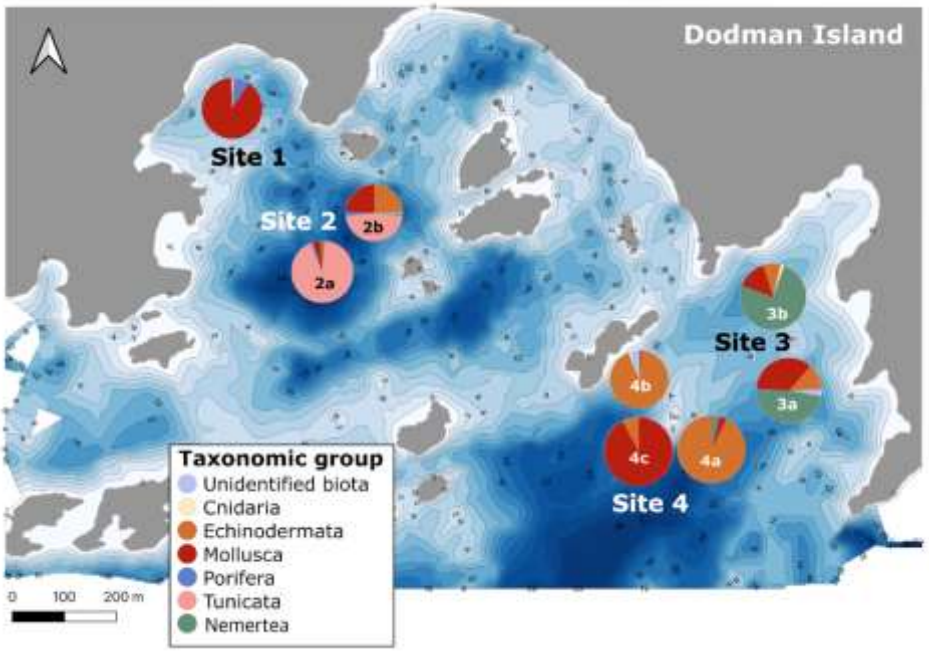

Figure 28: Map of Dodman Island. Pie charts represent relative cover of taxonomic croups identified on the images. Macroalgae were removed from the chart for clarity (Katz et al., 2025).

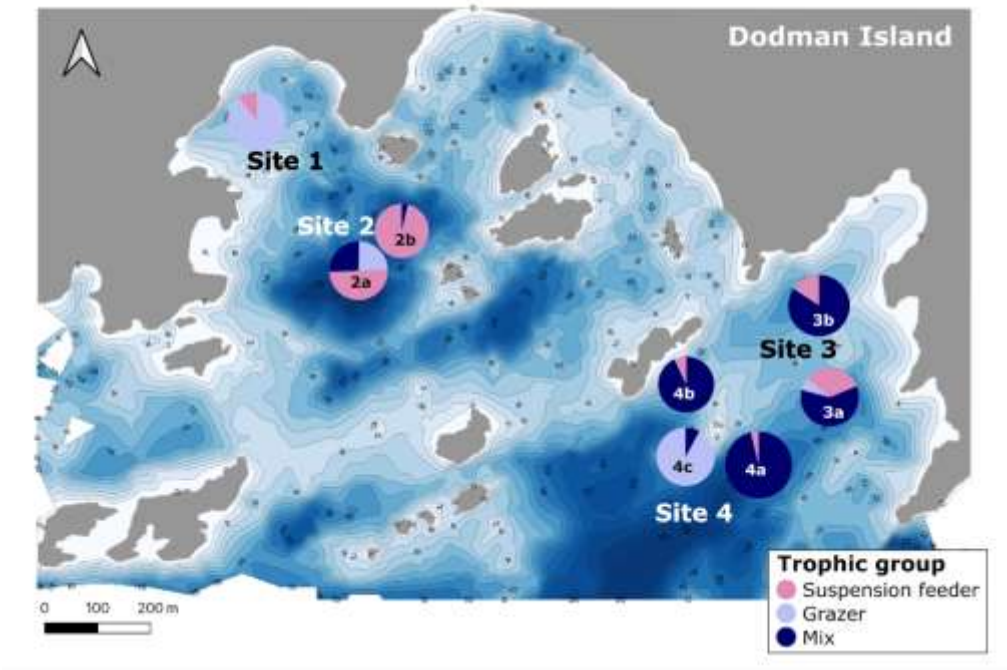

Figure 29: Map of Dodman Island. Pie charts represent relative cover of trophic groups identified on the images. Macroalgae were removed from the chart for clarity (Katz et al., 2025).

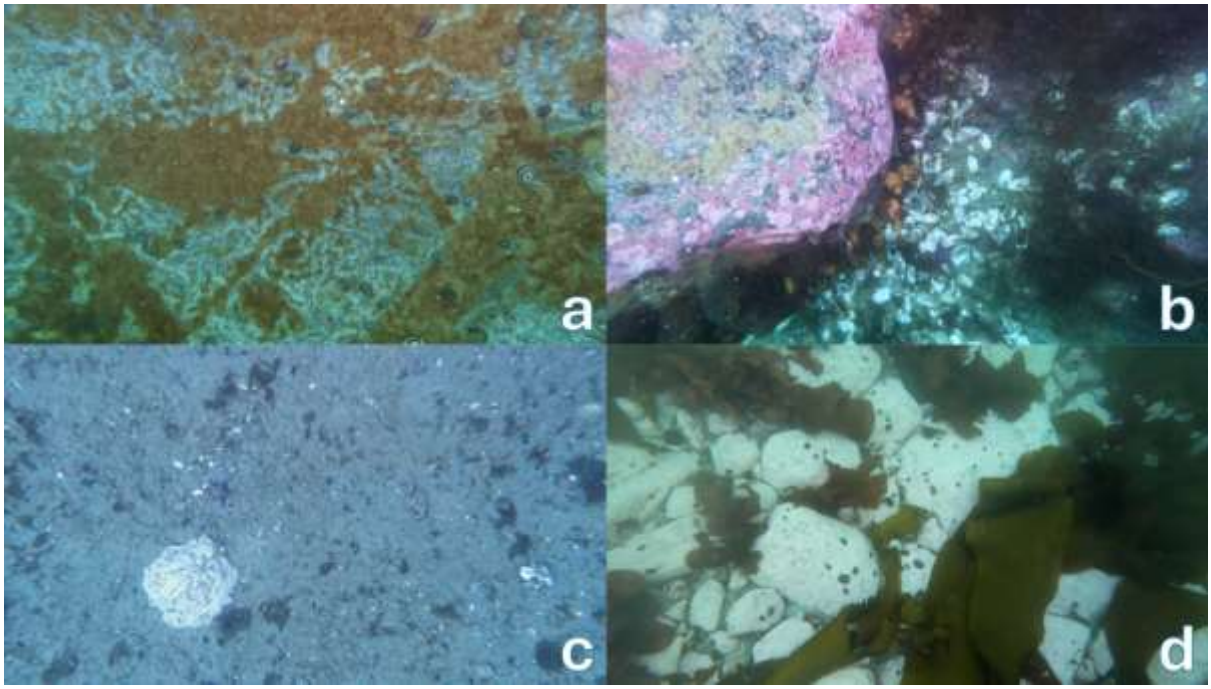

Figure 30: Sample images from the ROV, taken at approx. 1 m from the bottom. a) site 1: limpets and dwelling traces on rock. b) site 2b: dropstone with pink encrusting algae and ascidians. c) site 3a: pile of Parborlasia corrugatus. d) site 4c: rocks with sheet-like macroalgae and limpets.

Such small-scale heterogeneity is often obscured in broader-scale studies, which tend to emphasize regional variability (Gutt et al., 2013, 2016, 2019; Sahade et al., 2015), and a station like Dodman Island would be considered as one entity with an average community. In contrast, our sampling design enabled us to capture variability within the bay, offering a novel perspective of how benthic communities are structured across its contrasting areas. Furthermore, we found that biodiversity

patterns reflected not just species richness but also habitat diversity: sites with a greater mix of habitats (soft bottom patches, dropstones, macroalgae patches) supported higher alpha diversity and higher evenness, compared to sites dominated by one or two habitat types.

Building on this, in the sites of the northern WAP, we examined how heterogeneity manifests across spatial scales. This work used the data from the second cruise, and while each station was less extensively sampled than Dodman Island, we still managed to capture variability within and among stations, sites and even transects. Using NMDS, we found that, while sites and transects differed strongly from each other, there were many similar images across physically distant areas (Figure 31).

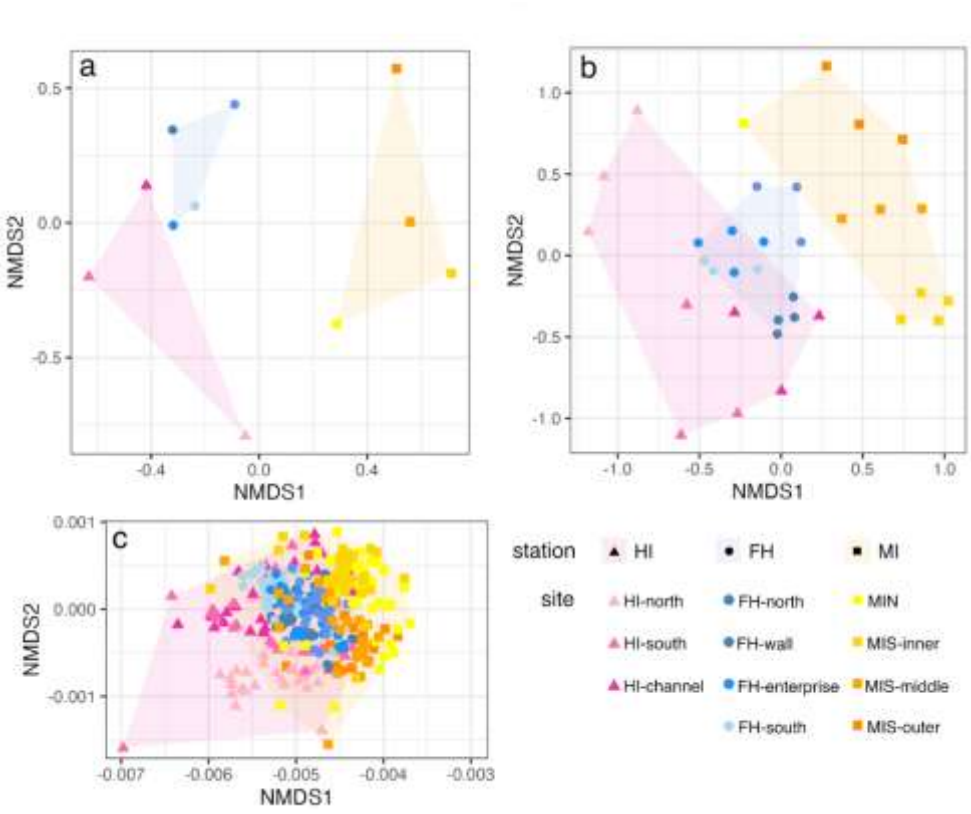

Figure 31: NMDS plots of benthic community data at 3 different scales: (a) unit=site, (b) unit=transect, (c) unit=image

The Hierarchical clustering analysis combined with a SIMPROF analysis identified 31 significant clusters of images across all stations, grouped by their similar benthic communities. Upon further investigation, this clustering is not solely driven by geographic separation (Figure 32). From now on, we define these groups of images with distinct communities as “microhabitats”, characterised by similar abundances and co-occurrence patterns of key taxa. The schematic representation in Figure 33 shows us that some of these microhabitats are widespread, occurring in the three stations at the same frequency (e.g. group ab), others are more localised (group e only found in site HI-north).

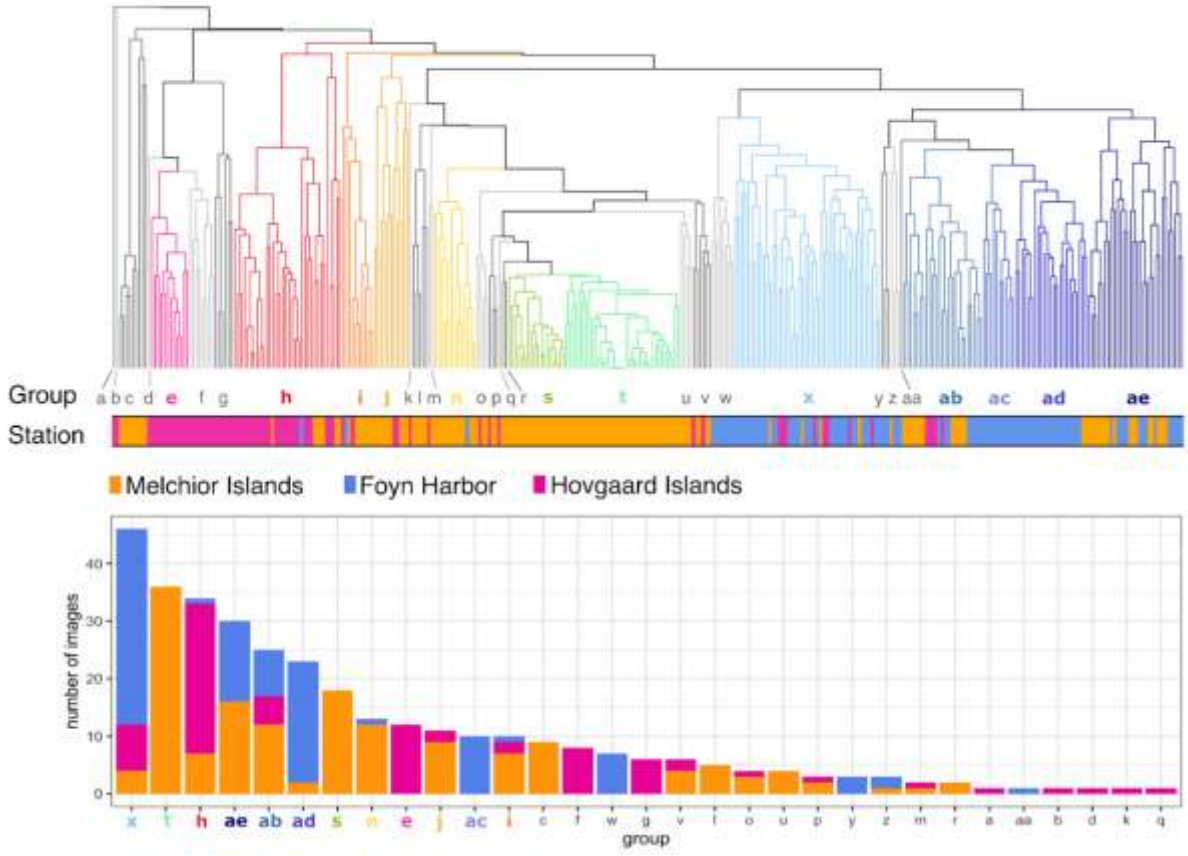

Figure 32: (top) SIMPROF dendrogram showing significant groupings ($p < 0.05$) of benthic images based on community composition, using Bray-Curtis similarity. Groups are color-coded, with coloured branches indicating different clusters, and main groups (+10 images) are highlighted. Horizontal bar below indicates sampling station of each image (Melchior Islands, Føyn Harbor, Hovgaard Islands). (bottom) Histogram showing the number of images per SIMPROF group, color-coded by station.

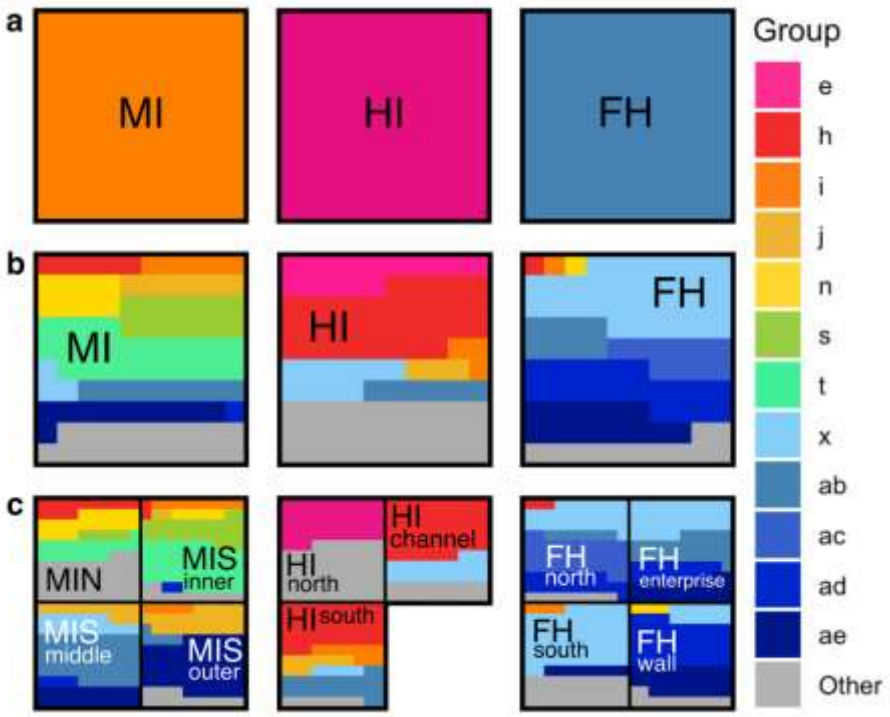

Figure 33: Schematic representation of the effect of spatial scale on benthic community interpretation across our 3 stations. Colors represent the main groups of images or "microhabitats" identified in Figure yy. (a) Station-level average community composition, shown as a solid color. (b) Microhabitat composition at the station-level. (c) Microhabitat composition at the site-level.

In other words, while the building blocks (or patches) of these benthic communities are often shared across sites and stations, the way they assemble into mosaics gives rise to seascapes that look entirely different. This revealed that the heterogeneity at site and station levels is largely driven by differences in the proportions of distinct "microhabitats", which we defined as groups of images characterized by similar abundances and co-occurrence patterns of taxa. Interestingly, having more microhabitats did not always translate into higher biodiversity; rather, the richness and complexity, as well as the connectivity between specific habitat types played a key role.

4.4.2 Identifying drivers of variability

Throughout this project, we found that drivers were highly scale-dependent with environmental features, such as ice-related processes, substrate type and macroalgal community, dominating large scale patterns, and species-level interactions becoming more apparent at finer spatial resolutions. In the following sections, we dive deeper into the main drivers we identified.

Substrate

In Dodman Island and in the northern WAP, using Bayesian Network Inference (BNI), we found that the presence or absence of many taxa were closely linked to the type of substrate, consistent with the literature. Substrate granulometry emerged as a central driver of benthic community structure, appearing as the focal node of the Dodman Island network (Figure 34), and appearing in almost every network across the northern WAP (Melchior Islands, Hovgaard Islands and Føyn Harbor; Figure S. 1-Figure S. 4).

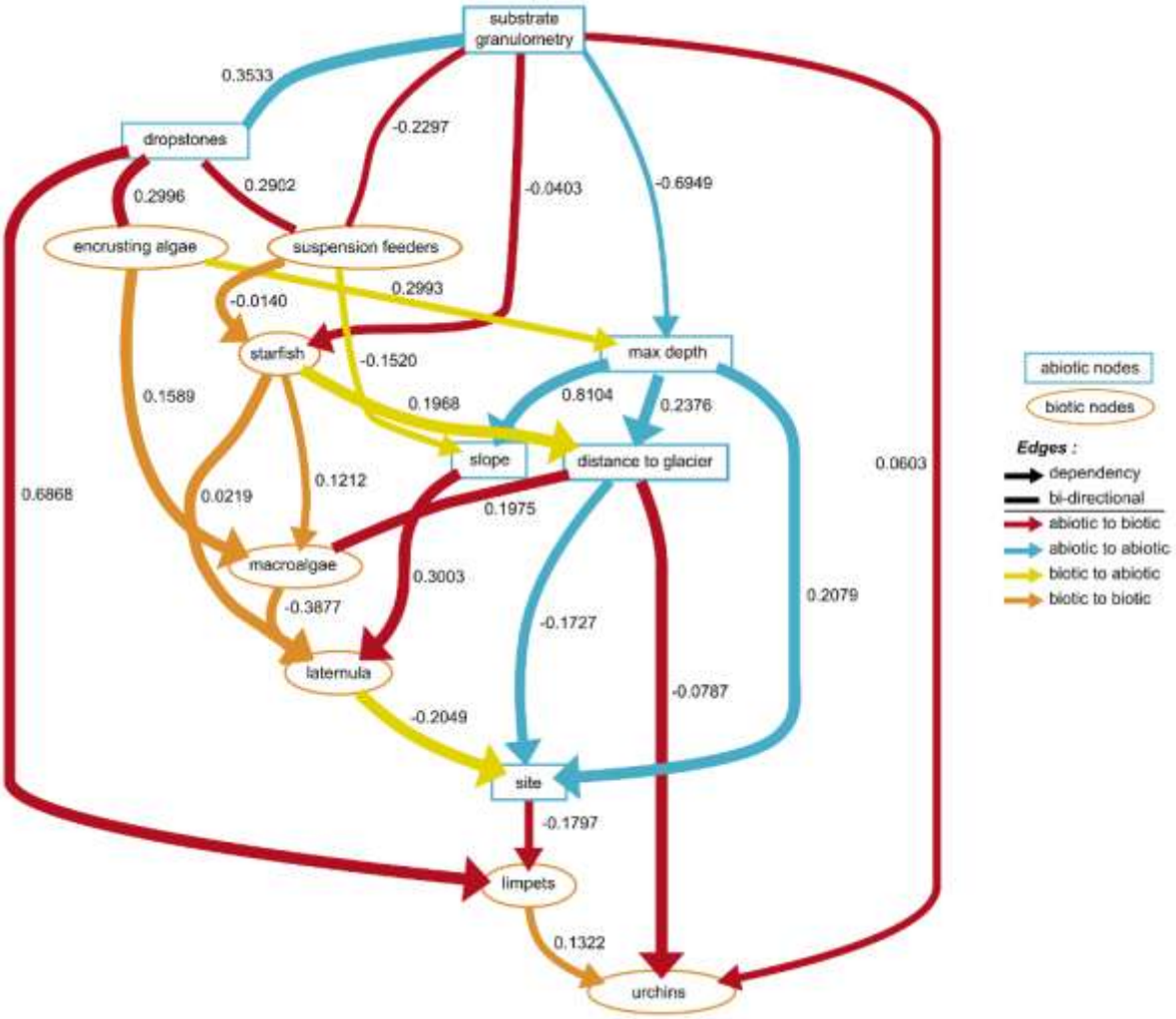

Figure 34: Bayesian Network of biotic and abiotic factors in Dodman Island. The lines between the nodes represent the edges, or dependencies, between the nodes. The lines are either directed (with an arrowhead in the direction of the dependency) or bi-directional (without an arrowhead). Width of the lines reflects the frequency at which the edge appeared in bootstrapped networks. The colour of the lines represents the type of connection (abiotic to abiotic, abiotic to biotic, etc.). The number next to the line is the Intensity Score (IS) of the connection (Katz et al. 2025).

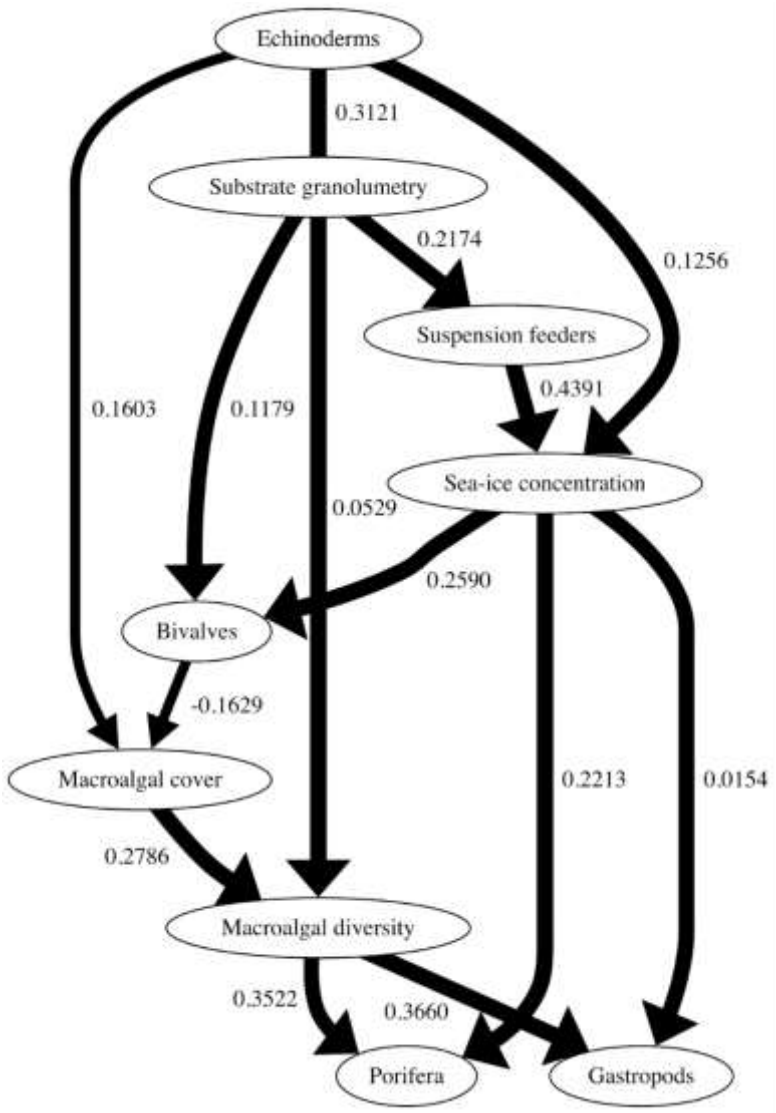

Figure 35: Bayesian Network of the northern WAP region. The arrows represent the directed dependencies between the nodes. The line without an arrowhead represents a bi-directional dependency. Width of the lines reflects the frequency at which the edge appeared in the bootstrapped networks. Each number represents the Influence Score (IS) of the connection.

Macroalgae

Macroalgae consistently emerged as connected nodes in networks at multiple scales (Figures x1-x6). However, their importance in the community was nuanced. *Macroalgal cover* is a connected node in the Dodman Island network but was less connected than most abiotic nodes (such as *Substrate granulometry* or *Distance to the glacier*). Indeed, macroalgal cover alone didn't explain the clustering of our microhabitats, reinforcing our hypothesis that benthic structure depends not only on the presence of macroalgae but rather on their local morphotypes and functional traits. With this in mind, we represented "macroalgae" as different nodes depending on the scale of the network: *Macroalgal cover* & *Macroalgal diversity* at regional (Figure 35) and station scales (Figure S. 1), and where possible, more specific morphotypes (e.g. *Red branching algae*, *Coralline algae*) at the site scale (Figure S. 2 Figure S. 3). At larger scales, macroalgal cover and diversity emerged as important nodes in the networks, and were found to usually have positive Influence Scores on other biotic nodes, which is consistent with their role as habitat formers, providing three-dimensional complexity, refuges, and heightened attachment structures that diversify ecological niches. Overall, the network results

support the idea that macroalgae play scale-dependent roles in structuring shallow Antarctic benthic communities: as broad indicators of sea-ice conditions, habitat productivity and complexity at large scales, and as direct biotic drivers and ecosystem engineers at finer ones. This highlights the need to treat macroalgae not just as a single environmental variable, but as an assemblage of morphotypes whose influence depends both on scale and local context.

Sea ice and glacier influence

Although the ROV dataset could not include sufficiently detailed sea-ice records or water column measurements to capture all ice-related processes, the results nonetheless highlight the importance of ice dynamics as drivers of benthic community composition at multiple spatial scales in the studied stations. At the regional scale, in the northern WAP, *Sea-ice concentration* emerged as an important

node in the network (Figure 35), connected to *Echinoderms*, *Suspension feeders*, *Bivalves*, *Gastropods* and *Porifera*. While these links do not necessarily indicate direct causal relationships between sea-ice and these taxa, they nonetheless could represent the food availability caused by the ice melting (Rossi et al., 2019). In the regional network (Figure 35), the association between *Sea-ice concentration* and *Suspension feeders* or *Bivalves* likely reflect this trophic relationship, where higher ice cover and its subsequent break-up enhances food availability for these groups through the release of sympagic algae (Rossi et al., 2019). From our networks, it is not directly clear how future declines in sea-ice cover will affect benthic communities, but we can however use the statistical

dependencies between macroalgae and other taxa to infer possible indirect changes in faunal composition due to changes in macroalgae abundance. At the station scale, the node *Distance to the glacier* was highly connected within the Dodman Island network (Figure 34), and could possibly reflect the influence of glacial runoff, and glacier calving on benthic assemblages. Our site closest to the glacier has much less species richness than the one at intermediate distance, located in the middle of the bay, suggesting a gradient of glacial influence on community composition. At the microhabitat scale, neither field observations nor available sea-ice datasets could explain the meter-scale variation we observed. This result suggests that while ice-related processes are clearly influential at broader scales, they may be less useful in explaining community patterns at very small spatial scales, where local biotic interactions and habitat complexity become more important.

Biotic interactions

In Dodman Island, *Starfish* was the most connected biotic node of the network (Figure 34). Predator-prey relationships with starfish were also detected in some of the site networks Føyn Harbor (Figure S. 4). Other network interactions (Figure 35, Figure S. 1 Figure S. 4) could represent competition for space, shared habitat preferences, facilitation and grazing. These findings reinforce the idea that Antarctic shallow benthos is not solely shaped by environmental drivers, but also by a dynamic web of species interactions that vary in strength across densities and contexts.

4.4.3 Recommendations for ROV surveys: the trade-off between efficiency and resolution

Using ROV surveys proved to be a time-efficient, non-destructive, reproducible and cost-effective method for image acquisition. This approach provided a broad overview of macrobenthic communities and allowed us to quantify biodiversity and heterogeneity across multiple spatial scales. Nevertheless, several limitations must be acknowledged when considering ROV imagery as the main sampling method. The constant-altitude, top-down perspective is advantageous in terms of survey efficiency,

remote control and potential for automation, but it inherently restricts observations to a two-dimensional view. When canopy-forming organisms such as macroalgae or sponges are abundant, they can obscure underlying organisms, which can lead to an underestimation of biodiversity. Similarly, the detectability of certain taxa depends strongly on the surrounding environment: cryptic species may be highly conspicuous in one context yet nearly invisible in another. For example, small white gastropods were easily detected on dark red sheet-like algae but far more difficult to discern against gravel. Comparisons with studies that rely on direct collection methods (e.g., hand-picking, trawling, dredging) are therefore problematic, as the assemblages captured will not be compatible. Brasier et al. (2018)) compared differences in faunal composition and abundance of samples taken with different sampling gear and found that trawling hauled lower abundance than imagery-based methods, while missing small or encrusting organisms, but was more successful in collecting infauna. Overall, while ROV surveys are powerful tools to document cover, size, microhabitat characteristics, and spatial co-occurrence patterns, they inevitably miss some components of biodiversity and should be interpreted with this in mind.

Another frequently raised issue concerns the reliability of species identifications from imagery. Many taxa cannot be distinguished with confidence from imagery, let alone from a top-down view, especially cryptic species or those defined by subtle morphological traits not visible in photographs. In some cases, field validation through hand-picking by SCUBA divers has confirmed the presence of certain taxa in the study area, but complete certainty of species identifications remains limited. For this reason, identifications are often made at a coarser taxonomic resolution, to remain consistent with what can be discerned from the imagery. Nevertheless, this level of resolution still allowed me to capture robust patterns of biodiversity, community structure, and spatial heterogeneity. In the context of benthic surveys in Antarctica, ROV imagery proved to be an excellent tool, but some practical considerations are essential to avoid major setbacks. The initial strategy was to conduct surveys in square “lawnmower” trajectories, covering ~100 m^2 per site. The resulting images could then be aligned into orthomosaics for analysing finescale spatial patterns. This approach was successful under ideal conditions (good weather, calm sea, good visibility, no drifting ice), but such conditions were rare. In practice, currents often caused the ROV to drift, floating ice repeatedly tangled the tether, and poor visibility from glacial runoff or recent calving prevented the alignment software from successfully reconstructing mosaics. Therefore, simplifying sampling surveys to linear transects proved to be far more tractable. Slight deviations from the ROV trajectory did not compromise results, deployments were faster and postprocessing of images was far more efficient. We therefore recommend transects as the default survey design in Antarctic environments, with square surveys for mosaics reserved for the exceptional cases where currents are absent, visibility is high, and light conditions are favourable.

5. DISSEMINATION AND VALORISATION

5.1. Training, collaboration, development of new techniques, policy relevance

Five doctoral theses were completed within the framework of the TANGO project, partly thanks to additional funding from the FNRS and the ULB, including an inter-university doctoral thesis (ULiege-UBO). Two PhD students, Martin Dogniez and Manon Bayat, were trained in the application of metabarcoding methods for gut and microbiome analyses and eDNA, also in collaboration with Isabelle George from ULB. M. Dogniez successfully developed molecular protocols further for challenging conditions, namely for non-model organisms coming from remote areas like the Southern Ocean; this work provided both students with important novel skill sets for their future careers. Metabarcoding and eDNA techniques are expected to be widely applied in future ecological research, including assessments of biodiversity at different levels. In view of the fast warming of certain Antarctic regions, generating baseline data of diet and microbiota components for a wide range of endemic meiobenthic invertebrates and for the biodiversity of benthic communities are both essential to follow future alterations in Antarctica due to global change.

The long-term experiment on thermal tolerance of the benthic keystone species *Odontaster validus* (Lamare et al., 2024) was only possible thanks to an international collaboration between the ULB team and researchers from Australia, New Zealand, Monaco, Sweden, Norway and the USA. This study revealed surprising new insights into the effects of global warming in the longer term. While adults of this sea star species could survive at higher temperatures, similarly to some other Antarctic taxa (Morley et al., 2022, 2024), their offspring were strongly affected showing reduced survival, growth and arresting of larval development. Such carry-over effects across generations need to be considered when predicting the effects of increasing seawater temperatures on stenotherm Antarctic organisms as they raise additional concerns for the functioning of marine ecosystems under global warming. Likewise, the observed spatial differentiation of gut microbiomes in a sea urchin illustrates that additional factors shaping the physiological response of endemic Antarctic taxa to global change need to be considered.

5.2. Conference attendances and presentations

- Katz, L., Mitchell, E., Danis, B. (2022). Studying spatial heterogeneities in benthic communties using underwater imagery. Poster presented at: Empowering Biodiversity research II, 24-25 May 2022, Tervuren
- Katz L, Mitchell E, Danis B (2023). Spatial heterogeneity in the Antarctic Peninsula : a case study in Dodman Island, using underwater imagery. Poster presented at: Benelux congress of Zoology 2023, 30-31 May 2023, Leiden
- Voisin, A., Lepoint, G., Danis, B., Guillaumot, C., Kristiansen, A., Pasotti, F., Saucède, T., Michel, L., 2021. Food web structure in a rapidly changing coastal environment: the West Antarctic Peninsula. International Conference on the Applications of Stable Isotope Techniques to Ecological Studies virtual interlude (IsoEcol 11.5), Gaming, Autriche, 19-21/05/2021

- Katz, L., Khan,T.M., Mitchell, E., Moreau, C., Robert, H., Danis, B. (2024). How benthic communities respond to environmental gradients in the West Antarctic Peninsula. Presented at: SCAR Open Science 2024, Pucon
- Katz, L., Mitchell, E., Moreau, C., Ramoisiaux, E., Robert, H., Wallis, B., Danis, B. (2024). Using a mini ROV to document cascading effects in benthic ecosystems of the Antarctic Peninsula. Poster presented at: SCAR Open Science 2024, Pucon
- Dogniez Martin, Camille Moreau, Léa Katz, Bruno Danis, Axelle Brusselman, Bruno Delille, Loïc Michel, Isa Schön & Gilles Lepoint. (2023). Investigating Antarctic benthic communities in a changing climate with a low environmental impact. Poster presentation at the FOCUS day 2023 in Liège (20 December 2023).
- Dogniez Martin, Camille Moreau, Léa Katz, Bruno Danis, Axelle Brusselman, Bruno Delille, Loïc Michel, Isa Schön & Gilles Lepoint. (2024). Using stable isotopes ratios to decipher changes in benthic food webs characteristics along the rapidly warming West Antarctic Peninsula. Poster presentation at the Benelux Association of Stable Isotopes Scientists symposium in Amsterdam (26 - 27 April 2024).
- Dogniez, M., Cadonici, D., Moreau, C., Latz, L., Danis, B., Brusselman, A., Delille, B., Michel, L., Schön, I., & Lepoint, G. (13 December 2024). *Benthic Food Webs in Antarctica ~ Would you care for some more (micro)algae?* [Paper presentation]. Benelux Zoology Congress 2024, Mons, Belgium. https://hdl.handle.net/2268/325575
- Michel, L., Danis, B., De Ridder, C., Dogniez, M., Dubois, P., Eleaume, M., Gallut, C., Le Bourg, B., Saucède, T., Voisin, A., & Lepoint, G. (May 2023). *Trophic plasticity in Antarctic echinoderms: an adaptive trait with implications at ecosystem wide scale?* [Paper presentation]. Workshop on Species Interactions in the Southern Ocean, Gent, Belgium. https://hdl.handle.net/2268/304780
- Brusselman, O. Crabeck, S. Muller, P. A. Araujo, M. Dogniez, G. Lepoint, L. Michel et al. "Glacier meltwater, a potential source of methane in West Antarctica Peninsula." Paper presented at EGU, Vienna, Austria, 16 April 2024. doi:10.5194/egusphere-egu24-18144
- De Borger, E., Buydens, M., Pasotti, F., Braeckman, U., Vanreusel, A. TANGO: Estimating tipping points in habitability of Antarctic benthic ecosystems under global future climate change scenarios. Poster presented at: APECS 2024 Belgian Polar Community Day. 30th April 2024. Ostend.
- Voisin, A., Dogniez, M., Moreau, C., Jeunet, L., Jaffrezic, E., Le Grand, F., Michel, L., Lepoint, G., Thébault, J., & Schaal, G. (June 2024). *Lipids as trophic biomarkers: use and inputs in a food web study of Antarctic benthic ecosystems* [Oral communication]. Lipids in the Ocean, Halifax, Canada. https://hdl.handle.net/2268/324111
- Voisin, A., Dogniez, M., Moreau, C., Thébault, J., Schaal, G., Michel, L., & Lepoint, G. (13 December 2024). *What do grazers really graze on?* [oral communication]. Zoology 2024, Mons, Belgium. https://hdl.handle.net/2268/325968
- Voisin, A., Dogniez, M., Lepoint, G., Michel, L., Thebault Julien, & Schaal Gauthier. (11 September 2025). *Frozen meals: What's on the menu for Antarctic benthic feeders?* [Paper presentation]. BE-Polar.

- Voisin, A., Dogniez, M., Julien Thébault, Lepoint, G., Michel, L., & Gauthier Schaal. (2025). *Biomarkers of change: tracking diets along an environmental gradient in an Antarctic benthic ecosystem* [oral communication]. 14th International Temperate Reef Symposium, Brest, France. https://hdl.handle.net/2268/335052
- Voisin, A., Dogniez, M., Lepoint, G., Michel, L., Thébault Julien, & Schaal Gauthier. (2025). *Frozen Clues: biochemistry to unravel resource partitioning among Antarctic consumers* [Poster presentation]. ZOOlogy 2025. https://hdl.handle.net/2268/338009

6. PUBLICATIONS

6.1. A1 publications

- Braeckman, U., Soetaert, K., Pasotti, F., Quartino, M. L., Vanreusel, A., Saravia, L. A., Schloss, I. R., & van Oevelen, D. (2024). Glacial melt impacts carbon flows in an Antarctic benthic food web. *Frontiers in Marine Science*, *11*. https://doi.org/10.3389/fmars.2024.1359597
- Katz, L., Khan, T.M., Moreau, C., Mitchell, E., Danis, B., 2025. Using Bayesian network inference and underwater imagery to understand the influence of environmental heterogeneities on benthic community structure in the Antarctic Peninsula. Polar Biol 48, 91. https://doi.org/10.1007/s00300-025-03407-4
- Lamare, M., Byrne, M., Danis, B., Deaker, D., Di Luccio, M., Dupont, S., Foo, S. A., Jowett, T., Karelitz, S., Sewell, M. A., Thomas, L. J., & Agüera, A. (2024). Antarctic cushion star *Odontaster validus* larval performance is negatively impacted by long-term parental acclimation to elevated temperature. *Science of The Total Environment*, *956*, 177213. https://doi.org/10.1016/j.scitotenv.2024.177213
- Voisin, A., Lepoint, G., Danis, B., Guillaumot, C., Kristiansen, A., Pasotti, F., Saucède, T., Michel, L. N. (2025). Food web structure in a rapidly changing coastal environment: the West Antarctic Peninsula. *Belgian Journal of Zoology*, *155*(1)119. https://doi.org/10.26496/bjz.2025.201
- Bayat, M., Lilli, G., George, I., Terrana, L., Moreau, C., Danis, B., Dogniez, M. et Michel, L. (Submitted). Realized dietary specialization in an Antarctic keystone species, the sea urchin Sterechinus neumayeri.

6.2. PhD Thesis

- Manon Bayat (submission planned for 2026). Trophic plasticity and gut microbiome variability under climate change context: a case study of a Southern Ocean sea urchin species. Free University Brussels (ULB
- Axelle Brusselman (submission planned for 2026). CO2 and CH4 fluxes along the atmosphere-sea ice-water column-sediment continuum. University of Liège.
- Martin Dogniez (submission planned for 2026). Evolution of benthic food webs across a Southern Ocean in transition. University of Liège
- Léa Katz (submitted and defended in December 2025). Spatial heterogeneity in Antarctic shallow benthos : Insights from ROV imagery and Bayesian network inference. Free University Brussels (ULB)
- Anthony Voisin (submission planned for 19 February 2026). **B**iodive**R**sity **U**nder rapid environmen**TAL** change: community structure, trophic interactions and functional responses in an antarctic benthic ecosystem. University of Liège/University of Western Brittany

6.3. Reports and theses

- Danis, B., Amenabar, M., Bombosch, A., Brusselman, A., Buydens, M., Delille, B., Dogniez, M., Katz, L., Moreau, C., Pasotti, F., Robert, H., & Wallis, B. (2023). Report of the TANGO 1 expedition to the West Antarctic Peninsula. Zenodo. https://doi.org/10.5281/zenodo.8013722

- Danis, B., Bayat, B., Brusselman, A., Coerper, A., De Borger, E., Delille, B., Dogniez, M., Katz, L., Moreau, C., Reade, A., Robert, H., Terrana, L, Voisin, A., Wallis, B. Report of the TANGO 2 expedition to the West Antarctic Peninsula. Zenodo. https://doi.org/10.5281/zenodo.11653690
- Master thesis: Barot, Floriane, and Bruno Danis. "Biodiversité Benthique Du Détroit de Gerlache (Péninsule Antarctique Occidentale) Évaluée Par La Drague Rauschert." Master Thesis, Université Libre de Bruxelles, 2023.
- Master thesis: Buron, Constance, Camille Moreau, Quentin Jossart, and Bruno Danis. "Diversité En Milieu Profond : Cas d'étude de La Famille Des Pterasteridae (Echinodermata : Asteroidea)." Master Thesis, Université Libre de Bruxelles, 2023.
- Master thesis: Deflandre, Lea, and Bruno Danis. "Diversité Benthique de La Péninsule Antarctique Ouest : Cas d'étude Sur l'île de Blaiklock," 2024.
- Master thesis: Dreidemy, Jeanne, and Bruno Danis. "Diversité des communautés benthiques en péninsule Antarctique occidentale: une approche à faible impact environnemental." Master Thesis, Université Libre de Bruxelles, 2022.
- Master thesis: Kassel, Maureen, Camille Moreau, Quentin Jossart, and Bruno Danis. "Phylogénie et Taxonomie Des Odontasteridae (Asteroidea, Echinodermata)." Master Thesis, Université Libre de Bruxelles, 2023.
- Master thesis: Cadonici, Davide,Variabilité des réseaux trophiques benthiques côtiers de la Péninsule Antarctique, Master thesis, University of Liège, 2024
- Master thesis : Hendrickx, Caroline, Variability of benthic food webs in macroalgae habitats in the West Antarctic Peninsula, Master thesis, University of Liège, 2025
- Master thesis : Pouleur Aurore, Étude isotopique d'un réseau trophique benthique en péninsule magellanique, Master thesis, University of Liège, 2023

7. ACKNOWLEDGEMENTS

The TANGO project was funded by BELSPO, where we acknowledge David Cox as liaison. For our research campaigns we thank captain Ben Wallis and crew of the RV Australis, and the dive leaders Francesca Pasotti and Lucas Terrana for TANGO 1 and TANGO 2 respectively. Thanks to Irene Schloss (CADIC) for logistic support of the campaign in Ushuaïa. The research leading to results presented in this publication was carried out with infrastructure funded by EMBRC Belgium - FWO international research infrastructure I001621N (UGent) and by FNRS equipment funding (U.N046.24) (ISOTOPY platform, ULiège). PhD thesis of Axelle Brusselman, Léa Katz and Martin Dogniez was supported by FRIA and FNRS scholarship, respectively. Sample analysis was supported by the analytical labs of the Marine Biology Research Group of Ghent University, Royal Netherlands Institute of Sea Research (NIOZ). Fatty acids analyses were realised at University of Western Brittany (UBO) thanks to a collaboration with LIPIDOCEAN analytical platform (Prof Gauthier Schaal). UBO has also funded the PhD thesis of Anthony Voisin. Lastly, we thank the follow up committee, for which we specifically acknowledge Huw Griffiths (British Antarctic Survey), Craig Smith (UHawaii), Angelika Brandt (Senckenberg, Frankfurt), Kerstin Jerosch (AWI Bremerhaven), Stephanie Langerock (Federal public service for Health, Food chain Safety and Environment), and Lisa Goudeseune (Belgian Biodiversity platform).

8. REFERENCE LIST

Abram, N. J., Purich, A., England, M. H., McCormack, F. S., Strugnell, J. M., Bergstrom, D. M., Vance, T. R., Stål, T., Wienecke, B., Heil, P., Doddridge, E. W., Sallée, J.-B., Williams, T. J., Reading, A. M., Mackintosh, A., Reese, R., Winkelmann, R., Klose, A. K., Boyd, P. W., … Robinson, S. A. (2025). Emerging evidence of abrupt changes in the Antarctic environment. *Nature*, *644*(8077), 621–633. https://doi.org/10.1038/s41586-025-09349-5

Agüera, A., Collard, M., Jossart, Q., Moreau, C., & Danis, B. (2015). Parameter Estimations of Dynamic Energy Budget (DEB) Model over the Life History of a Key Antarctic Species: The Antarctic Sea Star Odontaster validus Koehler, 1906. *PLOS ONE*, *10*(10), e0140078. https://doi.org/10.1371/journal.pone.0140078

Alexeev, V. A., Langen, P. L., & Bates, J. R. (2005). Polar amplification of surface warming on an aquaplanet in "ghost forcing" experiments without sea ice feedbacks. *Climate Dynamics*, *24*(7–8), 655–666. https://doi.org/10.1007/s00382-005-0018-3

Amiraux, R., Archambault, P., Moriceau, B., Lemire, M., Babin, M., Memery, L., Massé, G., & Tremblay, J.-E. (2021). Efficiency of sympagic-benthic coupling revealed by analyses of n-3 fatty acids, IP25 and other highly branched isoprenoids in two filter-feeding Arctic benthic molluscs: Mya truncata and Serripes groenlandicus. *Organic Geochemistry*, *151*, 104160. https://doi.org/10.1016/j.orggeochem.2020.104160

Amsler, C. D., Amsler, M. O., Klein, A. G., Galloway, A. W. E., Iken, K., McClintock, J. B., Heiser, S., Lowe, A. T., Schram, J. B., & Whippo, R. (2023). Strong correlations of sea ice cover with macroalgal cover along the Antarctic Peninsula: Ramifications for present and future benthic communities. *Elementa: Science of the Anthropocene*, *11*(1), 00020. https://doi.org/10.1525/elementa.2023.00020

Angulo-Preckler, C., Turon, M., Præbel, K., Avila, C., & Wangensteen, O. S. (2023). Spatio-temporal patterns of eukaryotic biodiversity in shallow hard-bottom communities from the West Antarctic Peninsula revealed by DNA metabarcoding. *Diversity and Distributions*, *29*(7), 892–911. https://doi.org/10.1111/ddi.13703

Atkinson, A., Hill, S. L., Pakhomov, E. A., Siegel, V., Reiss, C. S., Loeb, V. J., Steinberg, D. K., Schmidt, K., Tarling, G. A., Gerrish, L., & Sailley, S. F. (2019). Krill (Euphausia superba) distribution contracts southward during rapid regional warming. *Nature Climate Change*, *9*(2), 142–147. https://doi.org/10.1038/s41558-018-0370-z

Barnes, D. K. A., & Tarling, G. A. (2017). Polar oceans in a changing climate. *Current Biology*, *27*(11), R454–R460. https://doi.org/10.1016/j.cub.2017.01.045

Bokulich, N. A., Kaehler, B. D., Rideout, J. R., Dillon, M., Bolyen, E., Knight, R., Huttley, G. A., & Gregory Caporaso, J. (2018). Optimizing taxonomic classification of marker-gene amplicon sequences with QIIME 2's q2-feature-classifier plugin. *Microbiome*, *6*(1), 90. https://doi.org/10.1186/s40168-018-0470-z

Bolyen, E., Rideout, J. R., Dillon, M. R., Bokulich, N. A., Abnet, C. C., Al-Ghalith, G. A., Alexander, H., Alm, E. J., Arumugam, M., Asnicar, F., Bai, Y., Bisanz, J. E., Bittinger, K., Brejnrod, A., Brislawn, C. J., Brown, C. T., Callahan, B. J., Caraballo-Rodríguez, A. M., Chase, J., … Caporaso, J. G. (2019). Reproducible, interactive, scalable and extensible microbiome data science using QIIME 2. *Nature Biotechnology*, *37*(8), 852–857. https://doi.org/10.1038/s41587-019-0209-9

Braeckman, U., Pasotti, F., Hoffmann, R., Vázquez, S., Wulff, A., Schloss, I. R., Falk, U., Deregibus, D., Lefaible, N., Torstensson, A., Al-Handal, A., Wenzhöfer, F., & Vanreusel, A. (2021). Glacial melt disturbance shifts community metabolism of an Antarctic seafloor ecosystem from net autotrophy to heterotrophy. *Communications Biology*, *4*(1), Article 1. https://doi.org/10.1038/s42003-021-01673-6

Braeckman, U., Pasotti, F., Vázquez, S., Zacher, K., Hoffmann, R., Elvert, M., Marchant, H., Buckner, C., Quartino, M. L., & Mác Cormack, W. (2019). Degradation of macroalgal detritus in shallow coastal Antarctic sediments. *Limnology and Oceanography*, *64*(4), 1423–1441.

Braeckman, U., Soetaert, K., Pasotti, F., Quartino, M. L., Vanreusel, A., Saravia, L. A., Schloss, I. R., & van Oevelen, D. (2024). Glacial melt impacts carbon flows in an Antarctic benthic food web. *Frontiers in Marine Science*, *11*. https://doi.org/10.3389/fmars.2024.1359597

Brasier, M. J., Grant, S. M., Trathan, P. N., Allcock, L., Ashford, O., Blagbrough, H., Brandt, A., Danis, B., Downey, R., Eléaume, M. P., Enderlein, P., Ghiglione, C., Hogg, O., Linse, K., Mackenzie, M., Moreau, C., Robinson, L. F., Rodriguez, E., Spiridonov, V., … Griffiths, H. J. (2018). Benthic biodiversity in the South Orkney Islands Southern Shelf Marine Protected Area. *Biodiversity*, 1–15. https://doi.org/10.1080/14888386.2018.1468821

Brasier, M. J., Wiklund, H., Neal, L., Jeffreys, R., Linse, K., Ruhl, H., & Glover, A. G. (2016). DNA barcoding uncovers cryptic diversity in 50% of deep-sea Antarctic polychaetes. *Royal Society Open Science*, *3*(11), 160432. https://doi.org/10.1098/rsos.160432

Broyer, C. de, & Koubbi, P. (2014). *Biogeographic atlas of the Southern Ocean* [Map]. The Scientific Committee on Antarctic Research, Scott Polar Research Institute.

Brueggeman, P. (1998). *Underwater Field Guide to Ross Island & McMurdo Sound, Antarctica*.

Buschi, E., Tangherlini, M., Martire, M. L., & Corinaldesi, C. (2025). The juvenile Antarctic whelk Neobuccinum eatoni maintains a specialized microbiome in its proboscis even in adulthood. *Polar Biology*, *48*(2), 68. https://doi.org/10.1007/s00300-025-03388-4

Byrne, M., & Lamare, M. D. (2024). Climate change and polar marine invertebrates: Life-history responses in a warmer, high CO2 world. *Journal of Experimental Biology*, *227*(23), jeb245765. https://doi.org/10.1242/jeb.245765

Carlini, R., Coria, R., Santos, M. M., & Daneri, G. (2009). Responses of Antarctic marine fauna to environmental change. *Polar Biology*, *32*, 1427–1433. https://doi.org/10.1007/s00300-009-0640-7

Chown, S. L., Clarke, A., Fraser, C. I., & others. (2015). The changing form of Antarctic biodiversity. *Nature*, *522*, 431–438. https://doi.org/10.1038/nature14505

Clark, G. F., Stark, J. S., Palmer, A. S., Riddle, M. J., & Johnston, E. L. (2017). The Roles of Sea-Ice, Light and Sedimentation in Structuring Shallow Antarctic Benthic Communities. *PLOS ONE*, *12*(1), e0168391. https://doi.org/10.1371/journal.pone.0168391

Clark, M. S., Villota Nieva, L., Hoffman, J. I., Davies, A. J., Trivedi, U. H., Turner, F., Ashton, G. V., & Peck, L. S. (2019). Lack of long-term acclimation in Antarctic encrusting species suggests vulnerability to warming. *Nature Communications*, *10*(1), 3383. https://doi.org/10.1038/s41467-019-11348-w

Clarke, L. J., Suter, L., King, R., Bissett, A., Bestley, S., & Deagle, B. E. (2021). Bacterial epibiont communities of panmictic Antarctic krill are spatially structured. *Molecular Ecology*, *30*(4), 1042–1052. https://doi.org/10.1111/mec.15771

Clarke, L. J., Suter, L., King, R., Bissett, A., & Deagle, B. E. (2019). Antarctic Krill Are Reservoirs for Distinct Southern Ocean Microbial Communities. *Frontiers in Microbiology*, *9*, 3226. https://doi.org/10.3389/fmicb.2018.03226

Constable, A., Melbourne-Thomas, J., Corney, S., Arrigo, K., Barnes, D., Bindoff, N., Boyd, P., Brandt, A., Costa, D., Davidson, A., Ducklow, H., Emmerson, L., Fukuchi, M., Gutt, J., Hindell, M., Hofmann, E., Hosie, G., Iida, T., & Ziegler, P. (2014). Climate change and Southern Ocean ecosystems I: How changes in physical habitats directly affect marine biota. *Global Change Biology*, *20*. https://doi.org/10.1111/gcb.12623

Convey, P., Chown, S. L., Clarke, A., & others. (2014). The terrestrial biodiversity of Antarctica. *Ecological Monographs*, *84*, 203–244. https://doi.org/10.1890/12-2390.1

Coplen, T. B. (2011). Guidelines and recommended terms for expression of stable-isotope-ratio and gas-ratio measurement results. *Rapid Communications in Mass Spectrometry: RCM*, *25*(17), 2538–2560. https://doi.org/10.1002/rcm.5129

Couturier, L. I. E., Michel, L. N., Amaro, T., Budge, S. M., Da Costa, E., De Troch, M., Di Dato, V., Fink, P., Giraldo, C., Le Grand, F., Loaiza, I., Mathieu-Resuge, M., Nichols, P. D., Parrish, C. C., Sardenne, F., Vagner, M., Pernet, F., & Soudant, P. (2020). State of art and best practices for

fatty acid analysis in aquatic sciences. *ICES Journal of Marine Science*, *77*(7–8), 2375–2395. https://doi.org/10.1093/icesjms/fsaa121

Danis, B. (2024). *Report of the TANGO 2 expedition to the West Antarctic Peninsula*. Zenodo. https://doi.org/10.5281/ZENODO.11653689

Danis, B., Amenabar, M., Bombosch, A., Brusselman, A., Buydens, M., Delille, B., Dogniez, M., Katz, L., Moreau, C., Pasotti, F., Robert, H., & Wallis, B. (2023). *Report of the TANGO 1 expedition to the West Antarctic Peninsula*. Zenodo. https://doi.org/10.5281/ZENODO.8013722

Danis, B., Christiansen, H., Guillaumot, C., Heindler, F. M., Jossart, Q., Moreau, C., Pasotti, F., Robert, H., Wallis, B., & Saucède, T. (2021). The Belgica 121 expedition to the Western Antarctic Peninsula: A detailed biodiversity census. *Biodiversity Data Journal*, *9*, e70590. https://doi.org/10.3897/BDJ.9.e70590

Dayton, P. K., & Jarrell, S. C. (2017). Ecosystem Management in Antarctic Coastal Areas. *Ecological Applications*, *18*, 181–200. https://doi.org/10.1890/07-1950.1

Deregibus, D., Campana, G. L., Neder, C., Barnes, D. K. A., Zacher, K., Piscicelli, J. M., Jerosch, K., & Quartino, M. L. (2023). Potential macroalgal expansion and blue carbon gains with northern Antarctic Peninsula glacial retreat. *Marine Environmental Research*, *189*, 106056. https://doi.org/10.1016/j.marenvres.2023.106056

Deregibus, D., Quartino, M. L., Campana, G. L., Momo, F. R., Wiencke, C., & Zacher, K. (2016). Photosynthetic light requirements and vertical distribution of macroalgae in newly ice-free areas in Potter Cove, South Shetland Islands, Antarctica. *Polar Biology*, *39*(1), 153–166. https://doi.org/10.1007/s00300-015-1679-y

Dettai, A., Adamowizc, S. J., Allcock, L., Arango, C. P., Barnes, D. K. A., Barratt, I., Chenuil, A., Couloux, A., Cruaud, C., David, B., Denis, F., Denys, G., Díaz, A., Eléaume, M., Féral, J.-P., Froger, A., Gallut, C., Grant, R., Griffiths, H. J., … Ameziane, N. (2011). DNA barcoding and molecular systematics of the benthic and demersal organisms of the CEAMARC survey. *Polar Science*, *5*(2), 298–312. https://doi.org/10.1016/j.polar.2011.02.002

Dray, S., Bauman, D., Borcard, D., Clappe, S., Guenard, G., Jombart, T., Larocque, G., Legendre, P., Madi, N., & Wagner, H. (2026). *adespatial: Miltivariate Multiscale spatial analysis* (Version 0.3-28) [Computer software]. https://CRAN.R-project.org/package=adespatial

Ducklow, H. W., Fraser, W., Meredith, M. P., & others. (2013). West Antarctic Peninsula: An ice-dependent coastal marine ecosystem in transition. *Oceanography*, *26*, 190–203. https://doi.org/10.5670/oceanog.2013.62

Feng, J., Li, D., Zhang, J., & Zhao, L. (2022). Variations and Environmental Controls of Primary Productivity in the Amundsen Sea. *Frontiers in Marine Science*, *9*. https://doi.org/10.3389/fmars.2022.891663

Ferchiou, S., Tounsi, A., Fronton, F., Caza, F., Lejeune, M., Tornos, J., Boulinier, T., & St-Pierre, Y. (2025). Circulating microbiome DNA in Southern Ocean seabirds: A novel tool for disease surveillance in polar ecosystems. *Global Ecology and Conservation*, *62*, e03774. https://doi.org/10.1016/j.gecco.2025.e03774

Ferrero, L., Balazy, P., Kuklinski, P., & Sahade, R. (2026). Diversity and spatial distribution patterns of shallow benthic assemblages in Admiralty Bay, South Shetland Islands. *Marine Environmental Research*, *213*, 107640. https://doi.org/10.1016/j.marenvres.2025.107640

Folmer, O., Black, M., Hoeh, W., Lutz, R., & Vrijenhoek, R. (1994). DNA primers for amplification of mitochondrial cytochrome c oxidase subunit I from diverse metazoan invertebrates. *Molecular Marine Biology and Biotechnology*, *3*(5), 294–299.

Fox, A. J., & Vaughan, D. G. (2005). The retreat of Jones Ice Shelf, Antarctic Peninsula. *Journal of Glaciology*, *51*(175), 555–560. https://doi.org/10.3189/172756505781829043

Geller, J., Meyer, C., Parker, M., & Hawk, H. (2013). Redesign of PCR primers for mitochondrial cytochrome c oxidase subunit I for marine invertebrates and application in all-taxa biotic surveys. *Molecular Ecology Resources*, *13*(5), 851–861. https://doi.org/10.1111/1755-0998.12138

González-Aravena, M., Perrois, G., Font, A., Cárdenas, C. A., & Rondon, R. (2024). Microbiome profile of the Antarctic clam Laternula elliptica. *Brazilian Journal of Microbiology*, *55*(1), 487–497. https://doi.org/10.1007/s42770-023-01200-1

Gorodetskaya, I. V., Durán-Alarcón, C., González-Herrero, S., Clem, K. R., Zou, X., Rowe, P., Rodriguez Imazio, P., Campos, D., Leroy-Dos Santos, C., Dutrievoz, N., Wille, J. D., Chyhareva, A., Favier, V., Blanchet, J., Pohl, B., Cordero, R. R., Park, S.-J., Colwell, S., Lazzara, M. A., … Picard, G. (2023). Record-high Antarctic Peninsula temperatures and surface melt in February 2022: A compound event with an intense atmospheric river. *Npj Climate and Atmospheric Science*, *6*(1), 202. https://doi.org/10.1038/s41612-023-00529-6

Grant, R. A., Griffiths, H. J., Steinke, D., Wadley, V., & Linse, K. (2011). Antarctic DNA barcoding; a drop in the ocean? *Polar Biology*, *34*(5), 775–780. https://doi.org/10.1007/s00300-010-0932-7

Griffiths, H. J., Danis, B., & Clarke, A. (2011). Quantifying Antarctic marine biodiversity: The SCAR-MarBIN data portal. *Deep Sea Research Part II: Topical Studies in Oceanography*, *58*(1–2), 18–29. https://doi.org/10.1016/j.dsr2.2010.10.008

Gutt, J., Alvaro, M. C., Barco, A., Böhmer, A., Bracher, A., David, B., De Ridder, C., Dorschel, B., Eléaume, M., Janussen, D., Kersken, D., López-González, P. J., Martínez-Baraldés, I., Schröder, M., Segelken-Voigt, A., & Teixidó, N. (2016). Macroepibenthic communities at the tip of the Antarctic Peninsula, an ecological survey at different spatial scales. *Polar Biology*, *39*(5), 829–849. https://doi.org/10.1007/s00300-015-1797-6

Gutt, J., Arndt, J., Kraan, C., Dorschel, B., Schröder, M., Bracher, A., & Piepenburg, D. (2019). Benthic communities and their drivers: A spatial analysis off the Antarctic Peninsula. *Limnology and Oceanography*, *64*(6), 2341–2357. https://doi.org/10.1002/lno.11187

Gutt, J., Griffiths, H. J., & Jones, C. D. (2013). Circumpolar overview and spatial heterogeneity of Antarctic macrobenthic communities. *Marine Biodiversity*, *43*(4), 481–487. https://doi.org/10.1007/s12526-013-0152-9

Gutt, J., Isla, E., Bertolin, M., & others. (2015). Environmental drivers of biodiversity and ecosystem processes in the Southern Ocean. *Global Change Biology*, *21*, 1434–1453. https://doi.org/10.1111/gcb.12705

Ha, S.-Y., Ahn, I.-Y., Moon, H.-W., Choi, B., & Shin, K.-H. (2019). Tight trophic association between benthic diatom blooms and shallow-water megabenthic communities in a rapidly deglaciated Antarctic fjord. *Estuarine, Coastal and Shelf Science*, *218*, 258–267. https://doi.org/10.1016/j.ecss.2018.12.020

Havermans, C., Seefeldt, M. A., & Held, C. (2018). A biodiversity survey of scavenging amphipods in a proposed marine protected area: The Filchner area in the Weddell Sea, Antarctica. *Polar Biology*, *41*(7), 1371–1390. https://doi.org/10.1007/s00300-018-2292-7

Heindler, F. M., Christiansen, H., Frédérich, B., Dettaï, A., Lepoint, G., Maes, G. E., Van De Putte, A. P., & Volckaert, F. A. M. (2018). Historical DNA Metabarcoding of the Prey and Microbiome of Trematomid Fishes Using Museum Samples. *Frontiers in Ecology and Evolution*, *6*, 151. https://doi.org/10.3389/fevo.2018.00151

Henley, S. F., Cavan, E. L., Fawcett, S. E., Kerr, R., Monteiro, T., Sherrell, R. M., Bowie, A. R., Boyd, P. W., Barnes, D. K. A., Schloss, I. R., Marshall, T., Flynn, R., & Smith, S. (2020). Changing Biogeochemistry of the Southern Ocean and Its Ecosystem Implications. *Frontiers in Marine Science*, *7*. https://www.frontiersin.org/articles/10.3389/fmars.2020.00581

Hoegh-Guldberg, O., & Pearse, J. S. (1995). Temperature, Food Availability, and the Development of Marine Invertebrate Larvae. *American Zoologist*, *35*(4), 415–425. https://doi.org/10.1093/icb/35.4.415

Hoffmann, R., Al-Handal, A. Y., Wulff, A., Deregibus, D., Zacher, K., Quartino, M. L., Wenzhöfer, F., & Braeckman, U. (2019). Implications of Glacial Melt-Related Processes on the Potential Primary Production of a Microphytobenthic Community in Potter Cove (Antarctica). *Frontiers in Marine Science*, *6*, 655. https://doi.org/10.3389/fmars.2019.00655

Hui, E., Stafford, R., Matthews, I. M., & Smith, V. A. (2022). Bayesian networks as a novel tool to enhance interpretability and predictive power of ecological models. *Ecological Informatics*, *68*, 101539. https://doi.org/10.1016/j.ecoinf.2021.101539

Intergovernmental Panel On Climate Change (Ipcc). (2022). *The Ocean and Cryosphere in a Changing Climate: Special Report of the Intergovernmental Panel on Climate Change* (1st ed.). Cambridge University Press. https://doi.org/10.1017/9781009157964

Isla, E., Masqué, P., Palanques, A., Sanchez-Cabeza, J. A., Bruach, J. M., Guillén, J., & Puig, P. (2002). Sediment accumulation rates and carbon burial in the bottom sediment in a high-productivity area: Gerlache Strait (Antarctica). *Deep Sea Research Part II: Topical Studies in Oceanography*, *49*(16), 3275–3287. https://doi.org/10.1016/S0967-0645(02)00083-8

Jossart, Q., Sands, C. J., & Sewell, M. A. (2019). Dwarf brooder versus giant broadcaster: Combining genetic and reproductive data to unravel cryptic diversity in an Antarctic brittle star. *Heredity*, *123*(5), 622–633. https://doi.org/10.1038/s41437-019-0228-9

Katz, L., Khan, T. M., Moreau, C., Mitchell, E., & Danis, B. (2025). Using Bayesian network inference and underwater imagery to understand the influence of environmental heterogeneities on benthic community structure in the Antarctic Peninsula. *Polar Biology*, *48*(3), 91. https://doi.org/10.1007/s00300-025-03407-4

Kawaguchi, S., Atkinson, A., Bahlburg, D., Bernard, K. S., Cavan, E. L., Cox, M. J., Hill, S. L., Meyer, B., & Veytia, D. (2024). Climate change impacts on Antarctic krill behaviour and population dynamics. *Nature Reviews Earth & Environment*, *5*(1), 43–58. https://doi.org/10.1038/s43017-023-00504-y

Kennicutt, M., Bromwich, D., Liggett, D., Njåstad, B., Peck, L., Rintoul, S., Ritz, C., Siegert, M., Aitken, A., Brooks, C., Cassano, J., Chaturvedi, S., Chen, D., Dodds, K., Golledge, N., Le Bohec, C., Leppe, M., Murray, A., Nath, P., & Chown, S. (2019). One Earth Review Sustained Antarctic Research: A 21 st Century Imperative. *One Earth*, *1*, 95–113. https://doi.org/10.1016/j.oneear.2019.08.014

Kohlbach, D., Lange, B. A., Schaafsma, F. L., David, C., Vortkamp, M., Graeve, M., van Franeker, J. A., Krumpen, T., & Flores, H. (2017). Ice Algae-Produced Carbon Is Critical for Overwintering of Antarctic Krill Euphausia superba. *Frontiers in Marine Science*, *4*. https://doi.org/10.3389/fmars.2017.00310

Lamarche-Gagnon, G., Wadham, J. L., Sherwood Lollar, B., Arndt, S., Fietzek, P., Beaton, A. D., Tedstone, A. J., Telling, J., Bagshaw, E. A., Hawkings, J. R., Kohler, T. J., Zarsky, J. D., Mowlem, M. C., Anesio, A. M., & Stibal, M. (2019). Greenland melt drives continuous export of methane from the ice-sheet bed. *Nature*, *565*(7737), 73–77. https://doi.org/10.1038/s41586-018-0800-0

Lamare, M., Byrne, M., Danis, B., Deaker, D., Di Luccio, M., Dupont, S., Foo, S. A., Jowett, T., Karelitz, S., Sewell, M. A., Thomas, L. J., & Agüera, A. (2024). Antarctic cushion star Odontaster validus larval performance is negatively impacted by long-term parental acclimation to elevated temperature. *Science of The Total Environment*, *956*, 177213. https://doi.org/10.1016/j.scitotenv.2024.177213

Layman, C. A., Arrington, D. A., Montaña, C. G., & Post, D. M. (2007). Can stable isotope ratios provide for community-wide measures of trophic structure? *Ecology*, *88*(1), 42–48. https://doi.org/10.1890/0012-9658(2007)88%255B42:CSIRPF%255D2.0.CO;2

Massonnet, F., Barreira, S., Barthélemy, A., Bilbao, R., Blanchard-Wrigglesworth, E., Blockley, E., Bromwich, D. H., Bushuk, M., Dong, X., Goessling, H. F., Hobbs, W., Iovino, D., Lee, W.-S., Li, C., Meier, W. N., Merryfield, W. J., Moreno-Chamarro, E., Morioka, Y., Li, X., … Yuan, X. (2023). SIPN South: Six years of coordinated seasonal Antarctic sea ice predictions. *Frontiers in Marine Science*, *10*. https://doi.org/10.3389/fmars.2023.1148899

McClintock, J. B., Pearse, J. S., & Bosch, I. (1988). Population structure and energetics of the shallow-water antarctic sea star Odontaster validus in contrasting habitats. *Marine Biology*, *99*(2), 235–246. https://doi.org/10.1007/BF00391986

Mendes, C. R. B., Tavano, V. M., Dotto, T. S., Kerr, R., de Souza, M. S., Garcia, C. A. E., & Secchi, E. R. (2018). New insights on the dominance of cryptophytes in Antarctic coastal waters: A case study in Gerlache Strait. *Deep Sea Research Part II: Topical Studies in Oceanography*, *149*, 161–170. https://doi.org/10.1016/j.dsr2.2017.02.010

Michel, L. N., Danis, B., Dubois, P., Eleaume, M., Fournier, J., Gallut, C., Jane, P., & Lepoint, G. (2019). Increased sea ice cover alters food web structure in East Antarctica. *Scientific Reports*, *9*(1), 8062. https://doi.org/10.1038/s41598-019-44605-5

Milns, I., Beale, C. M., & Smith, V. A. (2010). Revealing ecological networks using Bayesian network inference algorithms. *Ecology*, *91*(7), 1892–1899. https://doi.org/10.1890/09-0731.1

Moline, M. A., Claustre, H., Frazer, T. K., Schofield, O., & Vernet, M. (2004). Alteration of the food web along the Antarctic Peninsula in response to a regional warming trend. *Global Change Biology*, *10*(12), 1973–1980. https://doi.org/10.1111/j.1365-2486.2004.00825.x

Moreau, S., Mostajir, B., Bélanger, S., Schloss, I. R., Vancoppenolle, M., Demers, S., & Ferreyra, G. A. (2015). Climate change enhances primary production in the western Antarctic Peninsula. *Global Change Biology*, *21*(6), 2191–2205. https://doi.org/10.1111/gcb.12878

Morley, S. A., Bates, A. E., Clark, M. S., Fitzcharles, E., Smith, R., Stainthorp, R. E., & Peck, L. S. (2024). Testing the Resilience, Physiological Plasticity and Mechanisms Underlying Upper Temperature Limits of Antarctic Marine Ectotherms. *Biology*, *13*(4), 224. https://doi.org/10.3390/biology13040224

Morley, S. A., Chu, J. W. F., Peck, L. S., & Bates, A. E. (2022). Temperatures leading to heat escape responses in Antarctic marine ectotherms match acute thermal limits. *Frontiers in Physiology*, *13*, 1077376. https://doi.org/10.3389/fphys.2022.1077376

Nester, G. M., Suter, L., Kitchener, J. A., Bunce, M., Polanowski, A. M., Wasserman, J., & Deagle, B. (2024). Long-distance Southern Ocean environmental DNA (eDNA) transect provides insights into spatial marine biota and invasion pathways for non-native species. *Science of The Total Environment*, *951*, 175657. https://doi.org/10.1016/j.scitotenv.2024.175657

Ni, X., Liu, X., Pang, S., Dong, Y., Guo, B., Zhang, Y., Wu, Y., Su, D., Xu, A., Yuan, Q., Wu, X., Yang, L., Wu, X., Wang, Z., Xiao, X., & Liang, Q. (2025). Global marine methane seepage: Spatiotemporal patterns and ocean current control. *Marine Geology*, *487*, 107589. https://doi.org/10.1016/j.margeo.2025.107589

Ochoa-Sánchez, M., Acuña Gomez, E. P., Ramírez-Fenández, L., Eguiarte, L. E., & Souza, V. (2023). Current knowledge of the Southern Hemisphere marine microbiome in eukaryotic hosts and the Strait of Magellan surface microbiome project. *PeerJ*, *11*, e15978. https://doi.org/10.7717/peerj.15978

Oliver, E. C. J., Donat, M. G., Burrows, M. T., & others. (2015). Marine heatwaves. *Trends in Ecology & Evolution*, *30*, 673–684. https://doi.org/10.1016/j.tree.2015.08.010

Pasotti, F., Saravia, L. A., De Troch, M., & others. (2015). Benthic responses to environmental change around Antarctic glacier fronts. *Marine Ecology*, *36*, 716–733. https://doi.org/10.1111/maec.12181

Peck, L. S., Morley, S. A., Pörtner, H.-O., & Clark, M. S. (2007). Thermal limits of burrowing capacity are linked to oxygen availability and size in the Antarctic clam Laternula elliptica. *Oecologia*, *154*(3), 479–484. https://doi.org/10.1007/s00442-007-0858-0

Peck, L., Webb, K., Miller, A., Clark, M., & Hill, T. (2008). Temperature limits to activity, feeding and metabolism in the Antarctic starfish Odontaster validus. *Marine Ecology Progress Series*, *358*, 181–189. https://doi.org/10.3354/meps07336

Pörtner, H. O., Roberts, D., Masson-Delmotte, V., & others. (2019). IPCC Special Report on the Ocean and Cryosphere in a Changing Climate. In *SROCC*. IPCC.

Posit team. (2022). *RStudio: Integrated Development Environment for R*. Posit Software, PBC. http://www.posit.co/

Quezada-Romegialli, C., Jackson, A. L., Hayden, B., Kahilainen, K. K., Lopes, C., & Harrod, C. (2018). tRophicPosition, an r package for the Bayesian estimation of trophic position from consumer

stable isotope ratios. *Methods in Ecology and Evolution*, *9*(6), 1592–1599. https://doi.org/10.1111/2041-210X.13009

R Core Team. (2021). *R: A Language and Environment for Statistical Computing*. R Foundation for Statistical Computing. https://www.R-project.org/

Rantanen, M., Karpechko, A. Yu., Lipponen, A., Nordling, K., Hyvärinen, O., Ruosteenoja, K., Vihma, T., & Laaksonen, A. (2022). The Arctic has warmed nearly four times faster than the globe since 1979. *Communications Earth & Environment*, *3*(1), 168. https://doi.org/10.1038/s43247-022-00498-3

Raynaud, D., Delmas, R., Ascencio, J. M., & Legrand, M. (1982). Gas Extraction From Polar Ice Cores: A Critical Issue For Studying The Evolution of Atmospheric CO2 and Ice-Sheet Surface Elevation. *Annals of Glaciology*, *3*, 265–268. https://doi.org/10.3189/S0260305500002895

Robeson, M. S., O'Rourke, D. R., Kaehler, B. D., Ziemski, M., Dillon, M. R., Foster, J. T., & Bokulich, N. A. (2021). RESCRIPt: Reproducible sequence taxonomy reference database management. *PLOS Computational Biology*, *17*(11), e1009581. https://doi.org/10.1371/journal.pcbi.1009581

Rossi, L., Sporta Caputi, S., Calizza, E., Careddu, G., Oliverio, M., Schiaparelli, S., & Costantini, M. L. (2019). Antarctic food web architecture under varying dynamics of sea ice cover. *Scientific Reports*, *9*(1), 12454. https://doi.org/10.1038/s41598-019-48245-7

Sahade, R., Lagger, C., Torre, L., Momo, F., Monien, P., Schloss, I., Barnes, D. K. A., Servetto, N., Tarantelli, S., Tatián, M., Zamboni, N., & Abele, D. (2015). Climate change and glacier retreat drive shifts in an Antarctic benthic ecosystem. *Science Advances*, *1*(10), e1500050. https://doi.org/10.1126/sciadv.1500050

Sands, C. J., Zwerschke, N., Bax, N., Barnes, D. K. A., & Moreau, C. (2023). The Growing Potential of Antarctic Blue Carbon. *Oceanography*, *36*(1), 16–17. https://doi.org/10.5670/oceanog.2023.s1.5

Schories, D., & Kohlberg, G. (Eds.). (2016). *Marine wildlife: King George Island, Antarctica: identification guide* (1. edition). Dirk Schories Publications.

Schwob, G., Cabrol, L., Saucède, T., Gérard, K., Poulin, E., & Orlando, J. (2024). Unveiling the co-phylogeny signal between plunderfish *Harpagifer* spp. And their gut microbiomes across the Southern Ocean. *Microbiology Spectrum*, *12*(4), e03830-23. https://doi.org/10.1128/spectrum.03830-23

Skinner, C., Mill, A. C., Newman, S. P., Newton, J., Cobain, M. R. D., & Polunin, N. V. C. (2019). Novel tri-isotope ellipsoid approach reveals dietary variation in sympatric predators. *Ecology and Evolution*, *9*(23), 13267–13277. https://doi.org/10.1002/ece3.5779

Smale, D. A., Barnes, D. K. A., & Fraser, K. P. P. (2007). The influence of ice scour on benthic communities at three contrasting sites at Adelaide Island, Antarctica. *Austral Ecology*, *32*(8), 878–888. https://doi.org/10.1111/j.1442-9993.2007.01776.x

Smith, C. R., DeMaster, D. J., Thomas, C., Sršen, P., Grange, L., Evrard, V., & DeLeo, F. (2012). Pelagic-benthic coupling, food banks, and climate change on the West Antarctic Peninsula Shelf. *Oceanography*, *25*(3), 188–201.

Song, W., Li, L., Huang, H., Jiang, K., Zhang, F., Chen, X., Zhao, M., & Ma, L. (2016). The Gut Microbial Community of Antarctic Fish Detected by 16S rRNA Gene Sequence Analysis. *BioMed Research International*, *2016*, 1–7. https://doi.org/10.1155/2016/3241529

Stammerjohn, S. E., Martinson, D. G., Smith, R. C., & Iannuzzi, R. A. (2008). Sea ice in the West Antarctic Peninsula region. *Deep-Sea Research Part II*, *55*, 2041–2058. https://doi.org/10.1016/j.dsr2.2008.04.026

Thibodeau, P., Song, B., Moreno, C., & Steinberg, D. (2022). Feeding ecology and microbiome of the pteropod Limacina helicina antarctica. *Aquatic Microbial Ecology*, *88*, 19–24. https://doi.org/10.3354/ame01981

Thurber, A. R., Seabrook, S., & Welsh, R. M. (2020). Riddles in the cold: Antarctic endemism and microbial succession impact methane cycling in the Southern Ocean. *Proceedings of the*

Royal Society B: Biological Sciences, *287*(1931), 20201134. https://doi.org/10.1098/rspb.2020.1134

Torre, L., Servetto, N., Eöry, M. L., Momo, F., Tatián, M., Abele, D., & Sahade, R. (2012). Respiratory responses of three Antarctic ascidians and a sea pen to increased sediment concentrations. *Polar Biology*, *35*(11), 1743–1748. https://doi.org/10.1007/s00300-012-1208-1

Turner, J., Maksym, T., Phillips, T., Marshall, G. J., & Meredith, M. P. (2013). Impact of changes in sea ice advance on the large winter warming on the western Antarctic Peninsula. *International Journal of Climatology*, *33*, 852–861. https://doi.org/10.1002/joc.3474

Vargas, S., Kelly, M., Schnabel, K., Mills, S., Bowden, D., & Wörheide, G. (2015). Diversity in a Cold Hot-Spot: DNA-Barcoding Reveals Patterns of Evolution among Antarctic Demosponges (Class Demospongiae, Phylum Porifera). *PLOS ONE*, *10*(6), e0127573. https://doi.org/10.1371/journal.pone.0127573

Vause, B. J., Morley, S. A., Fonseca, V. G., Jażdżewska, A., Ashton, G. V., Barnes, D. K. A., Giebner, H., Clark, M. S., & Peck, L. S. (2019). Spatial and temporal dynamics of Antarctic shallow soft-bottom benthic communities: Ecological drivers under climate change. *BMC Ecology*, *19*(1), 27. https://doi.org/10.1186/s12898-019-0244-x

Voisin, A., Lepoint, G., Danis, B., Guillaumot, C., Kristiansen, A., Pasotti, F., Saucède, T., & Michel, L. N. (2025). Food web structure in a rapidly changing coastal environment: The West Antarctic Peninsula. *Belgian Journal of Zoology*, *155*, 93–119. https://doi.org/10.26496/bjz.2025.201

Wangensteen, O. S., Palacín, C., Guardiola, M., & Turon, X. (2018). DNA metabarcoding of littoral hard-bottom communities: High diversity and database gaps revealed by two molecular markers. *PeerJ*, *6*, e4705. https://doi.org/10.7717/peerj.4705

Watts, J. (2021). *Antarctic Marine Wildlife: Antarctic Peninsula, Weddell Sea & Scotia Sea*. Jamie Watts Publications.

Weiss, R. F. (1981). "The production of nitrous oxide and methane in the sea." Environmental Science & Technology, 15(10), 1228-1234.

Wright, S. W., & Mantoura, R. F. C. (1997). Guidelines for collection and pigment analysis of field samples. In S. W. Jeffrey, R. F. C. Mantoura, & S. W. Wright, *Phytoplankton pigments in oceanography: Guidelines to modern methods.* (p. 661). UNESCO publishing.

Yu, J., Smith, V. A., Wang, P. P., Hartemink, A. J., & Jarvis, E. D. (2004). Advances to Bayesian network inference for generating causal networks from observational biological data. *Bioinformatics*, *20*(18), 3594–3603. https://doi.org/10.1093/bioinformatics/bth448

Zwerschke, N., Sands, C. J., Roman-Gonzalez, A., Barnes, D. K. A., Guzzi, A., Jenkins, S., Muñoz-Ramírez, C., & Scourse, J. (2022). Quantification of blue carbon pathways contributing to negative feedback on climate change following glacier retreat in West Antarctic fjords. *Global Change Biology*, *28*(1), 8–20. https://doi.org/10.1111/gcb.15898

9. ANNEXES

Measured sediment properties

Table S. 1: Measured sediment properties overaged over to top 2 cm (n = 3, average ± SD). Median grain size (d0.5, µm), grain size distribution percentages of clay, silt, very fine sand, fine sand, medium sand, coarse sand, and very coarse sand, and total organic carbon (TOC) and total nitrogen (TN) as percentage of dry sediment mass.

Location	subsite	d0.5	clay	silt	vfsand	Fsand	Msand	Csand	Vcsand	TOC	TN
Dodman Island	Pool 2	44.7 ± 3.8	41.3 ± 3.6	23.6 ± 0.5	24.4 ± 2.6	7.2 ± 1.3	1.5 ± 0.3	0.7 ± 0.2	0 ± 0	2.2 ± 0.3	0.4 ± 0
	Pool 3	105.4 ± 5.9	12.3 ± 2.4	12.5 ± 1.1	34.6 ± 1	30.7 ± 2.3	7.9 ± 1	1.1 ± 0.5	0.5 ± 0.3	0.3 ± 0.1	0.1 ± 0.1
	Pool 4	153.9 ± 18	2.2 ± 1.4	5 ± 1.9	30.3 ± 3.6	38.9 ± 2.4	15.4 ± 3.4	5.3 ± 2	2.9 ± 1.9	0.1 ± 0	0 ± 0
Blaiklock Island	Site 1	35.7 ± 4.2	50.4 ± 4.5	20.4 ± 1.8	17.6 ± 1.5	6 ± 0.6	2.3 ± 1	0.7 ± 0.5	0 ± 0	2.4 ± 0.1	0.4 ± 0
	Site 2	110.9 ± 13	23.8 ± 3.1	8.1 ± 0.7	21.3 ± 0.7	27.7 ± 1.3	14 ± 1.5	3 ± 1.2	0.5 ± 0.6	0.3 ± 0	0.1 ± 0
Melchior Island	Site 1	59.4 ± 11.9	37.3 ± 4	13.9 ± 1.7	16.8 ± 0.3	13.4 ± 2	10.5 ± 2.2	5.7 ± 1.4	0.9 ± 0.4	1 ± 0.2	0.2 ± 0
	Site 2	116.8 ± 116.2	29.1 ± 17.9	13.4 ± 6	17.8 ± 3.4	14.6 ± 5	14.6 ± 11.6	8.2 ± 9	1.2 ± 2	0.5 ± 0.3	0.1 ± 0
Hovgaard Island	Site 1	31.4 ± 0.7	58.1 ± 1	22.8 ± 0	14.4 ± 0.5	2.1 ± 0.4	0.9 ± 0.2	0.1 ± 0	0 ± 0	4.6 ± 0.1	0.7 ± 0
	Site 2	32 ± 3	54.1 ± 3.3	15.2 ± 0.5	14.9 ± 1.6	8.6 ± 1.2	3.8 ± 0.6	1.3 ± 0.2	0 ± 0	1.6 ± 0.2	0.2 ± 0
Føyn harbour	Site 1	49.5 ± 15.3	42.2 ± 6.8	14.4 ± 0.8	17.6 ± 0.9	13.7 ± 2.5	7.5 ± 2.9	2.8 ± 1.3	0.3 ± 0.3	1.6 ± 0.4	0.2 ± 0.1
	Site 2	40 ± 7.5	47.1 ± 5.8	16.8 ± 1	15.3 ± 0.9	7.1 ± 0.8	5.2 ± 0.7	4.5 ± 2.3	2.1 ± 2.1	3.1 ± 0.2	0.5 ± 0

Measured exchange fluxes across the sediment-water interface

Table S. 2: Averaged nutrient exchange fluxes (mmol m^{-2} d^{-1}, average ± SD) for sediment community oxygen consumption (SCOC), ammonia (NH_3), nitrate (NO_3^-), nitrite (NO_2^-), phosphate (PO_4^{3-}), dissolved silica (DSi).

Location	subsite	mode	SCOC	ammonia	nitrate	nitrite	phosphate	silica
Dodman Island	Pool 2	dark	26.11 ± 7.34	3.62 ± 6.09	0.8 ± 4.95	0.15 ± 0.31	0.05 ± 0.13	3.63 ± 10.36
		light	17.03 ± 6.88	2.71 ± 0.67	-6.56 ± 0.35	0.08 ± 0.01	-0.2 ± 0.04	-16.25
	Pool 3	dark	14.02 ± 4.97	1.2 ± 0.81	1.16 ± 3.15	NA	-0.1 ± 0.02	-7.67 ± 4.88
		light	21.45 ± 6.66	4.44 ± 4.34	-2.17 ± 0.59	0.15 ± 0.14	NA	3.62 ± 1.97
	Pool 4	dark	16.68 ± 3.02	1.21 ± 0.58	-0.04 ± 0.41	0.05 ± 0.02	-0.08 ± 0.14	3.31 ± 0.32
		light	10.82 ± 1.09	-0.45	-2.83	0.04	0.05 ± 0.02	-0.01 ± 5.32
Blaiklock Island	Site 1	dark	16.18 ± 2.13	0.93 ± 2.67	-1.05 ± 0.46	-0.02	-0.05 ± 0.05	-2.69 ± 2.18
		light	5.3 ± 1.79	-0.04 ± 0.71	-0.92 ± 0.27	-0.02 ± 0.03	-0.04	0.56 ± 11.47
	Site 2	dark	8.44 ± 0.66	1.7 ± 0.49	0.22 ± 0.73	0.05 ± 0.01	0.05 ± 0.07	-2.21 ± 2.26
		light	6.93 ± 1.58	0.21 ± 0.11	-0.07 ± 0.09	0.02 ± 0.02	0.01 ± 0.03	-2.09 ± 1.1
Melchior Islands	Site 1	dark	20.58 ± 3.46	0.51 ± 2.21	0.25 ± 3.24	0.29	0.11	NA
		light	16.16 ± 1.65	-0.03 ± 1.94	1.3 ± 0.13	0.1	0.2 ± 0.06	9.53 ± 0.83
	Site 2	dark	17.31 ± 1.75	0.45 ± 1.07	-0.59 ± 0.24	0.03 ± 0.01	-0.12 ± 0.08	-3.79
		light	-1.12 ± 5.45	NA	-2.12 ± 2.21	0.07	-0.07 ± 0.01	-3.16
Hovgaard Island	Site 1	dark	19.28 ± 2.13	1.14 ± 0.16	-1.44 ± 0.27	0.27 ± 0.21	-0.08 ± 0.02	-5.11 ± 0.1
		light	-4.8 ± 2.77	-1.76	-1.14 ± 0.51	0.06 ± 0.02	-0.12 ± 0.2	3.29
	Site 2	dark	19.77 ± 2.58	2.09 ± 0.06	1.23	0.03	-0.16 ± 0.08	-6.44
		light	8.4 ± 8.15	1.99 ± 1.99	-0.81 ± 0.46	0.05 ± 0.04	0.02 ± 0.08	5.39 ± 6.53
Føyn	Føyn Harbor	dark	20.49 ± 7.13	2.25 ± 1.07	2.88 ± 1.27	0.2 ± 0.1	-0.01 ± 0.12	NA
		light	2.3 ± 2.14	1.31 ± 0.11	0.51 ± 1.33	0.03 ± 0.07	-0.05	0.98 ± 8.72
	Governoren wreck	dark	32.86 ± 15.66	-1.21 ± 2.8	1.06	0.04	-0.17 ± 0.26	2.69

locations	station	mode	SCOC	ammonia	nitrate	nitrite	phosphate	silica
Dodman Island	Pool 2	dark	26.11 ± 7.34	3.62 ± 6.09	0.8 ± 4.95	0.15 ± 0.31	0.05 ± 0.13	3.63 ± 10.36
Dodman Island	Pool 2	light	17.03 ± 6.88	2.71 ± 0.67	-6.56 ± 0.35	0.08 ± 0.01	-0.2 ± 0.04	-16.25
Dodman Island	Pool 3	dark	14.02 ± 4.97	1.2 ± 0.81	1.16 ± 3.15	NA	-0.1 ± 0.02	-7.67 ± 4.88
Dodman Island	Pool 3	light	21.45 ± 6.66	4.44 ± 4.34	-2.17 ± 0.59	0.15 ± 0.14	NA	3.62 ± 1.97
Dodman Island	Pool 4	dark	16.68 ± 3.02	1.21 ± 0.58	-0.04 ± 0.41	0.05 ± 0.02	-0.08 ± 0.14	3.31 ± 0.32
Dodman Island	Pool 4	light	10.82 ± 1.09	-0.45	-2.83	0.04	0.05 ± 0.02	-0.01 ± 5.32
Blaiklock Island	Site 1	dark	16.18 ± 2.13	0.93 ± 2.67	-1.05 ± 0.46	-0.02	-0.05 ± 0.05	-2.69 ± 2.18
Blaiklock Island	Site 1	light	5.3 ± 1.79	-0.04 ± 0.71	-0.92 ± 0.27	-0.02 ± 0.03	-0.04	0.56 ± 11.47
Blaiklock Island	Site 2	dark	8.44 ± 0.66	1.7 ± 0.49	0.22 ± 0.73	0.05 ± 0.01	0.05 ± 0.07	-2.21 ± 2.26
Blaiklock Island	Site 2	light	6.93 ± 1.58	0.21 ± 0.11	-0.07 ± 0.09	0.02 ± 0.02	0.01 ± 0.03	-2.09 ± 1.1
Melchior Islands	Site 1	dark	20.58 ± 3.46	0.51 ± 2.21	0.25 ± 3.24	0.29	0.11	NA
Melchior Islands	Site 1	light	16.16 ± 1.65	-0.03 ± 1.94	1.3 ± 0.13	0.1	0.2 ± 0.06	9.53 ± 0.83
Melchior Islands	Site 2	dark	17.31 ± 1.75	0.45 ± 1.07	-0.59 ± 0.24	0.03 ± 0.01	-0.12 ± 0.08	-3.79
Melchior Islands	Site 2	light	-1.12 ± 5.45	NA	-2.12 ± 2.21	0.07	-0.07 ± 0.01	-3.16
Hovgaard Island	Site 1	dark	19.28 ± 2.13	1.14 ± 0.16	-1.44 ± 0.27	0.27 ± 0.21	-0.08 ± 0.02	-5.11 ± 0.1
Hovgaard Island	Site 1	light	-4.8 ± 2.77	-1.76	-1.14 ± 0.51	0.06 ± 0.02	-0.12 ± 0.2	3.29
Hovgaard Island	Site 2	dark	19.77 ± 2.58	2.09 ± 0.06	1.23	0.03	-0.16 ± 0.08	-6.44
Hovgaard Island	Site 2	light	8.4 ± 8.15	1.99 ± 1.99	-0.81 ± 0.46	0.05 ± 0.04	0.02 ± 0.08	5.39 ± 6.53
Foyn	Foyn Harbor	dark	20.49 ± 7.13	2.25 ± 1.07	2.88 ± 1.27	0.2 ± 0.1	-0.01 ± 0.12	NA
Foyn	Foyn Harbor	light	2.3 ± 2.14	1.31 ± 0.11	0.51 ± 1.33	0.03 ± 0.07	-0.05	0.98 ± 8.72
Foyn	Governoren wreck	dark	32.86 ± 15.66	-1.21 ± 2.8	1.06	0.04	-0.17 ± 0.26	2.69

Bayesian Networks

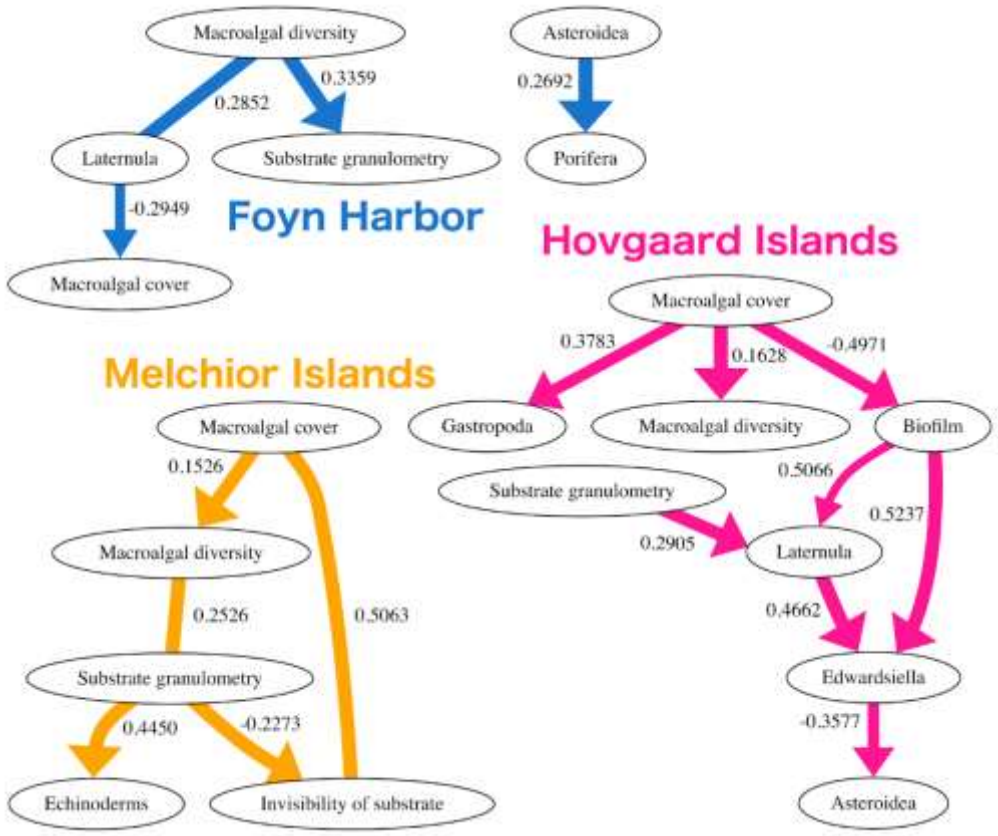

Figure S. 1: Station networks: Bayesian Networks of the northern WAP stations: Melchior Islands (MI), Hovgaard Islands (HI) and Føyn Harbor (FH). The arrows represent the directed dependencies between the nodes. The lines without an arrowhead represent bi-directional dependencies. Width of the lines reflects the frequency at which the edge appeared in the bootstrapped networks. Each number represents the Influence Score (IS) of the connection.

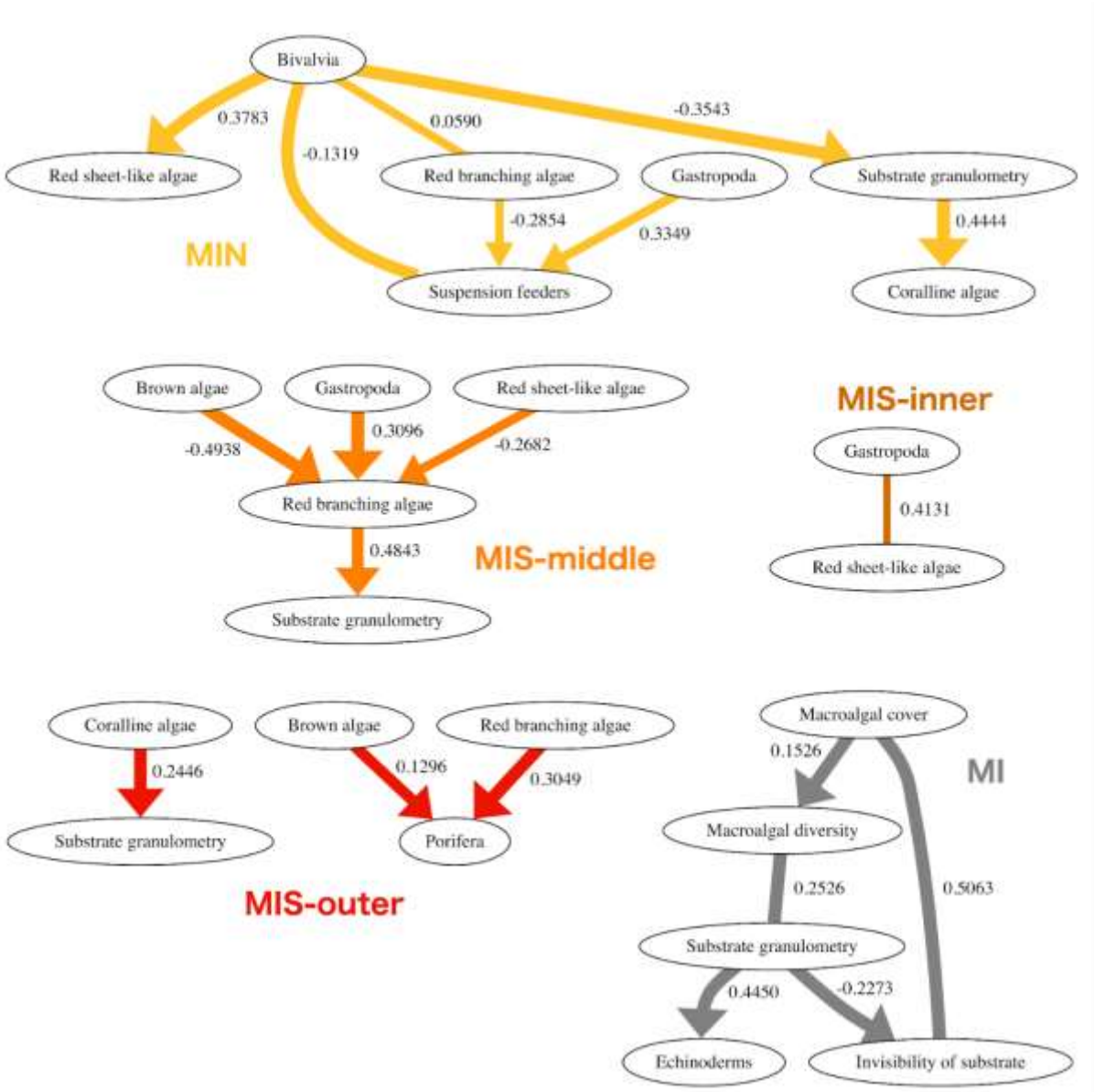

Figure S. 2: Bayesian Networks of Melchior Islands station (MI) and sites (MIN, MIS-inner, MIS-middle, MIS-outer). The arrows represent the directed dependencies between the nodes. The lines without an arrowhead represent bi-directional dependencies. Width of the lines reflects the frequency at which the edge appeared in the bootstrapped networks. Each number represents the Influence Score (IS) of the connection.

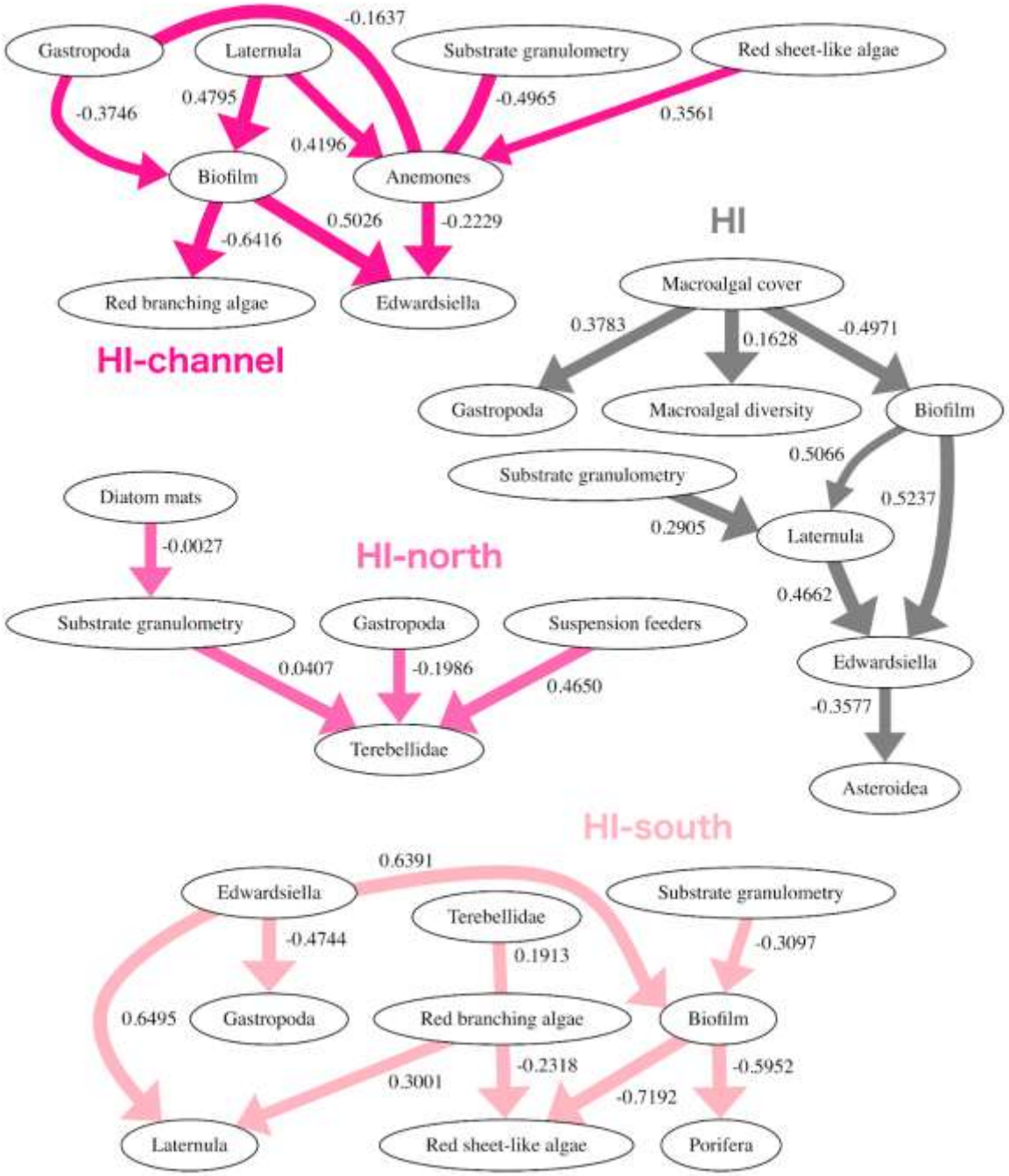

Figure S. 3: Bayesian Networks of Hovgaard Islands station (HI) and sites (HI-north, HIchannel, HI-south). The arrows represent the directed dependencies between the nodes. The lines without an arrowhead represent bi-directional dependencies. Width of the lines reflects the frequency at which the edge appeared in the bootstrapped networks. Each number represents the Influence Score (IS) of the connection.

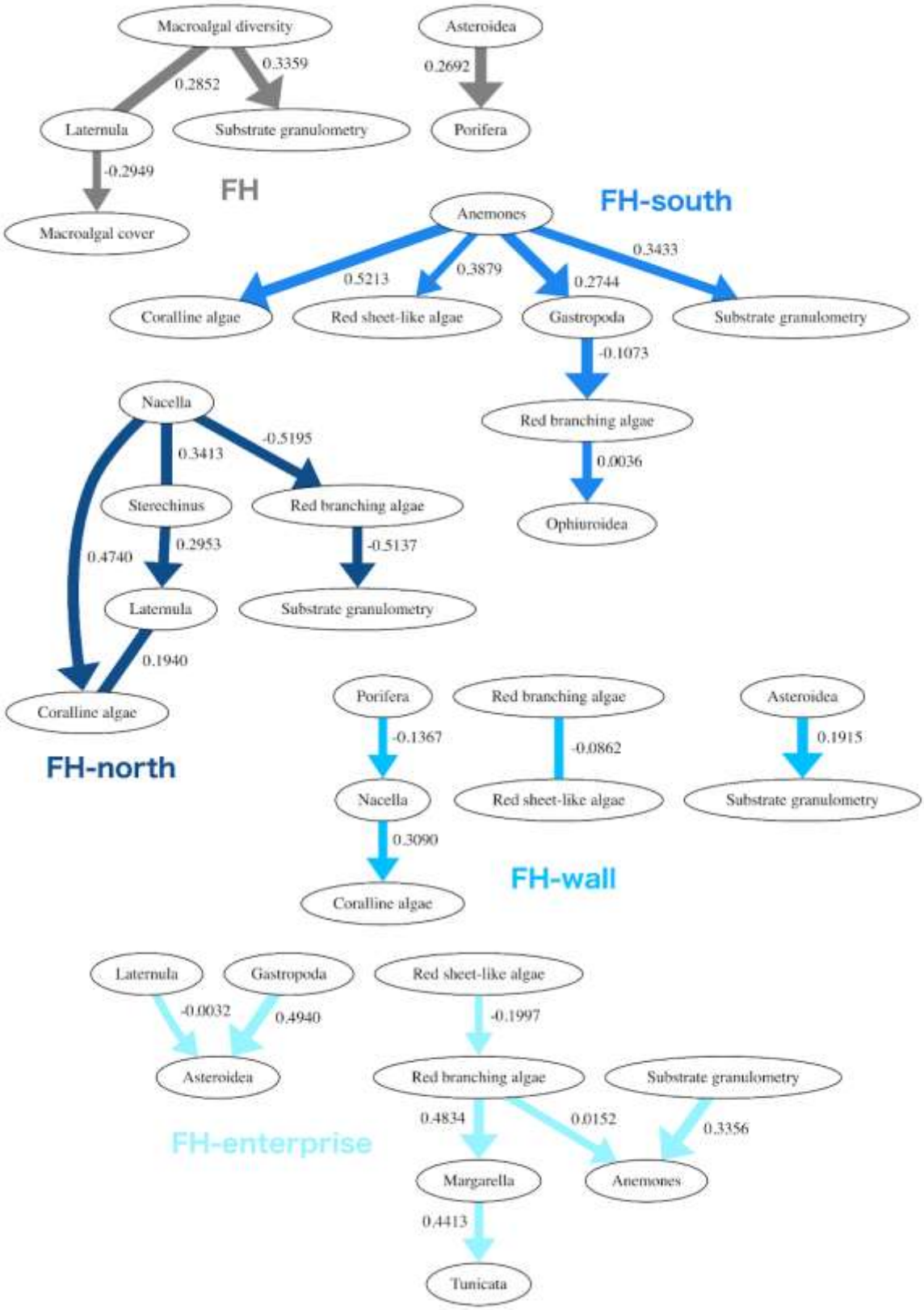

Figure S. 4: Bayesian Networks of Føyn Harbor station (FH) and sites (FH-north, FHsouth, FH-wall, FH-enterprise). The arrows represent the directed dependencies between the nodes. The lines without an arrowhead represent bi-directional dependencies. Width of the lines reflects the frequency at which the edge appeared in the bootstrapped networks. Each number represents the Influence Score (IS) of the connection.